

NUCLEIC ACID GATED NANOPORE DELIVERY OF ANTIBIOTICS

A THESIS SUBMITTED TO  
THE GRADUATE SCHOOL OF NATURAL AND APPLIED SCIENCES  
OF  
MIDDLE EAST TECHNICAL UNIVERSITY

BY

MURAT KAVRUK

IN PARTIAL FULFILLMENT OF THE REQUIREMENTS  
FOR  
THE DEGREE OF DOCTOR OF PHILOSOPHY  
IN  
BIOTECHNOLOGY

APRIL 2018



Approval of the thesis:

**NUCLEIC ACID GATED NANOPORE DELIVERY OF ANTIBIOTICS**

submitted by **MURAT KAVRUK** in partial fulfillment of the requirements for the degree of **Doctor of Philosophy in Biotechnology Department, Middle East Technical University** by,

Prof. Dr. Halil Kalıpçılar  
Dean, Graduate School of **Natural and Applied Sciences**

\_\_\_\_\_

Assoc. Prof. Dr. Can Özen  
Head of Department, **Biotechnology**

\_\_\_\_\_

Assoc. Prof. Dr. Çağdaş Devrim Son  
Supervisor, **Biological Sciences Dept., METU**

\_\_\_\_\_

Assoc. Prof. Dr. Veli Cengiz Özalp  
Co-Supervisor, **Bioengineering Dept.,  
Konya Food&Agriculture University**

\_\_\_\_\_

**Examining Committee Members:**

Prof. Dr. Meral Yücel  
Biological Sciences Dept., METU

\_\_\_\_\_

Assoc. Prof. Dr. Çağdaş Devrim Son  
Biological Sciences Dept., METU

\_\_\_\_\_

Prof. Dr. Füsün İnci Eyidoğan  
Faculty of Education, Başkent University

\_\_\_\_\_

Assoc. Prof. Dr. Ayşe Elif Erson Bensen  
Biological Sciences Dept., METU

\_\_\_\_\_

Assoc. Prof. Dr. Barış Ata Borsa  
Medical Microbiology Dept., Yeditepe University

\_\_\_\_\_

**Date:** 26.04.2018

**I hereby declare that all information in this document has been obtained and presented in accordance with academic rules and ethical conduct. I also declare that, as required by these rules and conduct, I have fully cited and referenced all material and results that are not original to this work.**

Name, Last name : Murat Kavruk

Signature :

## ABSTRACT

### NUCLEIC ACID GATED NANOPORE DELIVERY OF ANTIBIOTICS

Kavruk, Murat

Ph.D., Department of Biotechnology

Supervisor: Assoc. Prof. Dr. Çağdaş Devrim Son

Co-Supervisor: Assoc. Prof. Dr. Veli Cengiz Özalp

April 2018, 124 pages

Discovery of new strategies in administration of antimicrobial agents are essential in the ongoing battle against pathogens due to rapidly emerging antimicrobial resistance. Nanotechnology provide unique opportunities in this respect for the development of targeted drug delivery solutions for effective usage of current antibiotics. Mesoporous silica particles are micrometer-sized particles with nanometer-sized porous surface structure. They are advantageous molecules due to small size, biocompatibility, well-defined pore size and modifiable surface. Functional nucleic acids have potential to target the drug loaded nanoparticles.

From this perspective, affinity capability of aptamers and enzymatic cleavage of capability of nucleic acid oligos, targeting of nanoparticles was experimented in this study. Incorporation of *Staphylococcus aureus* aptamer and an oligo sequence specific to micrococcal nuclease were analysed against the hypothesis that, sealing of drug loaded nanopores with nucleic acids having a function to release the drug in the presence of a specific target, thus increasing the efficiency of drug and decreasing the risk of antibiotic resistance. *Staphylococcus epidermidis* was used as control

organisms and vancomycin was used as antimicrobial drug for proving the specificity of the system.

Nanoparticles with cleavega-oriented oligo sealing mechanism decreased the MIC of vancomycin against *S. aureus* strain from 1.061 $\mu$ g/mL to 0.332 $\mu$ g/mL, while affinity-oriented aptamer sealing mechanism functioned with a decreased MIC for *S. aureus* strain from 1.168 $\mu$ g/mL to 0.420 $\mu$ g/mL. In both mechanisms, MIC against *Staphylococcus epidermidis* increased proving the specificity of antibiotic delivery. The inhibitory performance of proposed targeted drug delivery mechanism proved its potential for further applications and developments.

Key words: Antimicrobial, mesoporous silica particles, functional nucleic acids, drug delivery.

## ÖZ

### NÜKLEİK ASİT KAPAKLI NANOGÖZENEKLİ ANTİBİYOTİK TAŞINIMI

Kavruk, Murat

Doktora, Biyoteknoloji Bölümü

Tez Yöneticisi: Doç. Dr. Çağdaş Devrim Son

Ortak Tez Yöneticisi: Doç. Dr. Veli Cengiz Özalp

Nisan 2018, 124 sayfa

Antimikrobiyal ajanların kullanımında yeni stratejilerin keşfedilmesi, hızla ortaya çıkan antimikrobiyal dirence bağlı olarak patojenlere karşı devam eden mücadelede önemlidir. Nanoteknoloji, mevcut antibiyotiklerin etkin kullanımı için hedeflenen ilaç taşınım çözümlerinin geliştirilmesi için eşsiz fırsatlar sunmaktadır. Mezoporlu silika parçacıkları nanometre boyutlu gözenekli yüzey yapısı ile mikrometre boyutlu parçacıklardır. Küçük boyutlu, biyouyumlu, iyi tanımlanmış gözenek boyutu ve değiştirilebilir yüzeyi nedeniyle avantajlı moleküllerdir. Fonksiyonel nükleik asitler ise, ilaç yüklü nanopartikülleri hedefleme potansiyeline sahiptir.

Bu açıdan, aptamerlerin afinite kabiliyeti ve nükleik asit oligolarının enzimatik parçalanması, bu çalışmada nanopartiküllerin hedeflenmesinde denenmiştir. *Staphylococcus aureus* aptamerinin ve mikrokokal nükleaza özgü bir oligo dizisinin dahil edilerek, ilaç yüklenen nano-gözeneklerin, spesifik bir hedefin varlığında ilacı serbest bırakmak için bir fonksiyona sahip olan nükleik asitlerle sızdırmaz hale getirilmesi, böylece ilacın verimini ve antibiyotik direnci riskini azaltmaktadır.

Antimikrobiyal ila olarak vankomisin, sistemin zelliđinin kanıtlanması iin kontrol organizması olarak *Staphylococcus epidermidis* kullanılmıřtır.

Enzimatik ynelimli oligo sızdırmazlık mekanizmasına sahip nanoparacıklar, *S. aureus* suřuna karřı vankomisin MİK deđerini 1,061µg/mL'den 0,332µg/mL'ye dřürürken, afinite ynelimli aptamer sızdırmazlık mekanizması, *S. aureus* suřuna karřı vankomisin MİK deđerini 1,168µg/mL'den 0,420µg/mL'ye dřürdüđü tespit edilmiřtir. Her iki mekanizmada da, *Staphylococcus epidermidis*'e karřı MİK'in artması, antibiyotik verilmesinin zgünlüđünü kanıtlamıřtır. Önerilen hedefe ynelik ila dađıtım mekanizmasının etki performansı, daha ileri uygulamalar ve geliřmeler iin potansiyelini kanıtlamıřtır.

Anahtar kelimeler: Antimikrobiyal, mezoporlu silika paracıkları, iřlevsel nükleik asitler, ila tařınım.



To My Mom and My Wife..

## ACKNOWLEDGEMENTS

The author wishes to express his deepest gratitude to his supervisor Assoc. Prof. Dr. Çağdaş Devrim Son and co-supervisor Assoc. Prof. Dr. Veli Cengiz Özalp for insight, helps, valuable suggestions and comments during the study. The author would like to thank to all his thesis committee for their suggestions and criticism.

The publication “NanoKeepers: stimuli responsive nanocapsules for programmed specific targeting and drug delivery” (DOI: 10.1039/C4CC04248D) was adapted with a permission from the corresponding publisher.

The publication “Antibiotic loaded nanocapsules functionalized with aptamer gates for targeted destruction of pathogens” (DOI: 10.1039/C5CC01869B) was adapted with a permission from the corresponding publisher.

The publication “Aptamers: Molecular Tools for Medical Diagnosis” (DOI: 10.2174/1568026615666150413154233) was adapted with a permission from the corresponding publisher.

The publication “Antimicrobial aptamers for detection and inhibition of microbial pathogen growth” (DOI: 10.2217/FMB.12.149) was adapted with a permission from the corresponding publisher.

The permissions for publications to which the author has contribution were given in Appendix A

This study was supported by The Scientific and Technological Research Council of Turkey (TUBITAK) Grant No: 1001 / 213M315.

## TABLE OF CONTENTS

ABSTRACT .....	v
ÖZ.....	vii
ACKNOWLEDGEMENTS.....	x
TABLE OF CONTENTS .....	xi
LIST OF TABLES.....	xiii
LIST OF FIGURES .....	xiv
LIST OF ABBREVIATIONS .....	xvii
CHAPTERS	
1. INTRODUCTION.....	1
1.1 Bacterial Infections and Antibiotics Utilization .....	1
1.2 Drug Resistance and Nanomaterial Strategies.....	8
1.3 Functionalized Nucleic Acids.....	17
1.3.1 Modified Oligo Sequences for Specific Nuclease.....	18
1.3.2 Aptamers for Specific Microorganisms .....	22
1.4 Utilization of Nanoparticles for Detection and Therapy .....	29
1.5 Aim of Study.....	34
2. MATERIALS AND METHODS .....	37
2.1 Materials .....	37
2.2 Methods .....	37
2.2.1 Characterization of Mesoporous Silica Particles .....	37
2.2.2 Synthesis of Probe-Capped Particles.....	39
2.2.3 Release Experiments .....	40
2.2.4 Bacterial Cultures.....	41
2.2.5 Antibacterial Activity.....	42
3. RESULTS AND DISCUSSION .....	45
3.1 Preparation of Mesoporous Silica Nanoparticles .....	45

3.1.1 Characterization and Modification of Mesoporous Silica Nanoparticles .....	45
3.1.2 Loading of Mesoporous Silica Nanoparticles .....	46
3.1.3 Calculated Loading Efficiency and Capping Concentration for Mesoporous Silica Nanoparticles .....	50
3.2 Modified Nucleic Acid Gates for Targeted Delivery of Antibiotics	51
3.2.1 Design of Modified Oligonucleotide Gates.....	51
3.2.2 Synthesis of Modified Oligonucleotide-Capped Silica Nanoparticles .....	53
3.2.3 Release Kinetics of Rhodamine B and Vancomycin from Modified Oligonucleotide-Capped Nanoparticles.....	57
3.2.4 MIC Analysis of Modified Oligonucleotide-Capped Nanoparticles .....	61
3.3 Aptamer Gates for Targeted Delivery of Antibiotics .....	65
3.3.1 Design of Aptamer Gates .....	66
3.3.2 Synthesis of Aptamer-Capped Silica Nanoparticles.....	68
3.3.3 Release Kinetics of Vancomycin from Aptamer-Capped Silica Nanoparticles.....	69
3.3.4 MIC Analysis of Aptamer-Capped Silica Nanoparticles .....	71
4. CONCLUSION .....	77
4.1 Future Studies .....	80
REFERENCES .....	87
APPENDICES	
A. PERMISSIONS FOR PUBLICATIONS .....	107
B. SHAPE CHARACTERISTICS OF GOMPERTZ MODEL.....	111
C. BET ANALYSIS METHOD AND SUPPORTIVE GRAPHICS .....	113
D. ANOVA CALCULATIONS OF MIC ANALYSIS .....	119
CURRICULUM VITAE.....	123

## LIST OF TABLES

### TABLES

Table 1 Drug development obstacles (Silver, 2011) .....	2
Table 2 History of introduction of new classes of antibiotic (Conly & Johnston, 2005).....	3
Table 3 Nanoparticle types used for drug delivery (De Jong & Borm, 2008; B. Kumar, Jalodia, Kumar, & Gautam, 2017).....	11
Table 4 Summary of Applications of Mesoporous Silica (MS) and Porous Silica Spheres (PSS) Materials (Hanrahan, O'Mahony, Tobin, & Hogan, n.d.).....	12
Table 5 Examples of aptamers recognizing live microorganisms. ....	26
Table 6 Probe, oligo and aptamer sequences.....	38
Table 7 Pore volume and surface area calculations as a result of BET experiment with different calculation methods; BJH and DFT for establishment of pore volume, surface area and pore diameter. ....	49

## LIST OF FIGURES

### FIGURES

Figure 1 Chemical structure of daptomycin as an example of large antibiotics (Ball, Goult, Donarski, Micklefield, & Ramesh, 2004).....	5
Figure 2 Chemical structure of vancomycin which was used as a model antibiotic in this study (Schäfer, Schneider, & Sheldrick, 2017).....	6
Figure 3 Number of published papers annually according to different topics accessed via Web of Science (Clarivate Analytics, 2018).....	9
Figure 4 Evolution of drug delivery systems since 1950 (K. Park, 2014).....	10
Figure 5 Classification of mesoporous particles based on their material. ....	13
Figure 6 Schematic diagram of the M41S materials (Allothman, 2012).....	14
Figure 7 Enzymatic cleavage site of micrococcal nuclease (MN) on nucleic acid sequences (Sigma-Aldrich, 2017a). ....	18
Figure 8 Specificity of different sequences (F. J. Hernandez et al., 2014).....	20
Figure 9 Fluorescence measurements of nuclease-activated nucleic acids coupled with fluorophore-quencher pairs (Kruspe et al., 2017).....	21
Figure 10 Main steps in a typical Cell-SELEX for serotype-specific aptamer enrichment. ....	25
Figure 11 pH-responsive chitosan nanoparticles encapsulating vancomycin (Kalhapure et al., 2017).. ....	31
Figure 12 Cyclodextrin-Mesoporous Silica Particles (CD-MSP) drug delivery system with different linkage (Stjern et al., 2017).....	33
Figure 13 Experimental setup for release kinetics of nanoparticles (Ozalp & Schafer, 2011). ....	41
Figure 14 Synthesis and characterization of modified silica particles.....	46
Figure 15 Nitrogen adsorption isotherms and pore size distribution of MCM-41 particles calculated by BJH method.....	47

Figure 16 Nitrogen adsorption isotherms and pore size distribution of MCM-41 particles calculated by DFT method. ....	48
Figure 17 Sizes of molecules to be incorporated in pores of mesoporous silica particles.....	50
Figure 18 Representation for quenching of fluorescence on modified oligonucleotide probe due to a complementary part at 3' and 5' ends via Nupack program (nupack.org). ....	53
Figure 19 Scheme of Modified Oligonucleotide-Capped Silica Nanoparticles approach for targeted drug delivery.....	55
Figure 20 Degradation profile of NK01 probe. ....	57
Figure 21 Evaluation of modified oligonucleotide-capped nanoparticles loading with Rhodamine B under simulated physiological conditions. ....	59
Figure 22 Evaluation of oligonucleotide-capped nanoparticles loading with vancomycin under simulated physiological conditions (10% human serum in 0.01 M PBS at 37 °C).....	61
Figure 23 Bactericidal efficiency of modified oligo-gated vancomycin loaded mesoporous silica particles. ....	63
Figure 24 Time-kill curves for <i>S. aureus</i> and <i>S. epidermidis</i> cultures after treating with modified oligonucleotide-nanoparticles with a concentration of 1 MIC calculated..	65
Figure 25 Fluorescence changes of the aptamer switch probes upon addition of 10 <sup>4</sup> <i>S. aureus</i> or <i>S. epidermidis</i> cells in 0.01 M PBS. ....	67
Figure 26 Scheme of Aptamer-Capped Silica Nanoparticles approach for targeted drug delivery.....	69
Figure 27 Evaluation of aptamer-capped nanoparticles loading with vancomycin under simulated physiological conditions (10% human serum in 0.01 M PBS at 37 °C).....	71
Figure 28 Bactericidal efficiency of aptamer-gated vancomycin loaded mesoporous silica particles. ....	73

Figure 29 Time-kill curves for <i>S. aureus</i> and <i>S. epidermidis</i> cultures after treating with aptamer-nanoparticles with a concentration of 1 MIC calculated. ....	75
Figure 30 Chemical structures of different antibiotics for experimenting mesoporous particle release kinetics (Atefyekta et al., 2016).....	81
Figure 31 Permission for publication “Antibiotic loaded nanocapsules functionalized with aptamer Gates for targeted destruction of pathogens” as a research paper. ....	107
Figure 32 Permission for publication “NanoKeepers: stimuli responsive nanocapsules for programmed specific targeting and drug delivery” as a research paper. ....	108
Figure 33 Permission for publication “Aptamers: Molecular Tools for Medical Diagnosis” as a book chapter.....	109
Figure 34 Permission for publication “Antimicrobial aptamers for detection and inhibition of microbial pathogen growth” as a review paper.....	110
Figure 35 Shape characteristics of the Gompertz model. ....	111
Figure 36 Multi-point BET plot of BET analysis .....	116
Figure 37 DFT Fitting Comparison of BET analysis .....	117
Figure 38 ANOVA statistics for MIC calculations of modified oligonucleotide-capped nanoparticles against <i>S. aureus</i> .....	119
Figure 39 ANOVA statistics for MIC calculations of modified oligonucleotide-capped nanoparticles against <i>S. epidermis</i> .....	120
Figure 40 ANOVA statistics for MIC calculations of aptamer-capped nanoparticles against <i>S. aureus</i> .....	121
Figure 41 ANOVA statistics for MIC calculations of aptamer-capped nanoparticles against <i>S. epidermis</i> .....	122



## LIST OF ABBREVIATIONS

AF488	: Alexa Flour 488
BET	: Brunauer–Emmett–Teller
BH1	: Blackhole I quencher
BJH	: Barrett-Joyner-Halenda
DFT	: Density functional theory
DLS	: Dynamic light scattering
FAM	: 6-carboxy fluorescein
MCM-41	: Mobil Composition of Matter
NK01	: NanoKeeper01 functional geate
NK02	: NanoKeeper02 unfunctional gate
PEG	: polyethylenglycol
Sulfo-GMBS	: Sulfo-N-succinimidyl 4-maleimidobutyrate sodium salt
ZEN	: IDT ZEN fluorescence quencher



## CHAPTER 1

### INTRODUCTION

#### 1.1 Bacterial Infections and Antibiotics Utilization

Antimicrobial discovery is in a global crisis and exploration of alternative antimicrobial sources is of utmost importance in the battle against microbial pathogens. A recent report shows that microbial infections is a major cause of death (World Health Organization, 2011). This is mainly due to the microorganisms' enormous adaptation capacity to overcome the effects of existing antimicrobial agents through various mechanisms. Many antibiotics have become ineffective against common pathogens. According to WHO data about 440,000 new cases of multi-drug resistant tuberculosis (MDR-TB) emerge annually. Similarly, there has been an increased incidence rate of methicillin-resistant *Staphylococcus aureus* (MRSA) and vancomycin-resistant Enterococci. Additionally, Salmonella recently has become a public health issue because of increased levels of antimicrobial resistance development as reviewed (Hur, Jawale, & Lee, 2012).

*Salmonella* spp. may be counted as a “model organism” for robustness of resistance mechanisms. Due to intense use of antibiotics in combat against Salmonella in both humans and animals (especially domestic chickens, cattle and swine) multi-drug resistance to quinolones, fluoroquinolones or extended-spectrum cephalosporins like ceftiofur and ceftriaxone has been emerged in serotypes such as *Salmonella* serotype Typhimurium, *Salmonella* serotype Enteritidis and *Salmonella* serotype Newport.

Even only for *Salmonella* spp. serotypes, different drug resistance mechanisms are at work that can be grouped as following:

- production of enzymes that inactivate antimicrobial agents through degradation or structural modification,
- reduction of bacterial cell permeability to antibiotics,
- activation of antimicrobial efflux pumps, and
- modification of cellular drug targets”

unfolding the complexity in fight against microorganisms (Hur et al., 2012). To further complicate the situation, multidrug resistance (MDR) has increased the number of antibiotic resistant microorganisms worldwide due to a snowball effect of increased antibiotics usage both quantitatively and qualitatively. This snowball effect is mainly due to unspecific broad-range antibiotic usage. These developments hinder the fight against infectious diseases in a global setting in addition to increased costs of drug development and increasing MDR-related mortality rates.

Table 1 Drug development obstacles (Silver, 2011)

<b>Intrinsic</b>	<b>Extrinsic</b>
Chemical libraries are limited	High cost of development for the firms
Penetration of drug candidates into Gram-negative bacterial wall barrier	Short-period of usage by patients
Structural features of drug candidates like molecular size and charge, common non-selective efflux pumps on the bacterial membranes	Market competitions between the firms
	Side effects of drugs
	Pharmaco -kinetics / -dynamics

To prevent a return to the “pre-antibiotic era” the requirement for novel antimicrobial compounds is greater than ever. However, the number of approved new antibiotics decreased by 56% between 1983 and 2002 due to both scientific and legislative reasons although infectious diseases are 3<sup>rd</sup> major reason of death in USA and 2<sup>nd</sup>

major reason of death in the world (Spellberg, Powers, Brass, Miller, & Edwards, 2004). Updates to this data are not clearly quantified, however recent surveys have published that, this trend has a potential to be more critical estimating 10 million deaths annually in following years (Boychev & Parsons, 2016). For every antibiotic \$400–\$800 million should be spent which is the biggest obstacle remaining to this day and getting worse with every resistance case of microorganisms. This trend is also expected to continue for the next decades due to the high costs involved in drug discovery and continuously emerging resistances in both hospitals and communities resulting a decrease in the feasibility of new antibiotics (Theuretzbacher, 2012). Summarized in Table 1 the intrinsic (related with the developmental stage) and extrinsic (related with the health and feasibility) obstacles in drug discovery (Silver, 2011).

Table 2 History of introduction of new classes of antibiotic (Conly & Johnston, 2005)

<b>Year introduced</b>	<b>Class of drug</b>
1935	Sulphonamides
1941	Penicillins
1944	Aminoglycosides
1945	Cephalosporins
1949	Chloramphenicol
1950	Tetracyclines
1952	Macrolides/lincosamides/streptogramins
1956	Glycopeptides
1957	Rifamycins
1959	Nitroimidazoles
1962	Quinolones
1968	Trimethoprim
2000	Oxazolidinones
2003	Lipopeptides

The obstacles mentioned above revealing an urgent situation with drug discovery. Only two major antibiotic classes have been developed clinically in past 40 years (Table 2) and they are not very successful against Gram-negative bacteria. Furthermore, bacteriostatic/bactericidal efficiency of drugs are diminishing in months to years upon starting clinical usage due to developing resistance mechanisms by bacteria (Coates, Halls, & Hu, 2011; Worthington & Melander, 2013).

With the beginning of millenia, both synthetic (“Oxazolidinones” against 50S ribosomal subunit inhibitor for interrupting formation of the 70S initiation complex which is a prerequisite for protein synthesis thus bacterial reproduction) and natural (“Lipopeptides” being composed of lipids and peptides and originated from bacteria) antibiotic started to be administered for clinical utilization. However, independent from being synthetic or natural, microorganisms are developing resistance to our newest arsenal. One of the noteworthy example is daptomycin, a lipopeptide naturally occurring in soil saprotroph *Streptomyces roseosporus* which had been found by a scientist Eli Lilly at Mount Ağrı (Eisenstein, Oleson Frederick B., & Baltz, 2010). Daptomycin is a member of the utmostly discovered class of drugs, lipopeptides (Figure 1). The molecule is able to self-assemble resulting a cell membrane embedding capability. Aggregation of daptomycin due to its amphoteric chemistry disrupts the membrane structure and creates holes for ion leakage (Ca<sup>2+</sup>-dependent potassium ion release) ending up with cell death in nearly 30 minutes (Silverman, Perlmutter, & Shapiro, 2003). And recently, it has been found that, membrane dislocalization due to daptomycin is causing a flip-flop (transbilayer lipid motion) effect on membrane proteins vital for cell membrane synthesis (Pogliano, Pogliano, & Silverman, 2012).

Based on these potentials, daptomycin is effective against some Gram-positive pathogens, like methicillin-resistant *S. aureus* (MRSA) and vancomycin-resistant Enterococcus (VRE) species. However, although it had showed success to some

extent, rapid resistance formation due to intense usage throughout the world will be the reasons for diminishing its efficiency in the near future. Starting with clinical usage in 2003, daptomycin-resistant strains of bacteria has been reported in less than a year and ending up with lethal cases (Marty et al., 2006). Although the exact mechanism of resistance is still unknown, there are some researches shedding light to the molecular mechanism. Baltz reported that “mutations associated with decreased susceptibility were mapped in *mprF*, *yycG*, *rpoB*, and *rpoC*, each giving about two-fold increase in the minimal inhibitory concentration (MIC) and combinations giving higher MICs.” (Baltz, 2009). These genes either control addition of lysine residue to phosphatidylglycerol and increase the ratio of lysyl-PG (LPG) in the cell membrane or antibacterial target candidates. Since lysine residue change the charge density,  $\text{Ca}^{2+}$ -dependent penetration and as a result efficiency of daptomycin decreases to two fold (from 6mg/kg to 12mg/kg). Studies showed that, intense usage of daptomycin resulting with the accumulation of various mutations ending up with such resistance (Dortet, Anguel, Fortineau, Richard, & Nordmann, 2013).

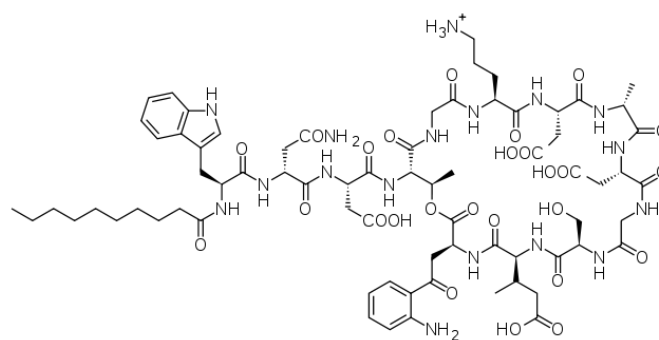


Figure 1 Chemical structure of daptomycin as an example of large antibiotics (Ball, Goult, Donarski, Micklefield, & Ramesh, 2004).

As in the cases of other antibiotic groups (like penicillins or cephalosporins), chemical modifications may lead to the  $\text{Ca}^{2+}$ -independently efficient daptomycins. However, more

complex and potent the bactericidal effect of the drug, more complex and severe resistance mechanisms will be evolved eventually.

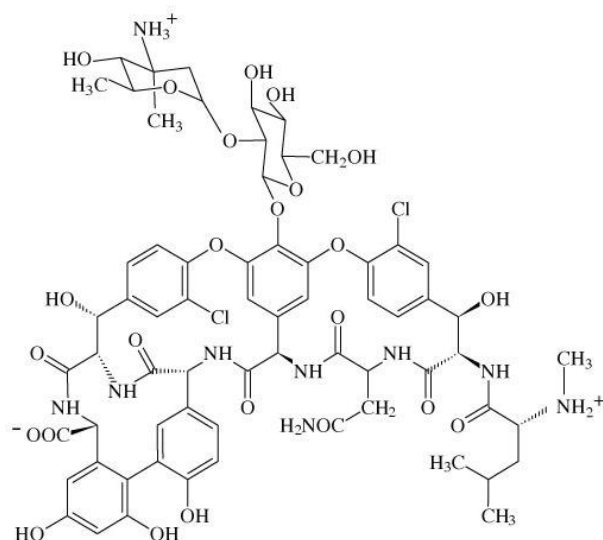


Figure 2 Chemical structure of vancomycin which was used as a model antibiotic in this study (Schäfer, Schneider, & Sheldrick, 2017)

In this study, vancomycin was chosen as a model antibiotic (Figure 2). Vancomycin is a broad-spectrum glycopeptide antibiotic utilized from *Streptomyces orientalis*, which is also a bacterium (currently known as *Amycolatopsis orientalis*). Its genus is a well known source both for currently used antibiotics like vancomycin (Brigham & Pittenger, 1956) and for new antibiotic research area like pargamicin (Igarashi et al., 2008), tolypomycin, nogabecin (Wink et al., 2003). Vancomycin disrupts the cell wall synthesis of Gram-positive bacteria by forming an asymmetric antibiotic dimer with C-terminal of polymeric lipid intermediates (Ala-Ala region), thus interfering the peptidoglycan synthesis (Barna & Williams, 1984; Reynolds, 1989).



This antibiotic was chosen since it is used as one of the last resorts against drug resistance bacteria including *S. aureus*. Vancomycin is actively and efficiently used against MRSA cases. One of such researches was conducted in China. Out of 140 MRSA clinical cases in hospitals, 35 was treated with vancomycin achieving more than 65% complete healing, and less than 10% mortality with nearly 98% of the patients were found to be cured with intravenous administration of 1-2 µg/mL of vancomycin also with some additional treatments according to the patients' condition (J. Tang et al., 2015). Even better results have been obtained *in vitro* studies with real clinical samples obtaining 0% resistance of 312 MRSA cultures tested with vancomycin screen agar, agar dilution technique and E strip technique (Kulkarni, Kulkarni, Nilekar, & More, 2017). However, vancomycin is also losing its efficiency with newly emerged resistance cases. Due to extensive use of vancomycin especially in hospitals against MRSA, intermediate resistance (8-16 µg/mL) and high-level resistance (32 µg/mL) *S. aureus* cases have been reported in both *in vitro* studies in India (Thati, Shivannavar, & Gaddad, 2011) and clinical studies in USA (Loomba, Taneja, & Mishra, 2010). The resistance mechanism has been studied by different groups and found that, more than one gene mutations (*walkR*, *vraSR*, *rpoB*, *yyqF/vraSR* system or the combination of these genes) related with cell wall synthesis (Gardete & Tomasz, 2014) or lateral transfer of *VanA gene* from vancomycin resistant *Enterococcus faecium* (Thati et al., 2011) may be some of the reasons for reduced sensitivity or insensitivity of *S.aureus* against vancomycin. However, there are still ongoing studies to reflect the exact mechanism of resistance. These publications indicate the lifespan of vancomycin usage is diminishing against critical cases. Thus, using vancomycin in this study may be counted as appropriate while proposing a drug release mechanism for more effective antibiotic administration.

## 1.2 Drug Resistance and Nanomaterial Strategies

Conventionally, two types of efficiency dependence mechanisms can be classified for antibiotic therapy based on pharmacodynamic and pharmacokinetic interactions; concentration-dependent antibiotics (for tissue penetration and maximum initial killing – e.g. aminoglycosides) and time-dependent antibiotics (maximum amount of time over MIC – e.g.  $\beta$ -lactams) (McKenzie, 2011). The clinical management of bacterial infections generally includes antibiotic treatment via oral or intravenous administration in any of these mechanisms. Since both of them are non-target strategies, high doses of antibiotics are required to obtain therapeutic effects in any of the alternatives. As a result of such practice, toxicity and bacterial resistance have been reported as the most common drawbacks (Hunter, Elsom, Wibroe, & Moghimi, 2012). Bacterial resistance is currently among the top health challenges worldwide as reviewed that 20% of MRSA cases have been resulted with mortality (Worthington & Melander, 2013).

In the last decades, the world was keeping hope in drugs such as carbapenems, as one of the latest weapons to battle against resistant bacteria (McKenna, 2013). Carbapenems (like imipenem or panipenem) are  $\beta$ -lactam antibiotics being effective to both Gram-negative and Gram-positive bacteria. However, a couple of years ago, several bacteria species have reported resistance to carbapenems, leaving the world defenseless against such infections (Gupta, Limbago, Patel, & Kallen, 2011). When the reasons for such rapid emergence of resistance were investigated, three main topics would come forward: uncontrolled access to antibiotics, inadequate actions after resistance emerges, sub- or supra-therapeutic dosage of antibiotics (Meletis, 2016). The first two topics may be counted as an issue of government and legislations, but third topic may also be counted as a scientific research area. There are other classifications or strategy proposals reviewed against antibiotic resistance (Uchil, Kohli, Katekhaye, & Swami, 2014), however the effective utilization of current

antibiotics remains a crucial step in any case. From this perspective, to preserve the life-saving potential of antibiotics, a more careful use should be implemented, including lowering the dosage by more efficient administration methods (Davies & Davies, 2010). The development of new approaches is therefore required to overcome this challenge.

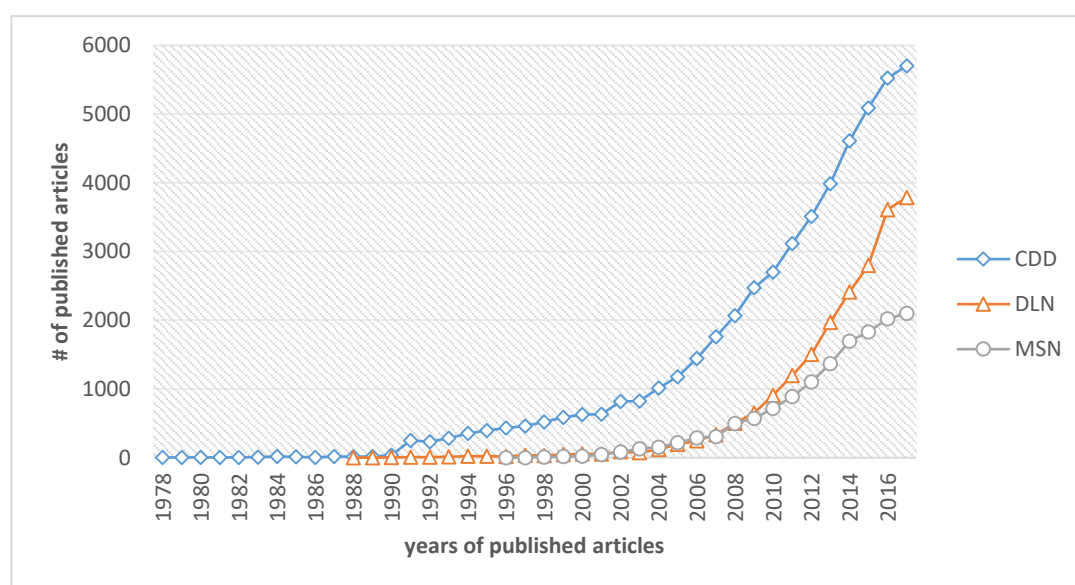


Figure 3 Number of published papers annually according to different topics accessed via Web of Science (Clarivate Analytics, 2018). CDD: controlled drug delivery, DLN: drug loaded nanoparticles, MSN: mesoporous silica nanoparticles

Controlled and targeted delivery systems have been widely investigated areas especially for cancer treatment or gene therapy over decades and still a hot topic in scientific area (Chen et al., 2017; Kompella, Amrite, Ravi, & Durazo, 2013; Upadhyay, 2014). As graphing in Figure 3, for the last 30 years (1978-2017) consistent increase in the number of published papers about this topic that can be accessed from Web of Science. Blue line indicates the number of papers having a topic “Controlled Drug Release” reaching nearly 6,000 papers annually. Orange line

represents the papers about the topic “Drug Loaded Nanoparticles”, and grey line represents “Mesoporous Silica Nanoparticles” which is also an important part of this research (Clarivate Analytics, 2018).

1950	1980	2010	2040
1st Generation		2nd Generation	
<u>Basics of Controlled Release</u>		<u>Smart Delivery Systems</u>	
Oral Delivery once/twice-a-day  Transdermal Delivery onca-a-week  Drug Release Mechanims dissolution, osmosis	Zero-Order Release zero vs first order release  Smart Polymers & Hydrogels environment-sensitive self-regulated release  Peptide & Protein Delivery biodegreable depot  Nanoparticles tumor-targeted delivery gene delivery	On-Off Insulin Release glucose-sensitive release  Targeted Delivery anticancer drugs, siRNA  Long-Term Delivery Systems 6-12 months with the minimal initial burst effect  <i>In vitro-In vivo</i> Correlation prediction of PK profiles from <i>in vitro</i> release study	

Figure 4 Evolution of drug delivery systems since 1950 (K. Park, 2014).

The trend of topics in the literature has a correlation with the expected future of controlled drug release as reviewed also in literature and summarized in Figure 4 (K. Park, 2014). With the development of biotechnology tools (like activity or affinity based targeting) and nanoparticle formulations (like mesoporous silica particles), 3<sup>rd</sup> generation of drug delivery systems are currently being developed with on-off switch systems and targeting a specific locations *in vivo*. Based on this trend, it can be proposed that controlled delivery systems based on adequately modified nanocapsules incorporate characteristics such as specific targeting, control of dose and drug release are strong candidates to overcome the side effects of conventional treatments like gastrointestinal side effects, allergic reactions, hepatotoxicity, kidney damage and many others reviewed in the literature (Xiong, Bao, Yang, Zhu, & Wang, 2014) as well as

drug resistance. From toxicological point of view, “effective” drug concentration (that can interact with organism) should be lowest apart from the clinically targeted tissue/organ, and from pharmacological point of view, drug concentration should be above its minimum effective drug concentration independent of its efficiency (or pharmacokinetics potential) in order to be effective. Drug-loaded nanomaterials are a combination of these two perspectives and will be exemplified below.

Table 3 Nanoparticle types used for drug delivery (De Jong & Borm, 2008; B. Kumar, Jalodia, Kumar, & Gautam, 2017). Most of the particles deliver the drug via encapsulating.

<b>Nanoparticle</b>	<b>Materials Used</b>
Carbon nanotubes	Metals, semiconductors
Dendrimers	Polymers like glycogen, amylopectins and proteoglycans
Fullerene based derivatives	Carbon based spherical in shape
Gold nanoparticles	Gold
Liposomes	Phospholipid vesicles
Magnetic nanoparticles	Magnetite Fe <sub>2</sub> O <sub>3</sub> , Maghemite coated with dextran
Nanoshells	Dielectric core and metal shell
Nanowires	Silicon, cobalt, gold or copper based nanowires
Natural materials or derivatives	Chitosan, dextrane, gelatine, alginates
Polymer carriers	Poly(lactic acid), poly(cyano)acrylates, polyethylenimine
Quantum dots	CdSe-CdS core shell
Silica nanoparticles	Silica
Solid lipid nanoparticle (SLN)	Melted lipid dispersed in Aqueous surfactant

There are different nanomaterials used for drug delivery and all of them have specific advantages over conventional drug administration (Table 3). Drug-loaded nanocapsules (DLNCs) are well suited for specific delivery of drugs for therapeutic applications in different human pathologies (F. J. Hernandez, Hernandez, Pinto, Schäfer, & Özalp, 2013). The concept of DLNCs relies on introducing a drug into

nanocapsules, followed by an adequate sealing of the structure in order to avoid leakage. Alternatively, the surface of the DLNCs is then functionalized such as to interact specifically with the target location, upon which the drug is released by an external stimulus making the system both controlled and targeted. DLNCs in this way improve drug pharmacokinetics, biodistribution, cell-specific targeting and drug kinetics, resulting in enhanced efficiency and improved tolerability.

Table 4 Summary of Applications of Mesoporous Silica (MS) and Porous Silica Spheres (PSS) Materials (Hanrahan, O’Mahony, Tobin, & Hogan, n.d.)

<b>Application</b>	<b>Thematic Area</b>	<b>Material Type / Product</b>
Quantum confined Nanowire host	Electronics/Energy	SBA-15
Heavy metal Ion removal from waste water	Environmental	SBA-15, SBA-16, MCM-48
Phosphate removal from waste water	Environmental	Metal (e.g. titanium) doped SBA-15
Removal of volatile organic carbon (VOCs) from indoor air	Environmental/Health	PSS
Methanolysis of styrene oxide	Catalysis	Metal (e.g. titanium) doped SBA-15
Improving the bioavailability of poorly water soluble drug molecules	Drug Delivery/ Pharmaceutical formulation	SBA-15
Enzyme encapsulation for bio catalysis	Catalysis	SBA-15 /PSS
Phospholipid extraction from biological matrices	Bio-Analysis/Sample Preparation	Metal doped SBA-15
Incorporation of spherical silica particles in pervaporation membranes for the separation of water from ethanol	Chemical Separation	PSS
Direct air capture of CO <sub>2</sub> by physisorbent materials	Energy	SBA-15

Mesoporous silica nanoparticles (MSN) have some intriguing potential as a DLNC like, having a multifunctional (both diagnostic and therapeutic) usage capability, biocompatibility, size tuning capability and surface functionalization although they are still in pre-clinical stages of development (Mai & Meng, 2013). Mesoporous particles are a type of porous particles with pores having diameters between 2 and 50 nm. Microporous particles are named for smaller diameters (<2nm), while macroporous particles for larger diameters (>50nm) according to the International Union of Pure and Applied Chemistry (Rouquerol et al., 1994). Main building blocks of these particles can be silica, alumina, titanium or zirconium (Figure 5). They can arrange in a crystalline or amorphous manner that can effect its technological usage. These particles have been discovered in 1992 by Mobil Oil Company named as M41S family (Kresge, Leonowicz, Roth, Vartuli, & Beck, 1992) and since then they have been utilized a wide range of applicatinos from photovoltaics to biosensors (Table 4). Mesoporous particles have different production alternatives like; sol-gel method, microwave assisted technique, chemical etching technique and templating approach (S. Kumar, Malik, & Purohit, 2017).

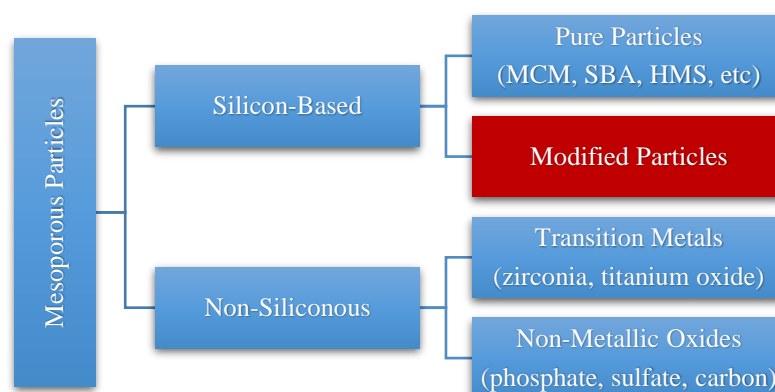


Figure 5 Classification of mesoporous particles based on their material. Nucleic acid-conjugated particles used in this study are classified as modified particles.

Mesoporous particles are preferable for biotechnology since pore sizes are large enough to load molecules, and small enough to be gated. Silica-based particles are preferable for “well defined pore sizes with the known biocompatibility of silica in a range of applications. An important property of a porous silica material is its ability to incorporate functional organics (R) on the silica wall.” (Adam Raw, n.d.).

MCM-41 type (hexagonal) mesoporous silica particles are molecular sieves and specific type of mesoporous particles known as MCM (Mobil Composition of Matter) since they have an array of regular mesopores (Figure 6). In addition to this regularity “pores can be tailored and finely tuned, very high surface area and reactivity, well-defined pore shape with a narrow size distribution, large amounts of internal hydroxyl groups, ease modification of the surface properties, enhanced catalytic selectivity, and excellent thermal, chemical and mechanical stability” (Golezani, Fateh, & Mehrabi, 2016). While cylindrical pore diameter can be ranged between 2 and 50 nm, hexagonal amorphous silica surrounding these pores length results in the range of microns. They can be synthesized by pH-regulated hydrothermal method allowing a degree of control over pore and particle size (Alothman, 2012; Golezani et al., 2016).



Figure 6 Schematic diagram of the M41S materials: MCM-50 (layered), MCM-41 (hexagonal) and MCM-48 (Cubic) mesoporous silica particle structures (Alothman, 2012).



In a recent study conducted by Zhou and his colleagues combined mesoporous silica nanoparticles with gelatin scaffold matrix for sustained and controlled vancomycin release against infected bone defects (X. Zhou et al., 2018). By doing so, they utilized the gelatin matrix for holding the DLNCs in a biodegradable and proper tissue engineering manner and MSNs for compact drug carrier. After observing a 209.8 nm diameter MSN size with TEM, 833.5 m<sup>2</sup>/g surface area and 2.4 nm mesopore size calculated by BET and BJH methods (which have been used in this study for same purposes also) both *in vitro* and *in vivo* efficiency of Van@MSNs/Gelatin fabrication were analyzed. What they concluded was; vancomycin had been still active while in Van@MSNs/Gelatin complex and having a longer duration of effective concentration (62.2% after 3 days) and bone implementation of Van@MSNs/Gelatin complex to artificially bone infected rabbits had showed decreased white blood cell (WBC) concentration indicating after 4 weeks indicating the *in vivo* efficiency. Also they observed no negative side effects on proliferation and differentiation of bone mesenchymal stem cells confirming the biocompatibility of MSNs. There are similar applications of MSNs used in biomedical applications for delivery of drug including antibiotics being reviewed in literature (Z. Li, Barnes, Bosoy, Stoddart, & Zink, 2012). In this study, MSNs was utilized in a similar manner with an addition of targeting and release capability via functionalized nucleic acids.

At this point, it may be appropriate to summarize an non-conventional alternative to fight against microorganisms and resistance mechanisms; antimicrobial aptamers (target affinity-purposed short nucleic acid molecules). While there is an increasing interest in search for more efficient antibiotic delivery constructs, there are also immense attempts to find new antibiotics for clinical usage. However, most of them will be clocked to an ever-shortening life cycle due to resistance. With the emergence of nanotechnological approaches new strategies will be developing. Potential antimicrobial effect of aptamers is worthy of noting. Drugs targeted to gram-negative bacteria have always been in demand, and especially, with the recent increase in the

incidence of multi-drug resistant gram-negative strains, this become an urgent challenge. However, it is very hard to find new agents among traditional sources for this purpose (Silver, 2011). This dilemma can be solved by implementing novel ways to obtain antimicrobial agents. Aptamer technology has a good potential to assist antimicrobial drug discovery since aptamers can be selected according to their antimicrobial properties and used as nucleic acid drugs. Recent research with aptamer sequences for antimicrobial properties together with advanced selection methods presents them as a potentially new source of antimicrobial discovery that can help in overcoming the challenges encountered by traditional discovery methods. Some of the scientific challenges in the discovery of novel antibiotics have recently been described as; i) chemical libraries are limited, ii) gram-negative organisms have a barrier to intracellular accumulation of drug candidates, and iii) the presence of non-selective efflux pumps, charge and size on drug candidate molecules (Silver, 2011). Aptamers have the potential for different mechanisms to exert their antimicrobial actions compared to traditional antibiotics. Since such antibiotic properties of aptamers originates from strong and specific affinity (at picomolar levels) for their target molecules, they can overcome above-mentioned challenges. Aptamers can prevent pathogen growth as a result of a specific binding to surface antigens of microbial cells. Aptamers are obtained through a chemical combinatorial method, which means that selection does not require any prior knowledge about the target pathogen organism. Also, it can be more easily modified or tweaked (changes of sequences around binding motif of nucleic acid sequences in order to fine tuning of aptamer structure) thus at least in theory, can provide faster adaptation to microbial resistance. Therefore, aptamers are attractive alternatives for antimicrobial discovery. Currently there is a need for new antibiotic sources and this demand will continue as long as the phenomenon called antibiotic resistance exists. Thus, targeted antimicrobials based on aptamer can be one of the cost-effective candidates considering *in vitro* selection of such nucleic acids for any kind of microorganisms. However, in the scope of this study, nucleic acid structures being functionalized

according to a specific role – like aptamers – has been utilized in a more specific manner to fight against antimicrobial resistance.

### **1.3 Functionalized Nucleic Acids**

Nucleic acids have been used as a raw material in biotechnological applications. Literature survey gives us two main types of usage based on thermodynamics properties of nucleic acids: ability to interact with its complementary sequences (e.g. siRNA, oligonucleotide sandwich assays (Drolet, Moon-McDermott, & Romig, 1996; X. Liu & Yuan, 2018)) or proteins (binding, cleavage (Frank J Hernandez et al., 2014)), and ability to acquire 3-D shape for affinity (e.g. aptamers (Escudero-Abarca, Suh, Moore, Dwivedi, & Jaykus, 2014) or DNAzymes (W. Zhou, Ding, & Liu, 2017)). Interaction of nucleic acids with cleavage enzymes and ligand affinity of aptamers were utilized in this study. The functionalization of nucleic acids is conducted for two main reasons; addition of other moieties for imaging or drug delivery based on their affinities, and modifications for increasing its properties (e.g. prevention from being cleaved). In this study, both of these functionalizations were utilized for nano-valve development: cleavage of double stranded nucleic acids being modified to gain a privilege to a bacteria-specific nuclease, and an affinity aptamer to a bacteria cell. Both of these functionalized nucleic acids have been used as nano valves to block the pores of silica particles. However both DNA and silica (isoelectric point nearly pI 3) is negative molecules, so blocking capability needs a definition. There has been a paper published specific to this topic. Shi and his colleagues described the surface of silica surface as “a disordered patchwork of hydrophilic and hydrophobic regions” and together with the water molecules near silica and DNA, they proposed ss and ds DNA binding mechanism with free energy calculations (B. Shi, Shin, Hassanali, & Singer, 2015). They also concluded that hydrogen bonding on hydrophilic patches is due to phosphate-silanol interactions and since ssDNA is more attractive than dsDNA as ssDNA is more flexible and has free unpaired bases for hydrogen bonding.

### 1.3.1 Modified Oligo Sequences for Specific Nuclease

Nucleases are nucleic acid cleaving enzymes functioning by hydrolysis of phosphodiester bonds and having a wide variety of roles from DNA repair to cell apoptosis. Also, it can be found extracellularly in bacteria and functioning in biofilm formation of *Vibrio cholera* (Seper et al., 2011) or a virulence factor for pathogenic *Staphylococcus aureus* (Berends et al., 2010). Micrococcal nuclease (MN) is an endonucleolytic cleavage enzyme with a IUBMB Enzyme Commission number of 3.1.31.1 that can hydrolyse double- or single-stranded substrate (Figure 7) (BRENDA, 2017). The enzyme is an extracellular nuclease of *Staphylococcus aureus* with a preference for AT and AU-rich regions as well as TT regions, yielding nucleoside 3'-phosphates and 3'-phosphooligonucleotide end-products (Dingwall, Lomonosoff, & Laskey, 1981).

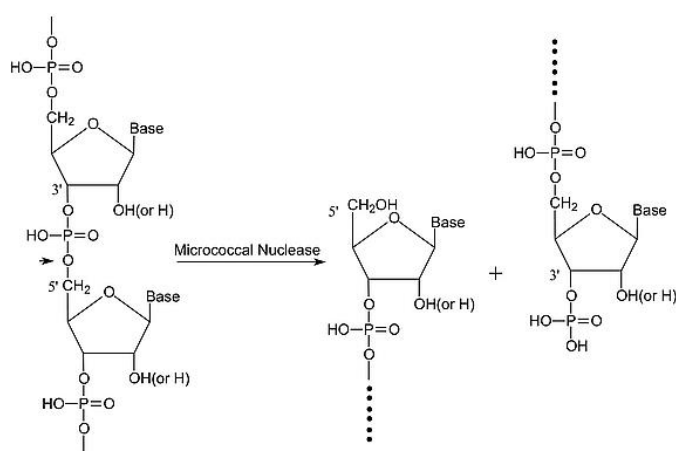


Figure 7 Enzymatic cleavage site of micrococcal nuclease (MN) on nucleic acid sequences (Sigma-Aldrich, 2017a). Sequence specificity of MN was utilized in constructing targeted drug delivery as MN cannot enzymatically cleave the methyl-modified nucleic acids.

It has been found that, MN of *S. aureus* plays a crucial role in virulence of bacteria by acting as a degrading enzyme against neutrophil extracellular traps (NETs). Extracellular traps can be produced by neutrophils, mast cells or eosinophils as an agent of defense mechanism. NETs are basically cellular DNA exposing outside of cell membrane like sticky tentacles and covered with antimicrobial peptides, histones, and cell-specific proteases providing a trap for different stimulus like bacteria, viruses or fungi that triggers a reactive-oxygen-species-mediated signaling cascade of neutrophils (Papayannopoulos, 2017; von Köckritz-Blickwede & Nizet, 2009). Thus, degradation of NETs by MN can be regarded an utilizable property for both diagnosis and therapy specific to *S. aureus*. And it has been utilized by Hernandez and his colleagues for developing novel molecular imaging approach for the specific, non-invasive detection of *S. aureus* based on the activity of its secreted nuclease, micrococcal nuclease (MN) (F. J. Hernandez et al., 2014). A library of chemically modified (LNA, 2'-fluoro- or 2'-O-methyl-modified pyrimidine RNA oligonucleotides) nucleic acid sequences were analyzed according to; resistance to serum nuclease and ability to be cleaved by *S. aureus* MN. Naturally occurring MN in serum does not possess the ability to cleave modified nucleotides such as methyl moiety substitution. And this property has been utilized by engineering oligo nucleotides sequences having a pair of deoxythymidines, between sequences of 2'-O-methyl-modified nucleotides and tested against both serum nucleases (Figure 8a) and bacteria with/without MN activity (Figure b8). Results of the study showed that using this platform, *S. aureus* could be monitored via secreted micrococcal nuclease activity on unmodified dT pair.

The findings of Hernandez are highly advantageous and specific as a diagnostic method; it does not offer a therapeutic option for bacterial infections. However, once an infection has been detected, a therapeutic approach that rapidly provides specific treatment for bacterial infections would be highly desirable. Being an important basis for the platform experimented in this study, the design of the oligo sequence for MN

activity utilization has been detailed in section 3.2.1 as one of the sealing options based on the nuclease activity of MN. The specific cleavage of the enzyme is a stimulus-response for specific targeting and controlled drug release. To demonstrate the applicability of this proof-of-concept study, we have selected *Staphylococcus aureus* as a clinical model of bacterial infection. *S. aureus* is a major cause of human disease, responsible for several conditions such as endocarditis and sepsis and has emerged as a major public health threat, with resistance to a variety of antibiotics (Prosperi et al., 2013).

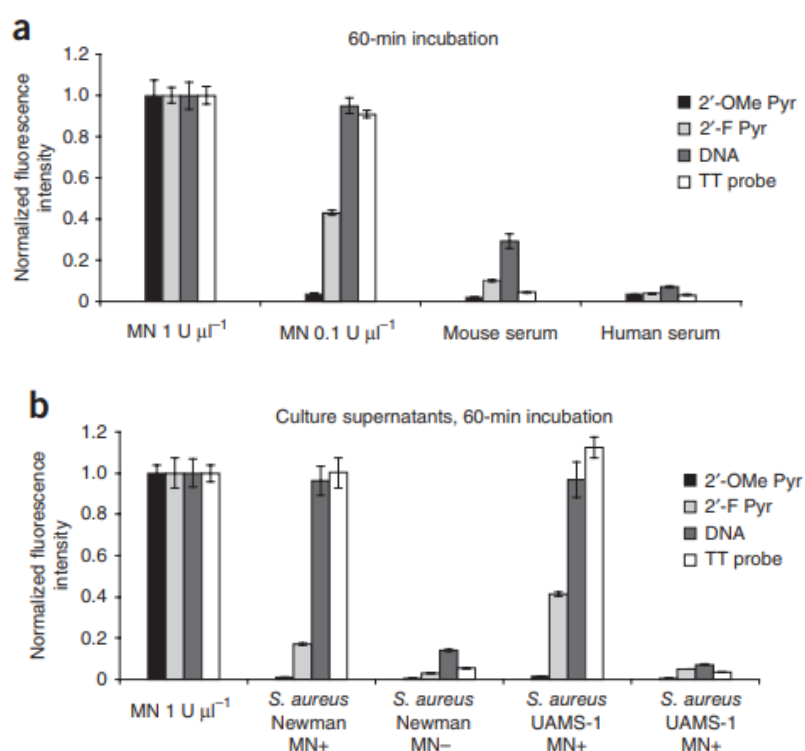


Figure 8 Specificity of different sequences (F. J. Hernandez et al., 2014). a) After 60 min incubation of different probes (1 native and 3 modified nucleic acids) under different conditions, only native DNA and TT probe were detected to be prone to micrococcal nuclease (MN) and DNA probe was also prone to human serum. b) TT probe was proved to be effective in detection of MN+ bacteria strains while performing better resistance to MN- strains than native DNA. The fluorescence readings were normalized with respect to background fluorescence.

Making use of extracellular nuclease is not specific to *S. aureus* and being analyzed in recent studies. For example, endonuclease I has been found the predominant DNase in *E. coli* lysates and experimented as a probe for rapid detection of urinary tract infections (Flenker et al., 2017). Another promising area of extracellular research is cancer research. For example, in breast cancer (BCa) cases “European Molecular Biology Laboratories – European Bioinformatics Institute (EMBL-EBI) database revealed that 143 out of 160 genes that encode putative nucleases are upregulated in BCa cell lines compared with whole blood”, so cancer-derived nucleases can be counted as biomarkers whose signal can be amplified and better alternative than detecting circulating tumor cells (CTCs) (Kruspe et al., 2017). By taking advantage of higher nuclease expression (EXO1, NEIL3, FEN1, DNA2, and ERCC1) in cancer progression three different nuclease-activated probes (dsDNA, ssDNA, 2’F-RNA) were analyzed with fluorescein quenching method against HCC1937 cancer cells. Fluorescence emission readings from fluorescence-quencher disruption in Figure 9 showed that up to 100 cells/mL concentration of cancer cells can be detected by measuring the BCa specific nuclease activity (Kruspe et al., 2017).

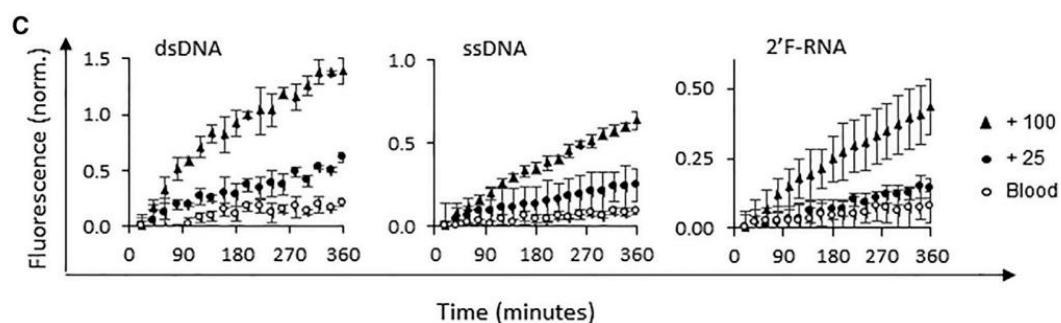


Figure 9 Fluorescence measurements of nuclease-activated nucleic acids coupled with fluorophore-quencher pairs (Kruspe et al., 2017). At 25 cells/mL sample concentration, circulating tumor cells (CTCs) are undetected from control blood samples. However at 100 cells/mL concentration, CTC detection was achieved by tumor cell-specific nuclease activity causing a disruption of quenching mechanism on nucleic acid probes.

It is important to note that this is the pioneer published result about nuclease usage for cancer detection and the nuclease-activated probes had been selected and derived from the same library that was utilized as nanopore sealing in this study (as NanoKeeper01 – NK01 – mentioned in Section 3.2). The literature survey summarized up to now shows that, the functionalization of nucleic acids by modification and usage as an agent for specific nucleases can role a part in the therapeutic approach with antibiotic loaded nanoparticles.

### **1.3.2 Aptamers for Specific Microorganisms**

Another functionalized nucleic acids being optimized on nanoparticles are aptamers. Exploring the nucleic acids for ligand binding molecules has opened a new research area at 1990's, where novel properties are exploited for the development of new analytical types of techniques. Aptamers have been used for developing various kinds of biosensors such as optical, fluorometric, electrochemical etc. Aptamers offer a very interesting alternative to previous widely used bioaffinity materials in diagnostics and also as therapeutic tool for drug delivery systems (Mairal et al., 2008). Since aptamers provide unique superior properties, techniques involving antibodies can potentially be replaced by aptamers in a variety of new configurations.

Nucleic acid aptamers are single-stranded, short and synthetic oligonucleotide sequences with high affinity to specific targets. Naturally, nucleic acid based regulatory elements, called a riboswitch, and contains target binding sequences. They are considered as nucleic acid antibodies with additional advantageous properties for biosensor development. Small size, artificial selection, *in vitro* chemical synthesis for economic production, relatively easy modification, and physical stability are the major superior properties of aptamers over antibodies. Aptamers can be selected in a test tube by a combinatorial procedure using whole cells, extracted membrane or soluble proteins. They are selected from large random sequence pools of libraries *in*



*in vitro* and they are typically short sequences with 15-60 base in length which provides enough diversity to sequences.

The specific affinity originates from unique secondary and tertiary structures. Aptamers are highly specific for structural differences in their targets. For example, the presence or absence of a phosphate group can be detected by ATP binding aptamer (Özalp, Nielsen, & Olsen, 2010; Ozalp, Pedersen, Nielsen, & Olsen, 2010). The completely *in vitro* selection of aptamers is one of the major advantages compared to antibodies that are produced through biological systems. Aptamers can be selected for different conditions whereas antibodies function under physiological conditions. Moreover, chemical synthesis of aptamers provides cost effective and reliable source as affinity molecule. Aptamers are selected following an artificial combinatorial selection method called Systemic Evolution of Ligands by EXponential enrichment (SELEX). The initial procedures were developed for selecting RNA aptamers to organic dyes (Ellington & Szostak, 1990) and to a protein (Tuerk & Gold, 1990). Later, many variations of the original SELEX procedure were developed to improve the methodology according to the requirements of new targets, such as capillary electrophoresis, SPR, AFM or single-bead based procedures. Briefly, single stranded DNA or RNA library is contacted with a desired target. Typical library complexity consists of  $10^{12}$ - $10^{16}$  different sequences. The random part of library members is usually 40-100 base long with fixed primer sequences at both end facilitating PCR amplification. The target-bound sequences are separated from unbound members via a chosen affinity separation method. The bound sequences are PCR-amplified and converted into single strand (Marimuthu, Tang, Tominaga, Tan, & Gopinath, 2012). Subsequently, this single strand is incubated with fresh target in the next cycle. This SELEX cycle is repeated as many as 20 times to obtain high affinity pools of sequences. The identity of members of DNA pools is obtained through cloning and sequencing techniques. Finally, aptamers are determined through sequence motif search and further affinity experiments. Although the aptamer selection procedure is

straightforward, improvements are being emerged such as SOMAmers (slow off-rate modified aptamers) partly because of some challenges in aptamer selection (Kraemer et al., 2011). For example, there should be at least one aptamer sequence for any target; however in practice failures are common in aptamer selection in laboratory settings. Mayer *et. al.* reported a 50% success rate in their attempts of selection for more than 300 selections on homogeneous targets (Mayer et al., 2010). A report documented that about 35 % of 900 aptamers in literature was DNA and the rest RNA aptamers (Cruz-Toledo et al., 2012). The targets ranged from dye molecules, toxins, nucleotides, peptides, proteins to whole virus particles and cells.

Traditional SELEX procedures have suffered from a significant drawback in that many of the cell surface receptors are extremely difficult to purify due to their hydrophobic properties. Even those that can be successfully purified may not retain their native conformation when immobilized for affinity separation, leading to non-functional aptamers that cannot recognize the natural structure of proteins as expressed on living cells. A promising approach in obtaining cell specific aptamers is a recent adaptation of traditional selection methodology. Cell-SELEX identifies aptamers by using whole cells as target during selection procedure and by a negative subtraction to eliminate common binders. This procedure has become quickly popular to obtain cell-specific aptamers that are essential in developing drug targeting systems since pathology modifies normal cell to have marker properties which can easily be used for selecting aptamers (Ozalp et al., 2010). Cell-SELEX is commonly used to obtain cancer cell-specific or bacteria-specific aptamer sequences, but the specific targets usually remain undefined due to the nature of the procedure (West, Isotta-Day, Ba-Break, & Morgan, 2016).

Figure 10 is a schematic representation of a typical cell-SELEX approach for obtaining serotype-specific aptamer sequences (Figure 10A). SELEX cycle consists of four main steps; incubation with target, affinity separation, negative selection and

finally amplification of target-bound sequences through PCR (Figure 10B Affinity separation for a bacterial cell in detail). Table 5 is a list of aptamers that are selected using whole microorganisms as target.

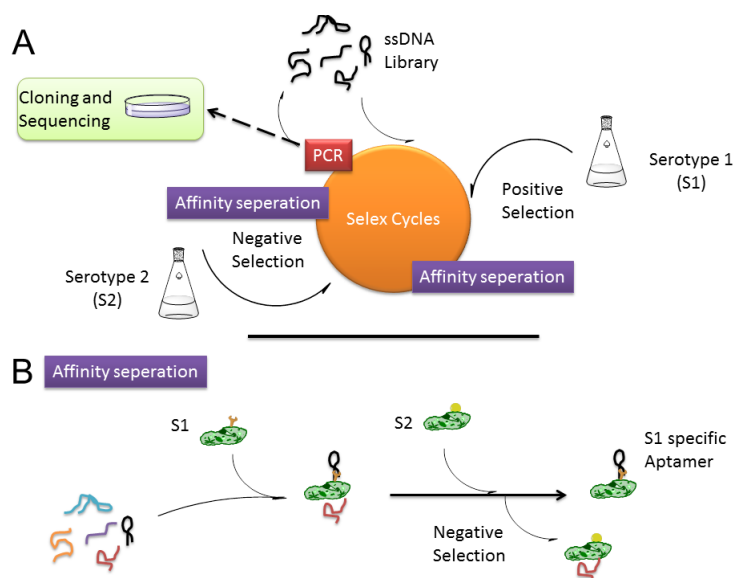


Figure 10 Main steps in a typical Cell-SELEX for serotype-specific aptamer enrichment. With combinatorial selection method of ssDNA from the library against a target and negative selection against negative control followed by a PCR amplification completes a one cycle of SELEX. Obtaining new ssDNA library from the previous cycle makes the beginning of a new cell-SELEX cycle.

The availability of cell-specific antigens is essential to develop any microorganism targeting system since the pathology modifies normal cell to have marker properties which can easily be used for aptamer selections (J. Zhou & Rossi, 2011). Antibodies have recently been the standard affinity molecule in a wide range of applications. Aptamers emerged as a class of affinity molecule that can replace antibodies in both diagnostic and therapeutic applications (Jayasena, 1999). Aptamers are excellent binding elements in sensing and diagnosis due to several inherent characteristics.

Table 5 Examples of aptamers recognizing live microorganisms. There are various DNA and RNA aptamers for various pathogenic microorganisms and viruses.

<b>Microorganism</b>	<b>Aptamer</b>	<b>Ref.</b>
<b>Gram negative Bacteria</b>		
<i>Campylobacter jejuni, A9a</i>	DNA	(Dwivedi, Smiley, & Jaykus, 2010)
<i>E. coli</i>	<i>O157:H7</i>	RNA (Lee, Han, Maeng, Cho, & Lee, 2012)
	<i>O111</i>	DNA (H. Li et al., 2011)
	B4	DNA (targeting lipopolysaccharide, (LPS)) (J G Bruno, Carrillo, & Phillips, 2008)
<i>Salmonella</i>	<i>O8</i>	DNA (G. Liu et al., 2012)
	<i>enteritidis</i>	RNA (Hyeon et al., 2012)
	<i>enterica, typhimurium</i>	DNA (Joshi et al., 2009)
	<i>enterica, typhimurium</i>	RNA (targeting type IVB pili) (Pan et al., 2005)
<i>Vibrio parahemolyticus</i>	DNA	(Duan, Wu, Chen, Huang, & Wang, 2012)
<b>Gram positive Bacteria</b>		
<i>Listeria monocytogenes</i>	DNA (targeting internalin A (InIA))	(Ohk, Koo, Sen, Yamamoto, & Bhunia, 2010)
<i>Staphylococcus aerus</i>	DNA	(Cao et al., 2009)
<i>Streptococcus pyogenes</i>	DNA (targeting M-type antigens)	(Hamula, Le, & Li, 2011)
<b>Bacterial Spore</b>		
<i>Bacillus anthracis</i> (nonpathogenic Sterne strain) spores	DNA	(John G Bruno & Carrillo, 2012)
<b>Virus</b>		
Vaccinia virus	DNA	(Labib et al., 2012)
Influenza A virus subtype H5 (H5N1)	RNA (Targeting virus envelope protein, Hemagglutinin (HA))	(S. Y. Park et al., 2011)
Influenza A virus subtype H9 (H9N2)	DNA (Targeting HA)	(Choi et al., 2011)
Herpes simplex viruses (HSV)	RNA (Targeting gD protein)	(Gopinath, Hayashi, & Kumar, 2012)
Herpes simplex viruse type 2(HSV-2)	DNA (Targeting gD protein)	(Moore et al., 2011)
Human immunodeficiency virus (HIV) type I	(Targeting gp120 envelope glycoprotein)	(Khati et al., 2003)

Comparative experiments proved that aptamers can successfully substitute antibodies in many formats including microarray (Lübbecke, Walter, Stahl, & Scheper, 2012), and aptamers are ideal bioaffinity molecules for intracellular targets due to their relatively small size, low cost, easy handling and possibility of chemical

modifications. First, artificial selection is a powerful *in vitro* technique providing aptamers for potentially any target and moreover to a specific region of the target. Moreover, DNA aptamers are relatively more stable than antibodies, which means they can survive in extreme conditions like high temperature (Liss, Petersen, Wolf, & Prohaska, 2002) and extreme pH values (Deng, Watson, & Kennedy, 2003), or high salt concentrations.

However, DNA aptamers in biological environments require the consideration of nucleases ubiquitously found in blood and intracellular environments. In this respect, microorganism can be a source of environmental nucleases. Various nucleic acid stabilization methods have been explored and successful results have been obtained especially with spielmegers (L-enantiomers of nucleic acids) (Boisgard et al., 2005) and secondary modifications (e.g., 2'-amino-, 2'-fluoro-) (Kubik, Bell, Fitzwater, Watson, & Tasset, 1997; Kujau & Wöfl, 1998; Padilla & Sousa, 1999). Locked nucleic acids (LNA) or UNA modifications recently proposed as a way to overcome nuclease susceptibility (F. J. Hernandez, Kalra, Wengel, & Vester, 2009; Veedu & Wengel, 2009).

Spielmege oligonucleotides are enantiomers of natural RNA and DNA molecules, from which aptamers possess the chemical properties. Selection of spielmeger requires elaborate methods compared to selection of aptamers because not only the oligonucleotides should be enantiomer, but also the targets be the equivalent mirror image. The D-enantiomers of proteins are currently very limited due to limitations in peptide synthesis. Thus, spielmegers were mostly selected for cytokines and short peptide hormones. However, protein spielmeger aptamers were selected for bacterial enterotoxins and cardiac troponin I by taking advantage of the fact that aptamers recognize only short domains of amino acid motifs (F. J. Hernandez et al., 2013). Locked nucleic acids (LNAs) is one of the most promising modified nucleotides strategies for increasing thermal and nuclease stability of nucleic acids. LNA is

initially developed as a derivative of RNA with a methylene bridge. The conformational flexibility is reduced by this bridge composed of a connection between the 2'-oxygen of ribose and the 4'-carbon which results in a locked 3'-endo conformation. An LNA-based aptamer diagnosis probe was constructed to improve the detection in biological fluids and to enhance the imaging properties (H. Shi et al., 2014). A *posteriori* modification of Ramos cell binding aptamers sequences (TD05) was prepared by adding 7 LNA and 3'-3'-T capping. The imaging ability of DNA/LNA chimera probe was tested in cell culture, serum and *in vivo* on Ramos cell implanted mouse models. The LNA incorporation was demonstrated to increase the stability of the probes at least ten times (H. Shi et al., 2014). The strategy of increasing stability of aptamers could be applied with greater efficiency by obtaining aptamer sequences consisting of solely LNA nucleotides. The major obstacle for achieving an LNA aptamer is the availability of a polymerase that can amplify LNA sequences. In fact, a recent discovery of such polymerases that can amplify LNA triphosphates was demonstrated and also a scheme for amplifying and re-generation of LNA-containing oligonucleotide libraries were proposed (Doessing, Hansen, Veedu, Wengel, & Vester, 2012; Dubois, Campbell, Edwards, Wengel, & Veedu, 2012).

The modifications usually should be applied *a priori* to the SELEX procedure rather than *a posteriori*. However, unnatural nucleic acids increase the cost of final application. On the other hand, nanoparticle conjugated aptamers have been reported to increase stability of aptamers to nucleases other than specific added properties (Zwanikken, Guo, Mirkin, & Olvera de la Cruz, 2011). In summary, aptamers are potentially alternative affinity reagents to antibodies in analytical applications due to low immunogenicity, rapid *in vitro* selection procedure, stability and relatively low cost of production. In this study, aptamers were utilized as their natural form for proof-of-concept analysis as detailed in Section 3.3.

## 1.4 Utilization of Nanoparticles for Detection and Therapy

There have been reported many nucleic acid targeted drug delivery examples for sensing or therapeutical purposes. The development of imaging probes aims to improve specificity and sensitivity of diagnostic tools through non-invasive and quantitative detection of specific biomolecules in tissues. A promising class of molecular imaging probes consists of nanoparticles (NPs) functionalized with a certain targeting agent. The aptamers-nanomaterial conjugates are of particular interest due to the unique properties of nanomaterials such as small size, increased surface-to-volume ratio, and a wide range of sensing formats, including metal and semiconductor core materials. To date, nanomaterials can be easily grafted with aptamers via direct covalent linkage or by non-covalent interactions. Gold nanoparticles (AuNPs) have widely been used in medical diagnosis due to their simple synthesis and unique spectral properties (e.g. surface plasmon producing). AuNPs can be synthesized from chemical reduction of AuCl<sub>4</sub> ions by agents like citric acid, and their size can be precisely controlled to have homogeneous particles with diameters in nanometer scales. AuNPs conjugated with aptamers have been extensively utilized in the medical diagnostics and imaging. The distance-dependent fluorescence quenching behaviour of AuNPs provides a tool of detection of the biomolecular interactions in close proximity. In addition to strong extinction peak in the visible and near infrared regions (Cho, Glaus, Chen, Welch, & Xia, 2010), gold nanoparticles ability to penetrate through tissue and easy surface modification make them convenient component of *in vitro* and *in vivo* systems (Ajnai et al., 2014). However, these favorable properties can be efficiently exploited if a targeting mechanism can be used in conjugation with gold nanoparticles. Aptamers can easily be conjugated to AuNPs via covalent binding through thiol moiety. For *in vitro* imaging and detection, Au particle aggregation was triggered with aptamer target interaction in order to develop a simple method for the detection of platelet-derived growth factors (PDGF) (Chang, Wei, Wu, Lee, & Lin, 2013). With the presence of PDGF, aptamers having

specificity and affinity to PDGF bind them and change conformation allowing partial-complementary probe to release from gold nanoparticles and conjugate with aptamers. Gold nanoparticles bind to DNA probes and aggregate in the solution, resulting in a change in their absorption spectrum that can be visually detected. Another research based on the aggregation of AuNPs was carried out for p53 tumor marker with its specific aptamer (Shwetha, Selvakumar, & Thakur, 2013). The sensitivity of detection was increased 10-fold by coupling aptamer affinity with the catalytic potential of AuNP with a chemiluminescence reaction. For *in vivo* imaging purposes, polyethylene glycol (PEG) are generally incorporated in order to increase stability and circulation time of aptamer-conjugated gold particles (Murphy et al., 2008). Gold nanoparticles were also coupled with aptamers noncovalently for the detection of analytes. For example, electrochemical sandwich assay was developed using screen-printed carbon electrode strips (Yeh et al., 2014).

The cellulose-derived polymer showed promise for drug delivery by combining cancer cell specificity of EpCAM aptamers and imaging capability of magnetic nanoparticles via MR imaging. Fluorophore-labelling of aptamers conjugated to magnetic nanoparticles is another popular design in developing diagnostic systems. Since polyA sequence has a strong affinity to gold nanoparticles and FAM fluorophore molecule, iodide or thiosulfate ions can act as displacing agent to separate polyA-tailed aptamer strands from AuNP and simultaneously activate the AuNP-quenched fluorophores by destroying the polyA-AuNP interaction.

A research team has developed a electrochemical aptamer platform for *Salmonella* spp. by using graphene (Ma et al., 2014). In this platform, glassy carbon electrode is modified with graphene oxide and aptamers specific to *Salmonella* were immobilized through AuNPs. Cyclic voltammetry measurements have shown that up to 3 CFU/mL can be detected. In another study, dual-aptamer-based sandwich system for the detection of *S. aureus* was reported based on detection of silver nanoparticles with



anodic stripping voltammetry (Abbaspour, Norouz-Sarvestani, Noori, & Soltani, 2015). In order to detect one of the most important human pathogens, *S. aureus*, the aptamers were conjugated to magnetic nanoparticle for easy isolation, and another aptamer sequence was conjugated with AgNP for signal amplification in electrochemical stripping voltammetry read-out. However, whether the target is a cancer cell or a pathogenic bacteria, the diagnosis can not always be coupled with therapy.

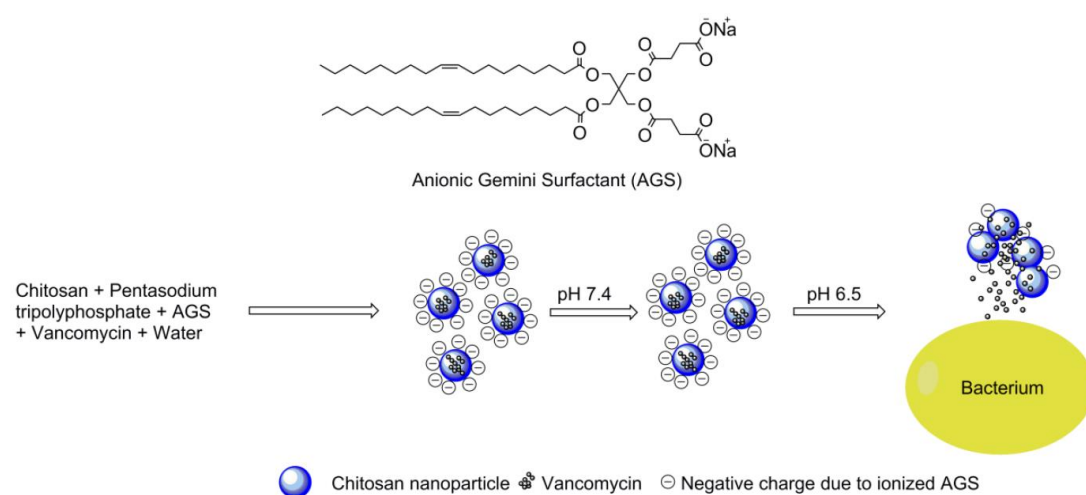


Figure 11 pH-responsive chitosan nanoparticles encapsulating vancomycin (Kalhapure et al., 2017). Vancomycin was encapsulated by chitosan nanoparticles and sealed by pH responsive AGS molecules. Change in the environmental pH causes the release of vancomycin molecules providing a target mechanism with a limited precision.

Some bacteria like cariogenic bacteria and *Staphylococcus aureus* decrease the pH in their surroundings allowing to develop a strategy for drug delivery. pH-responsive chitosan nanoparticles encapsulating vancomycin was studied against methicillin-resistant *S. aureus* (MRSA) (Kalhapure et al., 2017). Surface of chitosan was functionalized with anionic gemini surfactant (AGS) as twin-chain anionic

amphiphile (oleic acid with 2,2-dimethyl-5,5-bis(hydroxymethyl)-1,3-dioxane) making the particle pH-responsive (Figure 11). *In vitro* studies with MRSA gave a 8-fold decrease in MIC of AGS-chitosan-vancomycin complex (with a size of vancomycin loaded nanoparticles were measured 277nm with 32% vancomycin entrapment efficiency) at pH 6.5 (7.81 µg/mL) than pH 7.4 (62.5 µg/mL).

A limitation of existing DLNCs summarized in Section 1.2 is the fact that most stimuli-response delivery systems use bulk stimuli, including: light, magnetic field, ultrasound and pH (F. Tang, Li, & Chen, 2012). These stimuli are passive and non-specific approaches. Enzyme activity (mostly proteases) has been reported as alternative stimulus for controlled-drug release approaches, (F. Tang et al., 2012), however, the instability of peptides in physiological conditions (non-targeting proteases) may be an issue for peptide-based approaches. For example, it has been reported that only one protease, cathepsin L, is able to cleave more than a third of the human proteome, (Sée et al., 2009) indicating that unspecific degradation is expected for peptide-approaches.

In studies aimed to increase the targeting and efficiency of the drug delivery systems, the usage of mesoporous silica particles have started to increase. A team of researchers experimented a nanocapsule-mediated drug delivery by combining nucleolin aptamer with mesoporous silica particles encapsulating fluorescein. Nucleolin is an highly expressed protein on the surface of proliferating cancer cells, that makes the protein an ideal signboard for targeting. AS1411, 26-base DNA aptamer for nucleolin, was modified with 7-base sequence addition to 5'end for additional flexibility acting like hinge. With covalent binding of modified AS1411 on mesoporous silica nanoparticles (MSN) and allowing the aptamer to lock fluorescein dye inside MSN's via nonspecific affinity between nucleic acids and silica surface, drug loaded nanoparticle (DLN) platform was created. Observation of the DLN's interacting with nucleolin positive MDA-MB-231 cells under fluorescent microscope revealed that, release of

fluorescein occurred only in the presence of nucleolin and this interaction also triggered endocytosis of DLN's being about 190nm in size (F. J. Hernandez et al., 2013).

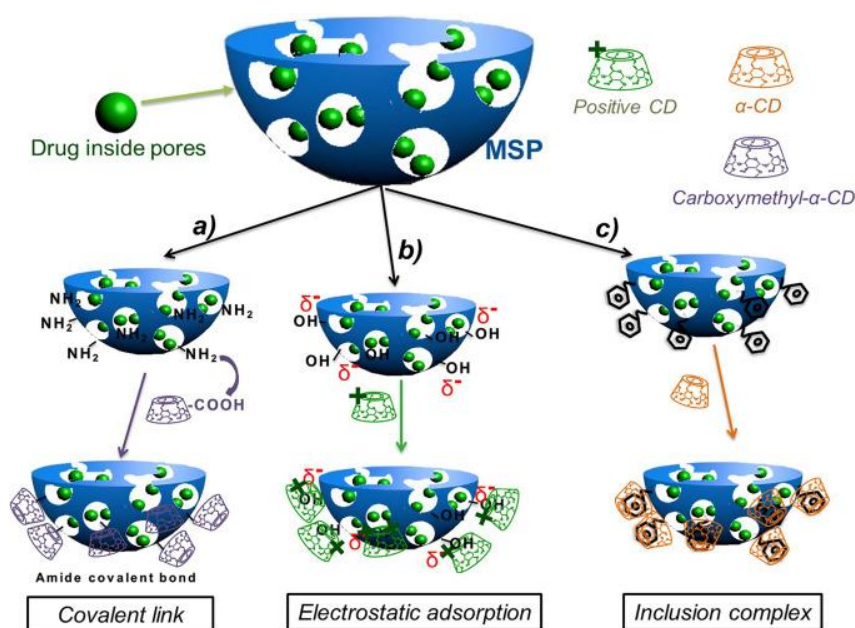


Figure 12 Cyclodextrin-Mesoporous Silica Particles (CD-MSP) drug delivery system with different linkage (Stjern et al., 2017). Three different sealing mechanisms were studied: covalent linking, electrostatic adsorption and inclusion complex formation.

In another study, silver core-embedded mesoporous silica nanoparticles (Ag-MSN) were synthesized in order to target antibiotics in drug-resistant infections (Wang et al., 2016). With this mechanism, both  $\text{Ag}^+$  and antibiotic can act synergistically against bacteria. The nanoparticle system was tested against model organisms of *E. coli* GN102 and *K. pneumoniae* 39 both of which are insensitive to tolevofloxacin hydrochloride (LEVO). By incorporating LEVO to Ag-MSN, researchers achieved to decrease MIC 20% according to LEVO alone proving the usage of nanoparticles as a shelf-life extender for current diminishing antibiotics. Other studies focused on

application areas of MSNs similar to this study. Instead of nucleic acids, cyclodextrin molecules can be used as gates of MSN pores. One such research was conducted (Stjern et al., 2017). Visualizing in Figure 12, cyclodextrin molecules combined with MSNs in three different ways for comparing its sealing capability against two different drugs; small/hydrophilic metronidazole and large/hydrophobic clofazimine. The study revealed that, metronidazole was best sealed with covalent linkage of cyclodextrin and co-loading of drugs showed a better sustained release possibly due to different size and hydrophilicity of drugs had been creating different bonding inside of MSNs. However, cyclodextrin in this study blocked the pores in a passive manner without any help for targeting of drugs.

Recent studies show that there is a trend trying to decrease the size of the nanoparticles for increased bioavailability during both imaging and therapeutic operations. One of which was conducted for developing a  $\beta$ -glucan-conjugated silica nanoparticle (SiNP) for delivering of tuberculosis drug, isoniazid (INH) (Hwang et al., 2018). The size of developed SiNP was 50nm allowing the cargoing of small molecules FITC, DOX as well as INH. And  $\beta$ -glucan conjugation stimulates the immune system thus coupling with the drug delivery. Such examples and reviews about nanoparticle usage for diagnosis and drug delivery from the literature can be extended (Khan, 2017; Wilczewska, Niemirowicz, Markiewicz, & Car, 2012). Nearly all of them have tried to propose alternative and innovative solution to similar challenges: better diagnosis for specific targeting and better therapy against specific agents. In this study, same expectations were tried to address with combination of and comparison of some strategies.

## **1.5 Aim of Study**

The present situation, challenges and the possible scientific solutions to the problem of antibiotic resistance of microorganisms have been summarized in the clauses

above. Under the scope of this study, development and efficiency of incorporation of functional nucleic acids on drug loaded nanocapsules for both selanig and specific targeting strategy was experimented. The strategy researched to combat with antibiotic resistance is basically based on targeting the delivery of antibiotics via alternative usage of bacteria-specific aptamers and MN activity-specific modified nucleic acids functioning as gates for release of antibiotics on silica-based drug carriages. Thus it is hypothesized that, whether targeted administration of antibiotics can lower the amount of drug usage and subsequently lower the antibiotic resistance due to uncontrolled drug usage with respect to non-targeted drug administration. As a proof-of-concept, *Staphylococcus aureus* was used as a model pathogen, *Staphylococcus epidermidis* was used as a control organism for specificity analysis. Vancomycin was used a model antibiotic known to be effective to both microorganisms, Rhodamine B was used as fluorescent dye for release experiments and for showing the diagnostic potential of the proposed system. MCM-41 (hexagonal pore opening) type mesoporous silica particles (as nanocapsules) was used a carrier for antibiotics and functionalized nucleic acids used as nanovalves for capping the nanocapsule and controlling the release of antibiotics.



## CHAPTER 2

### MATERIALS AND METHODS

#### 2.1 Materials

MCM-41 type (hexagonal) mesoporous silica particles were purchased from Sigma-Aldrich (Sigma-Aldrich, Ankara, Turkey). The properties of the particles were given by the supplier as follows; the unit cell size: 4.6-4.8 nm; pore volume: 0.98 cm<sup>3</sup>/g; pore size: 2.3-2.7 nm; spec. surface area: ~1000 m<sup>2</sup>/g (BET); bp: 2230°C; mp: >1600°C and bulk density: 0.34 g/mL. Micrococcal nuclease from *Staphylococcus aureus* (CAS number: 9013-53-0), Rhodamine B (CAS number: 81-88-9), (3-Mercaptopropyl)triethoxysilane (CAS number: 14814-09-6), vancomycin (CAS number: 1404-93-9) and all other chemicals were purchased from Sigma-Aldrich. Sulfo-GMBS (CAS number: 185332-92-7) was from Fisher Scientific. The oligonucleotides were synthesized by IDT DNA (Germany). The DNA sequences used in this study are given below in Table 6. The aptamer sequences was as reported in another study (Cao et al., 2009).

#### 2.2 Methods

##### 2.2.1 Characterization of Mesoporous Silica Particles

The particles used in this study were characterized by transmission electron microscopy (TEM). The samples were prepared by ultra-sonication of powders of mesoporous silica particles in ethanol for 5 min and drying of a droplet of suspension

on a standard holey carbon TEM grid. TEM analysis was carried out on Titan 60–300 electron microscope (FEI, Netherlands) operating at 300 kV in TEM mode (CIC NanoGune, San Sebastian, Spain). The average diameter of particles was determined by dynamic light scattering (DLS) with a Zetasizer ZEN 3600 Nano-ZS, (Malvern Instruments, Worcestershire, UK) (Yıldız Teknik University, MERKLAB). 2 mg MCM-41 particles were suspended in PBS buffer (0.01 M phosphate buffered saline; 0.138 M NaCl; 0.0027 M KCl; pH 7.4) for DLS investigation. Large aggregates of particles were first removed by low speed centrifugation at 500 rpm for 30 seconds with Sigma 3-18K (Sartorius AG, Göttingen, Germany) and the supernatant was used in DLS experiments. The average size was determined to be 183 nm.

Table 6 Probe, oligo and aptamer sequences. TT Probe was adapted from another study, NK01 probe is a modified version of TT probe, NK01 and NK02 oligo strands were used as model and control gating mechanisms. SA20, 23 and 34 aptamer sequences were adapted from another study. SA20-amino aptamer was used as aptamer-based gate development.

<b>TT probe</b>	5'- FAM- mCmUmCmGTTmCmGmUmUmC- ZEN-RQ -3'
<b>NK01 probe</b>	5'- FAM - TTmCmGmCmUmUmCmGmGmCmGmAmA- ZEN-RQ -3'
<b>NK01 oligo</b>	5'- NH <sub>2</sub> - TTmCmGmCmUmUmCmGmGmCmGmAmA -3'
<b>NK02 oligo</b>	5'- NH <sub>2</sub> -UmUmmCmGmCmUmUmCmGmGmCmGmAmA -3'
<b>SA20-hp</b>	AF488-GCGCCCTCTCACGTGGCACTCAGAGTGCCGGAAGTTCTGCGTTAT-(PEG)-AGGGCGC-BH1
<b>SA23-hp</b>	AF488-GGGCTGGCCAGATCAGACCCCGGATGATCATCCTTGTGAGAACCA-(PEG)-CCAGCCC-BH1
<b>SA34-hp</b>	AF488-CACAGTCACTCAGACGGCCGCTATTGTTGCCAGATTGCTTTGGC-(PEG)-GACTGTG-BH1
<b>SA20-amino</b>	NH <sub>2</sub> - GCGCCCTCTCACGTGGCACTCAGAGTGCCGGAAGTTCTGCGTTATAGGGCGC

NK01 and NK02 are NanoKeeper01 and 02 respectively. FAM and AF488 function as fluorescence while ZEN-RQ and BH1 are quenchers respectively. "m" represents 2'O-Methyl modification. Red colored nucleotides: added nucleotides complementary to 5' end for hairpin formation.

Brunnauer, Emmett and Teller (BET) surface analysis determines internal and external surface area and pore sizes (Quantachrome BET analyser, Yıldız Teknik



University, MERKLAB). About 100 mg of MCM-41 particle were used in the analysis. About 0.0906 g of MCM-41 powder was analyzed for 878.3 min (outgas time: 20 h at out gas temperature of 50°C).

### **2.2.2 Synthesis of Probe-Capped Particles**

The surface of MCM-41 particles was grafted with nucleic acid probes as described previously (Özalp & Schäfer, 2011) and detailed below as silanization, loading and capping steps.

#### **2.2.2.1 Silanization of MCM-41 Surface**

First step of probe-capped particles is silanization. This step was achieved by adding dry 50 mg of MCM-41 type silica particles to 20 ml 95 % EtOH at pH 3.8-3.9, which is prepared by adding 1 mM acetic acid and then mixing (3-Mercaptopropyl)triethoxysilane to 3 % (w/w) concentration. The mixture was stirred for 30 min at room temperature, followed by three-fold washing with ethanol by centrifugation (13,000 x g, 3 min).

#### **2.2.2.2 Loading and Capping of MCM-41 Particles**

The sulfhydryl-modified nanoparticles (1 mg) were loaded with vancomycin (100 µM) or Rhodamine (100 µM) by incubation in the corresponding solution in PBS buffer (0.01 M phosphate buffered saline; 0.138 M NaCl; 0.0027 M KCl; pH 7.4) overnight and used for 5 coupling reactions with amine-modified oligonucleotides (NK01, NK02 or aptamers). 2 mg/ml sulfo-GMBS (Sulfo-N-succinimidyl 4-maleimidobutyrates) were mixed with the sulfhydryl-modified nanoparticles in 0.01 M PBS buffer and stirred for 30 min. Next, the modified nanoparticles were washed 3 times with 0.01 M PBS buffer and followed by 1 hour incubation under stirring

conditions in 100  $\mu$ M solution of amine-modified oligonucleotide (50 nmol in 500  $\mu$ L 0.01 M PBS buffer containing either 100  $\mu$ M Rhodamine or 100  $\mu$ M vancomycin). Then, particles were washed three times with 0.01 M PBS buffer. Loading amount of Rhodamine molecules was estimated by measuring the fluorescence levels in particles samples with FS920 steady-state spectrofluorimeter from Edinburgh Instruments (Edinburgh, Scotland, UK) and by using a calibration graph and loading of vancomycin from the absorbance values at 280 nm. The amount of oligonucleotides immobilized on the surface of silica particles was calculated from absorbance values at 260 nm in a UV-VIS spectrophotometer (Nanodrop 2000, Thermo Scientific, Willmington, USA). For a typical preparation,  $10.4 \pm 1.8$  pmol oligonucleotides were immobilized per mg of particles. Coverage was estimated to be 48,760 probe molecules on average per nanoparticle, which corresponds to about one probe per 2.2 nm<sup>2</sup> of particle surface.

### **2.2.3 Release Experiments**

Release of Rhodamine dye from pores was followed by fluorescent spectrophotometric analysis (Nanodrop 3300, Thermo Scientific, Willmington, USA) at excitation of 535 nm and emission was recorded at 565 nm. Similarly, the release of vancomycin was measured by UV-VIS spectrophotometry (Nanodrop 2000, Thermo Scientific, Willmington, USA). The mesoporous silica particles capped by the probe molecules were stirred in a magnetic stirrer. The particles were trapped in dialysis membrane compartment (cellulose-based membrane at molecular cut of 12,000 Da) at the top of spectroscopy cuvette. Silica particles were large enough to be completely retained by dialysis membrane. A design of a two-compartment cuvette by using dialysis membrane was previously described in detail (Özalp & Schäfer, 2011) and graphically represented in Figure 13. All particles loaded with their cargo were washed extensively with PBS buffer before use. A typical nanoparticle leaked about 20% of its loaded cargo before a leak-free capping achieved.

The loading capacity of the particles with Rhodamine or vancomycin was determined by using 1 mg mixture of oligonucleotide capped silica particles in 0.01 M PBS buffer. Fluorescence or absorbance were recorded in a thoroughly mixed solutions. The amount of fluorescein released into the buffer was quantified by using a fluorescein calibration curve or absorbance standard curve. For a typical experiment, the maximum loading of Rhodamine dye was calculated to be 14.1 pmol/mg particle and the maximum loading of vancomycin to be 15.5 pmol/mg.

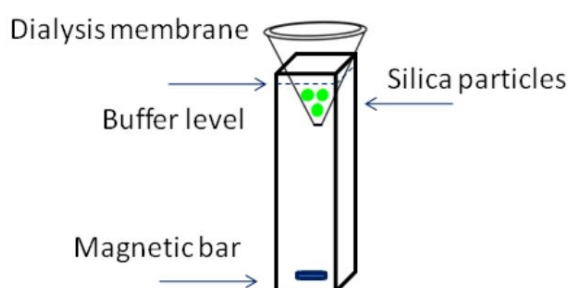


Figure 13 Experimental setup for release kinetics of nanoparticles (Ozalp & Schafer, 2011). Silica particles were placed inside a dialysis membrane which was placed at the top of a spectroscopy cuvette with 4mL volume and submerged in a 0.01M PBS. A small magnetic stirrer was used to mixed the content of the cuvette. Samples were taken with desired intervals for measurement

#### 2.2.4 Bacterial Cultures

The bacteria (*Staphylococcus aureus* (ATCC 29213) and *Staphylococcus epidermidis* (ATCC 2222)) were prepared by growing an inoculation from frozen stocks in a duration of 16 hours at 37 °C in commercially available tryptic soy broth (TSB) from Sigma-Aldrich having product code 22092 (St. Louis, Missouri, USA) by using 250mL Erlenmeyer flask and Hei-MIX 1000 Orbital Shaker and Incubator at 200 rpm speed (Heidolph AG, Schwabach, Germany). The targeted concentrations of bacterial

cultures were obtained through 1:9 serial dilutions by using 0.01 M PBS buffer. The colony counting experiments were performed by spreading 100  $\mu$ L diluted bacteria culture samples on agar plates of TSB via sterile glass beads from Paul Marienfeld GmbH (Lauda-Königshofen, Germany), growing overnight and then recording by counting the single colony forming units.

### **2.2.5 Antibacterial Activity**

Minimum inhibitory concentration (MIC) values of administered vancomycin were determined according to Clinical and Laboratory Standards Institute broth microdilution method M7-A7 (Clinical and Laboratory Standards Institute, 2006). The microdilution plates were incubated at 37 °C for 24 h and then the optical density of each well, at 600 nm (OD600), was determined with a spectrometer plate reader (EZ Reader). The dilution was performed with two-fold dilutions starting with 512  $\mu$ g/mL vancomycin concentrations. The MIC was determined in triplicate for each bacterial isolate. OD600 data (bacterial growth) were fitted by the Gompertz equation to calculate the MIC. Time-kill curve were conducted by overnight cultures diluted to yield an inoculum of  $10^3$  CFU/mL. The antibiotic concentrations used were equivalent to MIC for vancomycin. After 0, 3, 6, 12, 18 and 24 h of incubation in a shaking water bath at 37 °C, serial dilutions of 100  $\mu$ L samples were sub-cultured onto agar plates via sterile glass beads and incubated at 37°C for 24 h before CFU were counted.

The Gompertz model is widely used in many aspects of biology. It has been frequently used to describe the growth of animals and plants (fish, bird growth etc), as well as the number or volume of bacteria and cancer cells. It is extensively reviewed in a recent article (Tjørve & Tjørve, 2017). The Gompertz model is a sigmoid model and a special case of the four parameter Richards model, along with familiar models such as the negative exponential, the logistic, and the von Bertalanffy. The parameters describing Gompertz model are as follows:

- biometric measurements as functions of time;  $W(t)$ .
- survival:  $S(t)$ ,
- number of cells/bacteria or population size:  $N(t)$ ,
- density of cells or microorganisms;  $D(t)$ ,
- concentration of organisms  $C(t)$ ,
- volume  $V(t)$ ,
- body mass:  $M(t)$ ,
- length:  $L(t)$ .

The dependent variable (left hand side of the equation) can also be stated as relative values, for example given as  $W(t)/A$ , where  $A$  is the upper asymptote, or  $W(t)/W_0$ , where  $W_0$  is the initial value (or starting point on the x-axis). The latter then represents the value relative to the starting value. Sometimes the dependent variable is log-transformed, in particular when modelling microbial growth. Gompertz calculations were conducted in Sigmaplot program (version 11, San Jose, USA). Shape characteristics of the Gompertz model was given in Appendix B.



## CHAPTER 3

### RESULTS AND DISCUSSION

#### 3.1 Preparation of Mesoporous Silica Nanoparticles

The aim for the characterization of the commercially available nanoparticles was to validate and/or batch-specific determination of physical properties of nanoparticles and to be sure whether these properties are suitable for the study.

##### 3.1.1 Characterization and Modification of Mesoporous Silica Nanoparticles

In the process of particle characterization, Transmission Electron Microscopy (TEM) analysis was done in order to observe the particles and pore sizes, pore mouths and pore walls. TEM image in the Figure 14A) gave us the hexagonal pore walls, nearly 4 nm pore diameter and ordered pore distributions. Following these findings about pore structure, particle size was determined via dynamic light scattering (DLS) method. The graph in Figure 14B gives the distribution of MCM-41 nanoparticles as determined by DLS. Since the particle size was measured in aqueous solution, the size measurements would be the hydrodynamic size including the shell of water molecule layer around particles due to non-covalent interactions. The average diameter of particles was observed  $182.8 \pm 2.3$  nm. This size is in accordance with the previous results related with mesoporous silica particles (F. J. Hernandez et al., 2013) and smaller than some of the drug delivery system summarized in section 1.4 (Kalhapure et al., 2017). After validating some basic properties conjugation strategy for probe immobilization on silica nanoparticles was done. Details of the procedure were given

in Section 2.2.2 and schematically represented in Figure 14C, conjugation strategy was based upon the silanization of silica particles with (3-Mercaptopropyl)triethoxysilane for amine-modified functional nucleic acid gates (aptamer or cleavage resistant oligonucleotide) to be covalently bound via sulfo-GMBS linker.

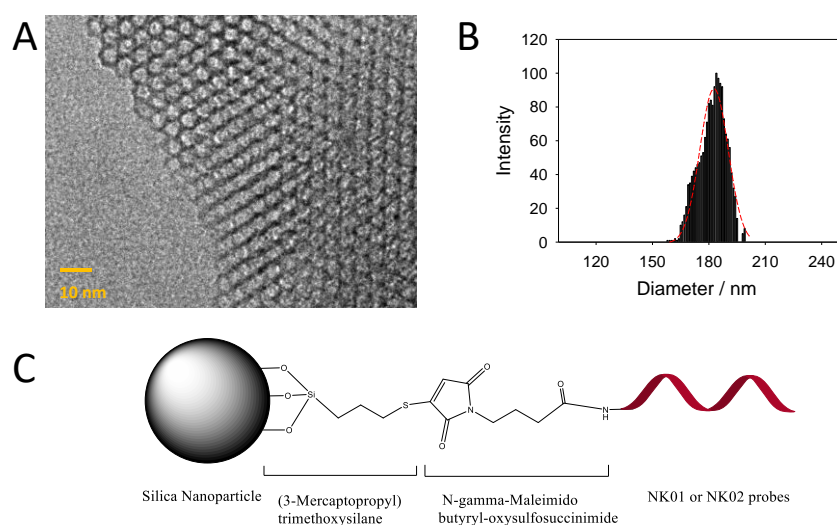


Figure 14 Synthesis and characterization of modified silica particles. A) TEM image of MCM-41. B) DLS result of MCM-41 for obtaining hydrodynamic size distribution. C) surface modification of MCM-41 for nucleic acid conjugation for either modified oligo sequence or *S. aureus* aptamers.

### 3.1.2 Loading of Mesoporous Silica Nanoparticles

Since the volumetric capacity of the particles is as important as their sizes, Brunauer, Emmett and Teller (BET) method was performed in order to determine the isothermal adsorption of an inert gas (nitrogen) to calculate the total internal and external surface area of materials (Collins, 2012). N<sub>2</sub> uptake was determined at various pressures to obtain an isotherm plot which can be used to calculate pore size and distributions.



Figure 15 and Figure 16 are isotherm graphs for MCM-41, which fits to main type of mesoporous particles (Type IV according to IUPAC classification). The N<sub>2</sub> sorption measurements with typical inflection point at about 0.6 p/p<sub>0</sub> indicated a mesoporous structure for the nanoparticles, demonstrating type IV isotherms (Appendix C).

Pore size distribution function (PSDF) of a solid matrix is one of the most important structural feature of drug-delivery vehicle. This is given in Figure 15 and Figure 16 from two different method, BJH (Barrett-Joyner-Halenda) and DFT (density functional theory), resulting in pore volume versus pore width graphs. PSDF graphs can be used for determining mean pore size, specific surface area, porosity and permeability.

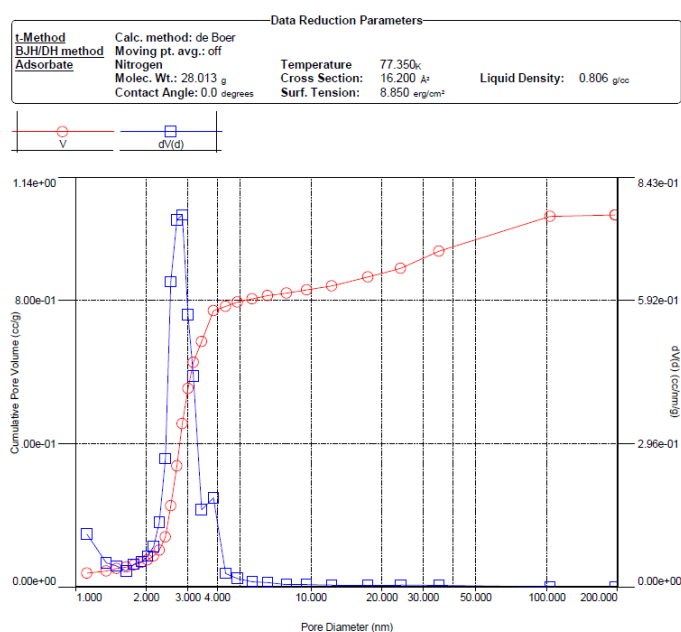


Figure 15 Nitrogen adsorption isotherms and pore size distribution of MCM-41 particles calculated by BJH method. The data and the graph was obtained form Quantachrome QuadraWin program. By using the derivative (blue line) of calculated volumetric measurement (red line) from BET analysis an estimation of 2.8 nm pore size was obtained.

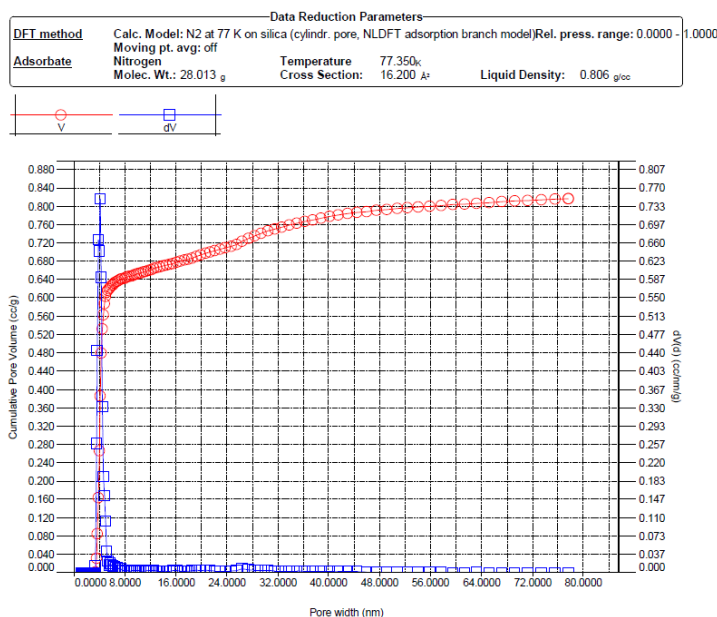


Figure 16 Nitrogen adsorption isotherms and pore size distribution of MCM-41 particles calculated by DFT method. The data and the graph was obtained from Quantachrome QuadraWin program. By using the derivative (blue line) of calculated volumetric measurement (red line) from BET analysis an estimation of 4.1 nm pore size was obtained.

The BET analysis resulted in two different pore size, depending on application of the methods (BJH or DFT). BJH method determined a similar pore size to size as given by the supplier (Collins, 2012; Sigma-Aldrich, 2017b). However, DFT uses a modified Kelvin equation in the calculations and considers better some internal hexagonal cylindrical architectures including MCM type materials. Therefore, pore size of 4.093 nm is assumed to be closer to real size compared to 2.8 nm as calculated by BJH method (Figure 15 and Figure 16). In fact, this is reported in literature that BJH method estimates pore sizes smaller than the real one by several tens of angstroms compared to DFT method estimates as evaluated with electron microscopy determinations (Kruk, Jaroniec, & Sayari, 1997). As can be validated from the TEM analysis given in Figure 14A of Section 3.1.1, a 4.1 nm pore size of DFT method is more realistic rather than 2.8 nm pore size of BJH method. Pore volume and surface

area values were automatically calculated. Quantachrome QuadraWin is a program developed by Quantachrome Instruments (Florida, USA) from the isotherms and given in Table 7. Supportive graphs of the BET analysis is given in Appendix C.

Table 7 Pore volume and surface area calculations as a result of BET experiment with different calculation methods; BJH and DFT for establishment of pore volume, surface area and pore diameter.

	<b>BJH Method</b>	<b>DFT Method</b>
<b>Pore Volume (cc/g)</b>	1.036	0.816
<b>Surface Area (m<sup>2</sup>/g)</b>	1245.649	810.359
<b>Pore Diameter (nm)</b>	2.833	4.093

4.1 nm pore size is appropriate for the molecules to be incorporated since the size of the molecules are smaller than 4.1 nm. Figure 17 gives the molecular size of the Rhodamine B and vancomycin. They have different chemical properties. In terms of size, hydrogen bonding capacity and flexibility. Rhodamine B can be regarded as smaller and more hydrophobic of these two molecules with 479.017 g/mol molecular weight, 7 rotatable bond, for hydrogen bonding 1 donor, 5 acceptor locations (NCBI, 2018a) with 1-1.2 nm size as seen in Figure 17A. On the other hand, vancomycin is larger in size with more hydrogen bonding and flexibility with 1,449.265 g/mol molecular weight, 13 rotatable bond, for hydrogen bonding 19 donor, 26 acceptor locations (NCBI, 2018b) and 2.2-3.2 nm size as seen in Figure 17B. Vancomycin is also one of the model molecules to challenge drug delivery kinetics of proposed systems including mesoporous silica particles (Atefyekta et al., 2016; Cauda, Onida, Platschek, Muhlstein, & Bein, 2008).

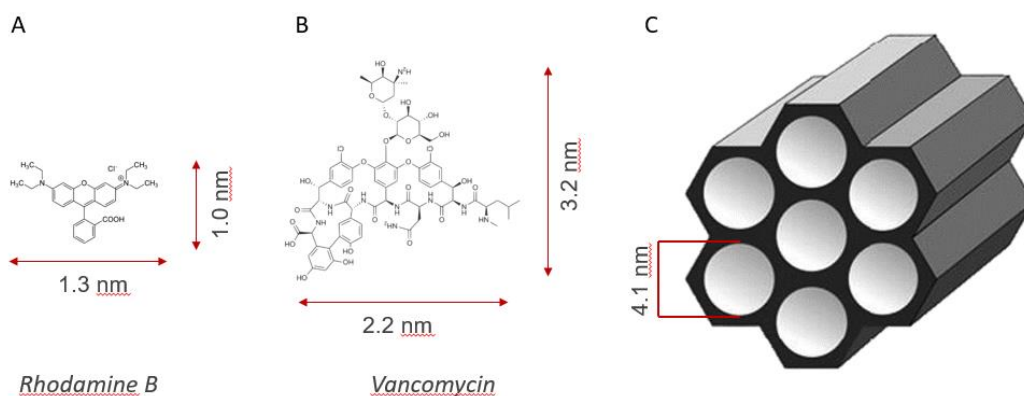


Figure 17 Sizes of molecules to be incorporated in pores of mesoporous silica particles. A) rhodamine B is relatively small molecule than vancomycin B) vancomycin is a large molecule and similar in size with pores openings. It has 13 rotatable bonds making it flexible for change its 3D shape with respect to thermodynamic interactions. C) Measured pore diameter of MCM-41 type mesoporous silica particles.

### 3.1.3 Calculated Loading Efficiency and Capping Concentration for Mesoporous Silica Nanoparticles

Two different encapsulating mechanisms (can be called as “gates” or “valves”) in this study; cleavage-oriented approach of bacteria endonuclease specific modified oligo sequence and affinity-oriented *S. aureus* specific aptamer sequence. For modified oligonucleotide-capped nanoparticles the concentration of encapsulated vancomycin was observed with spectrophotometric measurement at 280 nm and calculated to be 15.5 pmol/mg of mesoporous silica particles (meaning 22.5  $\mu\text{g/g}$  vancomycin in terms of administrating concentration) and concentration of encapsulated Rhodamine B was calculated to be 14.1 pmol/mg of mesoporous silica particles (meaning 6.8  $\mu\text{g/g}$  Rhodamine B in terms of administrating concentration). Similar loading capacity was observed with oligonucleotide-capped nanoparticles as loaded vancomycin was calculated to be 12.1 pmol/mg of mesoporous silica particles (meaning 17.5  $\mu\text{g/g}$  vancomycin in terms of administrating concentration). These calculations were based

on measuring the remaining vancomycin in the solution and abstracting it from initially added amount of vancomycin in terms of the volume of the solution, concentration and the molecular weights of the molecules.

Following the capping procedure through immobilization of  $11.8 \pm 1.3$  pmol aptamers (SA20hp) per mg nanoparticles or  $10.4 \pm 1.8$  pmol oligonucleotides (NanoKeeper 01 or NanoKeeper 02). The modified oligo sequences used for cleaving by MN is called NanoKeeper in this study. Because, apart from the aptamer-based gating mechanism, they are opened by cleaving, not by affinity binding, thus modified oligo sequences “keep” the drug inside pores and cannot function as “valve” for regenerative opening-closing action. NanoKeeper01 is the one that can be cleaved and NanoKeeper02 is the one with no cleavable site, thus can be regarded as “blunt” against MN. Oligo and aptamer capping mechanisms are two different strategies for capping the nanopores and detailed in Sections 3.2.1 and 3.3.1 respectively.

### **3.2 Modified Nucleic Acid Gates for Targeted Delivery of Antibiotics**

To demonstrate the applicability of targeted antibiotic delivery, this proof-of-concept study used *S. aureus* and *S. epidermidis* as clinical models of bacterial infection. *S. aureus* is a major cause of human disease, responsible for several conditions such as endocarditis, osteomyelitis and sepsis and has emerged as a major public health threat, with resistance to a variety of antibiotics. Bacteria specific and modified oligonucleotide gating mechanism was the first strategy for targeting of antibiotic delivery for *S. aureus*.

#### **3.2.1 Design of Modified Oligonucleotide Gates**

In order to engineer an oligonucleotide gate on nanopores with serum nuclease resistance ability, a modified sequence produced in another study was utilized and

further modified. The aim of utilizing and modifying such probe is to seal the nanopores with conjugation on nanoparticles while having the ability to cleave from the nearest possible site on nanopore conjugated end (5' end) thus maximizing the possibility of pore opening by cleaving the highest amount of nucleic acid strand from covalent linkage. NanoKeepers approach (detailed in Section 3.2.2) is proposed to be useful in designing therapeutic approaches because specific nucleases are found in specific bacteria.

*S. aureus* specific nuclease (MN) has been previously used as trigger for fluorescent hairpin probes, which is a oligonucleotide probe sequence (11mer) with 2 central thymidines, flanked by 2'-O-Methyl nucleotides (mCmUmCmGTTmCmGmUmUmC), modified at both ends with a fluorophore and a quencher (TT probe), where the m means 2'-O-Methyl nucleotides and TT means DNA thymidines (F. J. Hernandez et al., 2014). The TT oligonucleotide probe results in specificity to MN, probably conferred by the TT sequence. At the same time, the oligo is resistant to endogenous nucleases in mouse and human serum due to the 2'-O-Methyl nucleotides. In a similar approach, TT oligonucleotide sequence was incorporated into the probe and attached to mesoporous nanocapsules. To this end, we have engineered the TT probe (Figure 18) into a hairpin structure such as to widely block the porous orifice and in this way aim at retaining the loaded drug inside the nanocapsule.

As represented in Figure 18; TT probe adapted from another research (F. J. Hernandez et al., 2014) was modified in terms of sequence into NanoKeeper01 probe (derived from the TT probe for the sake of this study) were performed for comparison purposes. The 2'-O-methyl modified nucleotides are resistant to MN cleavage of *S. aureus*, leaving only a –TT– region for cleavage. By changing the position of thymidine dimer to 5' end and adding –AA– region to 3' end, hairpin structure was obtained allowing the quenching mechanism with a fluorescence and a quencher. Following this change,

subsequent experiments were conducted in order to be sure that whether NanoKeeper probes were still functional in terms of being prone to cleavage and being able to seal the pores.

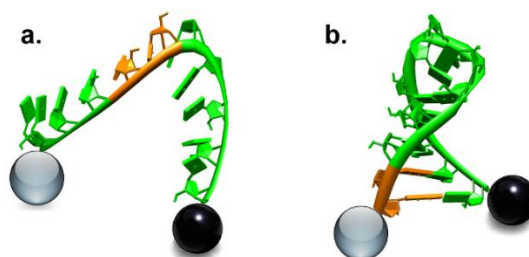


Figure 18 Representation for quenching of fluorescence on modified oligonucleotide probe due to a complementary part at 3' and 5' ends via Nupack program (nupack.org). a) the TT probe adapted from original study where the unmodified and MN prone –TT– region (orange area) is at the center of the sequence (F. J. Hernandez et al., 2014). b) NanoKeeper oligo nucleotide, derived from the TT probe in which the same –TT– region was shifted toward 5' end in order to create complementary with –AA– region at 3' end. Grey sphere represents the fluorescence, while black spheres represents quencher molecule.

### 3.2.2 Synthesis of Modified Oligonucleotide-Capped Silica Nanoparticles

Due to the change of the unmodified TT position in methyl-modified oligonucleotide, the risk of affecting the degradation efficiency by MN emerged. Therefore, a position-modified oligonucleotide sequence (FAM-TTmCmGmCmUmUmCmGmGmCmGmAmA–Quencher), denoted NK01 was designed in order to understand the degradation of NK01 upon nuclease activity by MN and resistance to degradation in serum (Figure 19) were found to be similar to those reported by the TT probe, (F. J. Hernandez et al., 2014) thus, indicating the utility of NK01 for being incorporated into the NanoKeepers approach.

As opposed to existing concepts of DLNCs, NanoKeepers were incorporated for the aim of fulfilling three functions: i) to block the nanopore, retain the loaded drug inside the nanocapsule and provide specificity to *S. aureus* nuclease (Figure 19a), ii) to be resistant to endogenous nucleases (serum nucleases), and iii) to provide specific targeting based on nuclease activity going along with active drug release: Upon specific degradation by MN (Figure 19b), the oligonucleotide is detached from the nanocapsule and subsequently, the antibiotic is released (Figure 19c). Combining these three functionalities into one single nanodevice represents a significant progress over currently existing nanoparticle-based approaches.

As the procedure detailed Section 2.2.2 and schematically represented in Figure 19, after the characterization of mesoporous silica particles, their surface was modified with a sulfo-linker as NK01 oligos were prepared with an amine group (NK01-NH<sub>2</sub>) at the 5'-end, which facilitates coupling reactions to the nanoparticle surface. Oligonucleotide NK01, composed of a pair of deoxythymidines (orange) and several 2'-O-methyl modified nucleotides (green), was designed to maximize sensitivity to micrococcal nuclease (MN). In addition, the forming hairpin structure of NK01 works as a cap to retain the previously loaded antibiotic. When NanoKeepers encounter with MN regarding the presence of pathogenic *S. aureus*, the oligo NK01 is expected to be detached as result of nuclease activity and the encapsulated antibiotic is released.



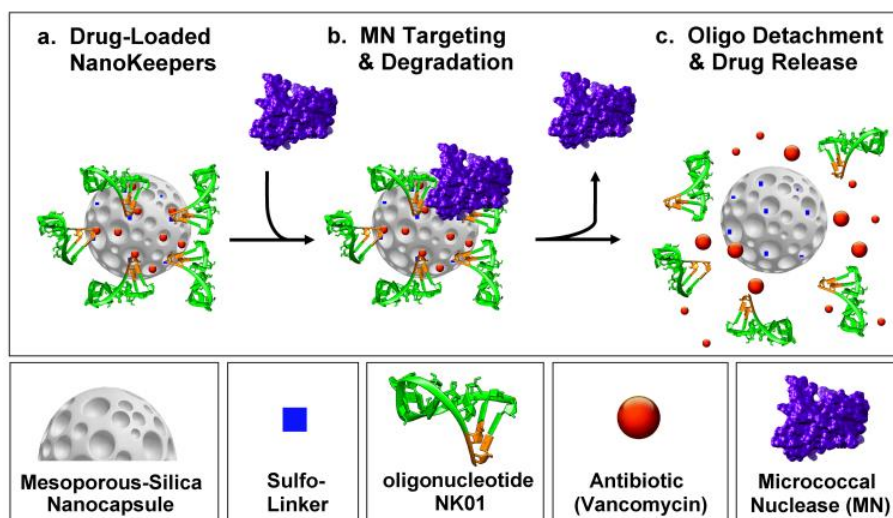


Figure 19 Scheme of Modified Oligonucleotide-Capped Silica Nanoparticles approach for targeted drug delivery. Surface of the mesoporous silica particles are represented as grey porous spheres, sulfo-linker used for creating covalent linkage between nanoparticles and oligonucleotides are blue squares in the figure. 5' amine-capped and methyl modified oligonucleotide strands are shown in green having orange areas for emphasizing the micrococcal nuclease (MN) sensitive, unmodified – TT – region. Orange spheres represents the model antibiotic, vancomycin that is encapsulated in gated-nanoparticles and can only be released in the presence of MN enzyme shown as purple molecule in the figure.

In order to proof such expectations from proposed gating mechanism, first, the blocking capacity of NK01 oligos for cargo molecules inside the nanocapsules was tested as described in section 2.2.3 with Rhodamine B loading. Briefly, the NanoKeepers were loaded with Rhodamine B and thereafter blocked with the oligo NK01-NH<sub>2</sub>. The important step of loading and capping procedure is to supply the nanopores with the target molecule (Rhodamine B or vancomycin) at the capping stage also by adding the related molecule in the capping buffer (0.01 M PBS) with a similar concentration of loading buffer (100 μM of either Rhodamine B or vancomycin). Otherwise the loaded molecules will release via simple diffusion process from the pores at 30 min incubation of sulfo-linker binding step and subsequent 1 h incubation of oligo binding step.

After loading and capping procedure, the nanoparticles were incubated; in PBS as a control for capping ability since upon any failure of capping, leakage can be observed with increasing fluorescence readings, in 10% serum samples (in 0.01 M PBS solution) to mimic endogenous nuclease background (control) to simulate the stability of oligonucleotide gate under *in vivo* conditions, and the serum samples spiked with MN for the observation of the opening of oligonucleotide gate. Each of the indicated conditions was incubated for 60 min at 37°C. The samples were taken for spectrofluorometer readings with appropriate filters for Rhodamine B. Triplicate measurements were reported in the experiments; the results shown are given as average of normalized fluorescence intensity and the error bars show the standard deviations.

NK01 probe was tested with PBS (control), PBS solution containing 1 U MN/ $\mu$ L, 10% of mouse or human serum. In PBS, and 10% of either human or mouse serum, fluorescence levels remain low after 60 min incubation. This proved sealing capability and the stability of oligonucleotide gating mechanism. Following this verification of the gating mechanism, release kinetics experiment were performed in order to understand the drug delivery capability of the system. The results of the robustness of the system in different conditions were summarized in Figure 20.

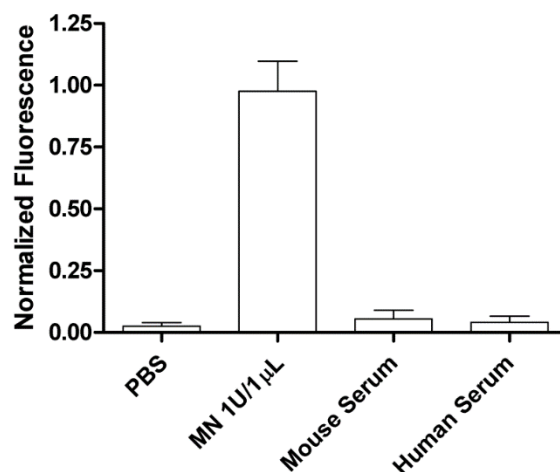


Figure 20 Degradation profile of NK01 probe. Due to hairpin structure of the NK01, fluorescence and quencher were in close proximity, thus allowing the fluorescence readings with any degradation of NK01. Y-axis represent the normalized fluorescence measurements were taken with respect to background fluorescence of solutions. Increase fluorescence readings were taken in MN 1U/mL solutions. Triple measurements were carried out in each sample; the results showed average fluorescence intensity and the error bars were standard deviations (n=3 independent experiments,  $p < 0.05$ ).

### 3.2.3 Release Kinetics of Rhodamine B and Vancomycin from Modified Oligonucleotide-Capped Nanoparticles

In order to understand the release kinetics of molecules from the nanoparticles, Rhodamine B and vancomycin were loaded in oligonucleotide-capped nanoparticles in separate experiments. To understand the specificity of NanoKeeper-NK01 oligos further, a non-responsive control sequence was used, which is denoted NK02 (NH<sub>2</sub>-UmUmmCmGmCmUmUmCmGmGmCmGm AmA). TT motif sequence in NK01 is replaced by 2'-O-Methyl Uracils (UmUm) in NK02 in order to decrease degradation activities from MN enzymes. NK02 was immobilized on the surface of nanocapsules following the same approach as NK01.

Rhodamine loaded mesoporous nanoparticles were challenged against three different conditions; NK01-capped particles in 10% human serum (in 0.01M PBS) with micrococcal nuclease, NK02-capped particles in 10% human serum (in 0.01M PBS) with micrococcal nuclease, and NK01-capped particles in 10% human serum (in 0.01M PBS) without micrococcal nuclease. First condition had the optimum environment for drug delivery mechanism to work. In the second condition, suboptimal capping mechanism was used in order to prove the specificity of endonuclease related drug release, and in the final condition effect of serum conditions were experimented as a control.

By taking samples from these setups and observing Rhodamine B concentration by fluorescence readings, release of Rhodamine B was tracked (Figure 21). A release of Rhodamine B occurred in serum samples spiked with 1 U/mL MN and containing the correct capping mechanism, NK01, proving specific release upon MN activity. In samples containing only serum, a minimal release of Rhodamine B is observed, revealing a favourable low-leakage capsule stability at simulated physiological environment. The non-specificity studies carried out by capping Rhodamine B containing nanoparticles with a control oligomer (NanoKeepers-NK02) gave also similar result with the serum-only conditions even in the presence of MN. All the measurements were carried out in triplicate; the results show average fluorescence intensity and the error bars represent standard deviations. Samples were taken at different time intervals completing with t=24h sampling step. These results demonstrate the viability of the concept of serum nuclease resistant modified oligonucleotide-capped nanoparticles as drug delivery systems based on nuclease activity with specific targeting for MN and, hence, their potential physiological applications.

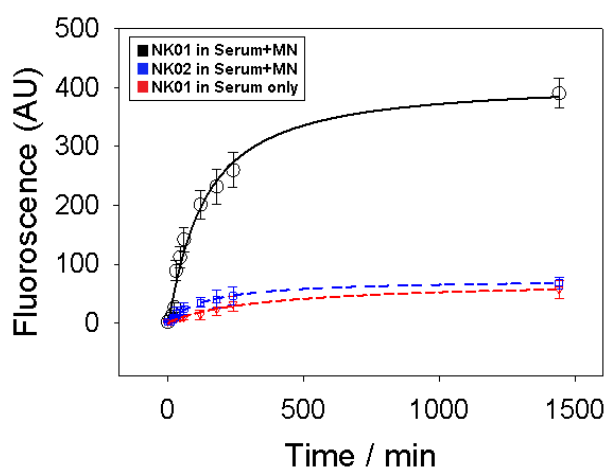


Figure 21 Evaluation of modified oligonucleotide-capped nanoparticles loading with Rhodamine B under simulated physiological conditions. Black line represents the nanoparticles containing NK01 oligo as capping mechanism and in serum containing 1 U/mL MN (10% human serum in 0.01 M PBS at 37 °C). Blue and red lines are control setups with “blunt” NK02 probe-capped nanoparticle not having unmodified TT region and NK01 probe-capped nanoparticle in serum without MN. Y-axis represent the fluorescence measurement with respect to times of sample taking for measurement depicted in X-axis. Triple measurements were carried out in each sample; the results show average fluorescence intensity and the error bars were standard deviations (n=3 independent experiments,  $p < 0.05$ ).

It was an important achievement for the drug delivery system with no release of cargo molecules (Rhodamine B) by NK02 oligonucleotide-capped mesoporous silica particles in the presence of MN and signal levels resembled rather those of NK01 oligonucleotide-capped in serum only. This demonstrated that NK02 oligo with no cleavable site was similarly capable of closing the nanopore of mesoporous silica particles and no opening was triggered by enzymatic activity of MN. Hence, the specific recognition and then cleavage of the TT DNA motif of NK01 oligonucleotide-capped mesoporous silica nanoparticles was indeed the responsible mechanism for the delivery of the cargo molecules in presence of MN. This observation confirmed that the bacteria specific nuclease activity can be utilized as the trigger mechanism for drug delivery construct in this study.

The inhibitory efficiency of oligonucleotide-capped nanoparticles was subsequently evaluated in bacterial cultures grown in TSB medium in order to verify the results obtained with Rhodamine B. Nanoparticles were loaded with vancomycin (as a model for common antibiotic for treating *S. aureus* infections) as 22.5 µg/g vancomycin concentration in nanoparticle and capped with NK01 oligonucleotide. The detection and quantification of vancomycin during a release determination study can be easily followed by simple UV spectrophotometry absorbance due to aromatic rings on the molecule (Nieto & Perkins, 1971).

Vancomycin loaded mesoporous nanoparticles were challenged against four different conditions; particles with no capping mechanism (for observing the unmodified reselase), NK01-capped particles in 10% human serum (in 0.01M PBS) with 10<sup>4</sup> CFU/mL of *S. aureus*, NK01-capped particles in 10% human serum (in 0.01M PBS) with 10<sup>4</sup> CFU/mL of *S. epidermidis*, and NK01-capped particles in 10% human serum (in 0.01M PBS) without any bacteria. First condition was conducted to observe the simple diffusion of drugs. Second condition had the optimum environment for drug delivery mechanism to work. In the third condition, of *S. epidermidis* was used in order to prove the strain specificity of drug release, and in the final condition effect of simulated serum environment was experimented as a control similar to Rhodamine B release experiment.

During 24h, the susceptibility of two cultures was observed, namely that of *S. aureus* which produces MN, and *S. epidermidis*, a genus of Staphylococcus that has been reported to produce undetectable levels of MN (F. J. Hernandez et al., 2014). These vancomycin-loaded nanoparticles were characterized to confirm almost leakage-free stability and release only by specific activation of MN (Figure 22). Also the capping mechanism performed a decreased release rate than simple diffusion which did not seem to effect the inhibitory concentration as experimented an proved in the next section.

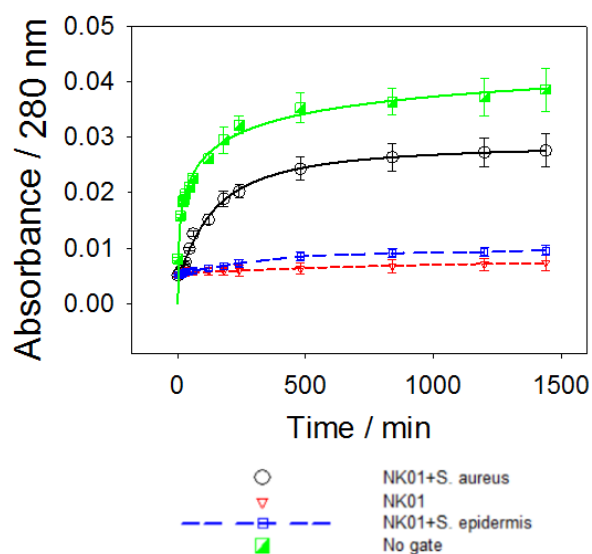


Figure 22 Evaluation of oligonucleotide-capped nanoparticles loading with vancomycin under simulated physiological conditions (10% human serum in 0.01 M PBS at 37 °C). Green line represents the leakage of vancomycin without any capping mechanism on drug loaded nanoparticles. Black line represents the nanoparticles containing NK01 oligo as capping mechanism and in serum containing  $10^4$  CFU/mL *S. aureus*. Blue represents the NK01-capped nanoparticles with control microorganism,  $10^4$  CFU/mL *S. epidermidis*. Red line represents only vancomycin loaded, NK01-capped nanoparticle. Y-axis represent the absorbance measurement with respect to times of sample taking for measurement depicted in X-axis. Triple measurements were carried out in each sample; the results show average fluorescence intensity and the error bars were standard deviations (n=3 independent experiments, p<0.05).

### 3.2.4 MIC Analysis of Modified Oligonucleotide-Capped Nanoparticles

The bacterial susceptibility was determined by minimum inhibitory concentrations (MICs) in 96-well microtiter plates using the microdilution method according to the Clinical and Laboratory Standards Institute (Swenson et al., 2009). Tryptic soy broth (TSB) was used for susceptibility testing for *Staphylococcus* spp. cultures. By administrating different concentrations of (two-fold dilutions) of vancomycin loaded serum nuclease resistant oligonucleotide-capped nanoparticles in wells of microplate

with corresponding bacteria strain the experiment setups were set. After incubation (with shaking at 37 °C) for 24 h, turbidity of the wells were measured at 600 nm. Fitting the data with OD versus log[Vancomycin concentration] graphs and with the help of Gompertz equation given in Figure 23, MIC values with respect to drug loaded nanoparticles and unmodified drug administration were plotted for each bacteria strain.

The MICs of vancomycin-modified oligonucleotide-capped nanoparticles for *S. aureus* and *S. epidermidis* (control) were found to be 0.332 µg/mL and 10.483 µg/mL, respectively. These results mean a 31-fold increased efficiency between *S. aureus* and *S. epidermidis*, thus indicating specific targeting in the case of *S. aureus* and lower toxicity for *S. epidermidis*. The MIC for vancomycin only, used as control in our study, amounted to 1-2 µg/mL (Figure 23) which is in agreement with previous studies (Rehm & Tice, 2010). Importantly, *S. epidermidis* was only affected by high doses of vancomycin-Nanokeepers (10.483 µg/mL). This suggests that at an appropriate dose (e.g. at 1 MIC = 0.332 µg/mL), NanoKeepers approach could be safe for non-targeted bacteria or cells while efficiently killing the targeted bacteria *S. aureus*. Statistical background these findings was given in Appendix D.



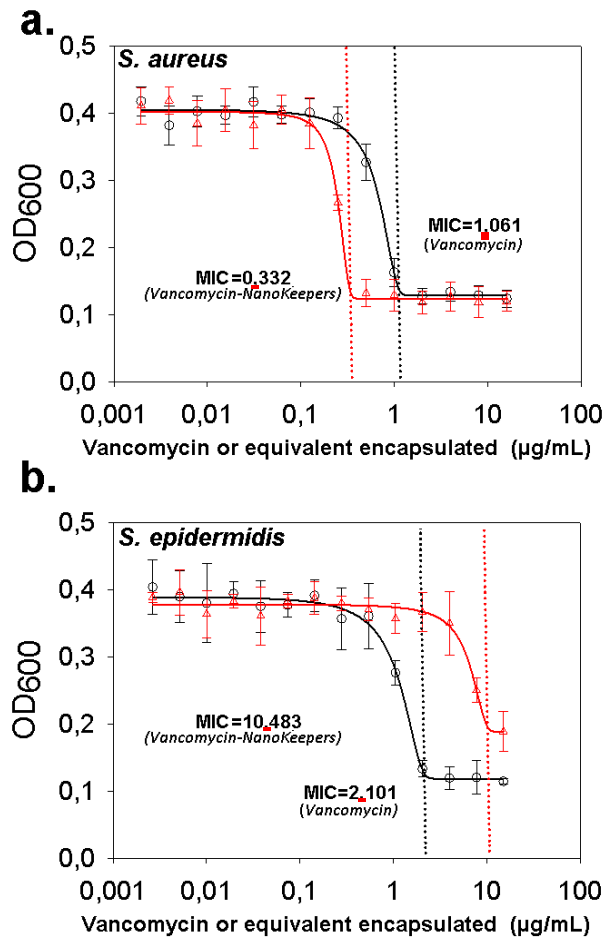


Figure 23 Bactericidal efficiency of modified oligo-gated vancomycin loaded mesoporous silica particles. Susceptibility of a) *S. aureus* and b) *S. epidermidis* cultures were challenged against serial two-fold dilutions of vancomycin-NanoKeepers (red lines) or vancomycin only as control (black lines). After a 24 h incubation period at 37 °C, the cell viability was measured by optical density (OD) detection at 600 nm, and the minimum inhibitory concentrations (MICs) were determined. All the measurements were performed in triplicate; the error bars indicate the standard deviations. Statistical background was given in Appendix D.

The concept of the proposed targeted drug delivery system was proved with the MIC analysis for modified oligonucleotide-capped nanoparticles. However, for verification purposes, time-kill plots of different bacteria/nanoparticle combinations for verification purposes. This verification was carried out by comparing kill curves and

growth curves of *S. aureus* and *S. epidermidis* in presence and absence, respectively, of vancomycin-loaded modified oligonucleotide-capped nanoparticles. Time-kill curves have been previously used *in vitro* to provide more detailed information about the time course of the antimicrobial effects (Dilworth, Sliwinski, Ryan, Dodd, & Mercier, 2014). Figure 24 depicts the effect of 1 MIC concentration of vancomycin-loaded nanoparticles (calculated in previous experiment via Gompertz equation) and the change in density of viable bacteria as a function of time. After each time indicated in the Figure 24, the log of CFU/mL was determined. All the measurements were performed in triplicate; the error bars indicate the standard deviations.

As graphically represented in Figure 24, vancomycin-loaded oligonucleotide-capped nanoparticles were an effective therapeutic strategy against *S. aureus*, with a moderate response after 2 h; followed by a strong and prolonged bactericidal activity from 6 to 24 h (red dashed line), and as compared to the *S. aureus* growth curve (black line). In contrast, the viability of *S. epidermidis* was not affected by vancomycin-oligonucleotide-capped nanoparticles (green line), being similar to the control *S. epidermidis* growth curve (blue line). These results clearly demonstrate the bactericidal efficiency of NanoKeepers for *S. aureus* and the limited effects on the viability of non-targeted bacteria. The results also confirm the safety and efficiency of oligonucleotide-capped mesoporous silica nanoparticles as a potential therapeutic approach. In addition, a decrease in MIC values is one of the promising results of this study since, resistance level of pathogenic bacteria is considered and classified according to the MIC values. Also, higher the MIC, higher the concentration of drug to be administered and higher the risk of side effects and unwanted new antimicrobial resistances.

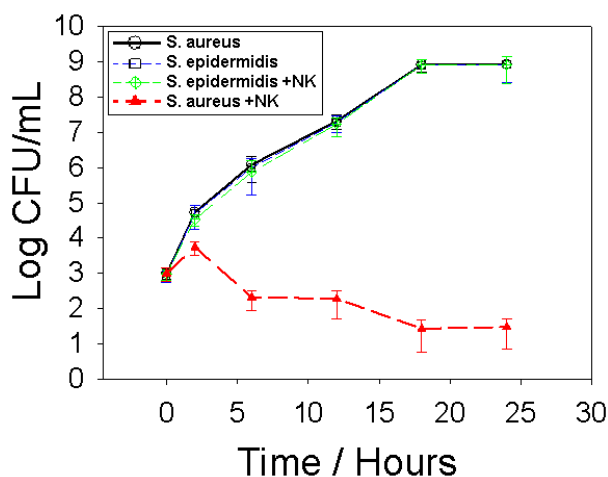


Figure 24 Time-kill curves for *S. aureus* and *S. epidermidis* cultures after treating with modified oligonucleotide-nanoparticles with a concentration of 1 MIC calculated.  $10^3$  CFU/mL initial concentrations of *S. aureus* and *S. epidermidis* cultures were used for normal growth in TSB medium at 37 °C (black and blue lines). Same bacteria concentration was challenged against 1 MIC of (0.332  $\mu\text{g/mL}$ ) vancomycin encapsulated by oligonucleotide-capped mesoporous silica nanoparticles (green and red lines). After a 24 h incubation period at 37 °C and sampling at different time intervals, the cell viability was measured by optical density (OD) detection at 600 nm, with further TSB agar plate colony counting. Y-axis represents the log scale of bacteria counting while X-axis represents time for expressing sampling intervals. All the measurements were performed in triplicate; the error bars indicate the standard deviations.

### 3.3 Aptamer Gates for Targeted Delivery of Antibiotics

In developing a *S. aureus* specific aptamer-based molecular gate, an aptamer sequences that had been reported in another research and was used as reported in literature (Cao et al., 2009). The aptamer was selected against whole cells of *S. aureus* and negative selection was performed with *S. epidermidis*. Thus, the aptamer sequences recognized specifically *S. aureus* and did not bind to the closely related strain *S. epidermidis*. Among the aptamer sequences were tested for their ability to form a structure switching probe structure and the best responding one was covalently attached to the surface of silica nanoparticles as a capping agent. The release kinetics

were determined with bacteria spiked serum solutions and compared to the previous studies with aptamer-gated silica nanoparticles.

### 3.3.1 Design of Aptamer Gates

In experimenting the potential application of aptamer sequences as capping agent on mesoporous nanoparticles first of all, *S. aureus* specific aptamer sequences were converted to hairpin structure as can be seen in Section 2.1 (Table 6). Among three potential aptamer sequences being reported elsewhere (Cao et al., 2009) the specific aptamer sequence of this study was experimentally determined from the response of switch probe designs. The probe is an intramolecular signal-transduction aptamer design that consists of the aptamer sequence and a short-stem DNA sequence complementary to the other end of the aptamer sequence and separated by a polyethylene glycol (PEG) linker. The reason for incorporating a PEG linker was to be sure than large enough of conformation change and opening of hairpin was achieved in order to disrupt the quenching of fluorescence. A fluorophore (Alexa Fluor 488) and quencher (Black Hole 1) were covalently attached at the two ends of the sequence. The interaction of *S. aureus* surface antigens with the aptamer sequence disrupts the hairpin structure and leads to rearrangement of the structure, separating quencher and fluorophore from each other and higher the fluorescence means the higher the conformation change of the aptamer upon binding to *S. aureus* surface antigen. This leads to an increase in fluorescence that depends on the presence of the target that can be seen in Figure 25.

Modified aptamer sequences were challenged against in four different combinations; in the first three combinations are *S. aureus* versus different aptamers coded as SA20, SA23 and SA34. Final combination was SA20 versus *S. epidermidis* in order to understand the specificity of the aptamer. Among the three probes, SA20hp responded with highest fluorescence peak in the presence of  $10^4$  *S. aureus* cells (Figure 25, black

line). Although SA23hp and SA34hp resulted in fluorescence increases, the responses were about 25% and 40% lower than SA20hp respectively. Based on these results, we have selected SA20hp as the molecular gate aptamer in the rest of the study. The response of SA20hp probe was also challenged with *S. epidermidis* and only a slight response was obtained at about 82 % lower than that of *S. aureus* cells. The aptamer capping was performed with SA20 aptamer without PGE linker both retaining the 3'end complementary addition with an assumption of the maximum sealing and maximum conformational change upon binding to target surface antigen of *S. aureus*.

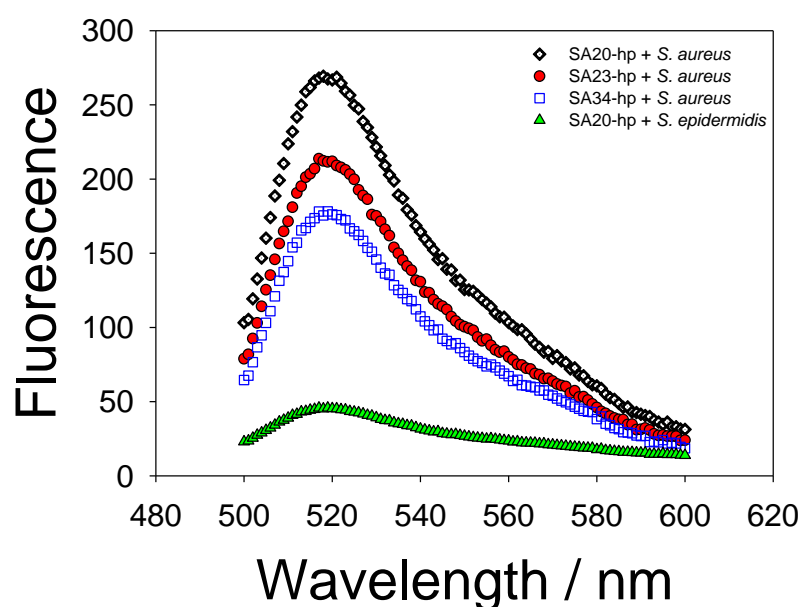


Figure 25 Fluorescence changes of the aptamer switch probes upon addition of  $10^4$  *S. aureus* or *S. epidermidis* cells in 0.01 M PBS. Emission spectra was recorded for  $\lambda$  ex. at Green \_ 480 nm after 15 min incubation at 37 °C, The y-axis is fluorescence at arbitrary units while X-axis represents the wavelengths in nm scale. Black dots represents the fluorescence readings of SA20 aptamer with *S. aureus*, red dots represents SA23 aptamer with *S. aureus* and Blue dots represents SA34 aptamer with *S. aureus*. Green dots are fluorescence measurements of SA20 aptamer with *S. epidermidis* as control the specificity of SA20 aptamer.

### 3.3.2 Synthesis of Aptamer-Capped Silica Nanoparticles

The blocking and retaining capacity of aptamer gates were tested with MCM-41 type silica particles, which was the same as used in modified oligonucleotide capping (Section 3.2). The pores (average diameter 2.7 nm) were functionalized with a sulfo-linker for allowing subsequent amine coupling as the aptamer had been functionalized with an amine group (aptamer-NH<sub>2</sub>) at the 5'- end in order to facilitate the coupling to the nanoparticle surface as previously described (F. J. Hernandez et al., 2013).

Figure 26 is a schematic depiction of strategy as used in this study. A) Silica nanoparticles were loaded with vancomycin and coupled to the amine-modified aptamer-gate oligonucleotides. B) The hairpin structure of *S. aureus* binding aptamer sequence works as a cap to retain the previously loaded antibiotic, vancomycin. C) When aptamer-nanoparticles encounter *S. aureus* surface antigens, the aptamer-gate is detached as result of ligand-target binding and the encapsulated antibiotic is released, D) Closed/open forms of aptamer gates. The antibiotic vancomycin was absorbed into the pores of mesoporous silica nanoparticles and capped with SA20hp gatekeeper molecule. When the nanoparticles bind to their target molecules on the surface of *S. aureus* cells via gatekeeper aptamer sequences, the cargo antibiotic is released to kill bacteria. Otherwise, vancomycin is entrapped in the pores and thus inactive. This construct with assumptions and expectations were experimented as release kinetics, MIC analysis and time-kill curve studies.

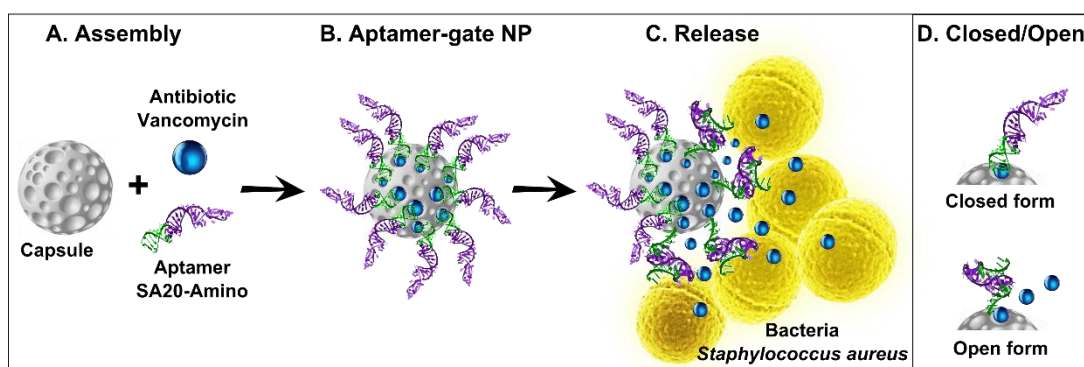


Figure 26 Scheme of Aptamer-Capped Silica Nanoparticles approach for targeted drug delivery. Surface of the mesoporous silica particles are represented as grey porous spheres, sulfo-linker used for creating covalent linkage between nanoparticles and aptamers. Aptamers are shown in purple having green areas as PEG attachment for increasing the flexibility of the aptamer over the nanoparticles. Blue spheres represents the model antibiotic, vancomycin that is encapsulated in gated-nanoparticles and can only be released in the presence of *S. aureus* interacting with aptamer thus changing its conformation over pores of nanoparticles.

### 3.3.3 Release Kinetics of Vancomycin from Aptamer-Capped Silica Nanoparticles

The encapsulation ability and release kinetics of aptamer-capped nanoparticles were investigated by monitoring vancomycin release by UV absorbance at 280 nm as in the case of modified oligonucleotide-capping experiments. The nanoparticles were loaded with vancomycin and thereafter blocked with the aptamer hairpin structures. Subsequently, they were incubated in 10% human serum samples (in 0.01 M PBS) to mimic endogenous background, and serum samples spiked with either *S.aureus* or *S.epidermidis* cells. These vancomycin-loaded and aptamer-capped mesoporous silica particles were characterized to confirm almost leakage-free stability and release only by specific actuation of aptamer-ligand interaction as shown in Figure 27. Aptamer-capped nanoparticles loaded with vancomycin were incubated with serum, to observe their stability and cargo keeping under physiological conditions (red dashed line). The

leakage was about  $5 \% \pm 0.2$  (n=3) at the end of 24 hours incubation (Figure 27, red line).

Next, the release of entrapped vancomycin was triggered by addition of  $10^4$  cells of bacteria *S. aureus*. This concentration was chosen in order to warrant binding and opening of the majority of hairpin aptamer molecules resulting in the release of vancomycin. Indeed, the addition of *S. aureus* cells increased the release dramatically, as anticipated (Figure 27, black line). This leakage amount was lower than our previous reports with ATP binding aptamers (Ozalp & Schafer, 2011). The improvement in leakage prevention could result from the size difference of cargo molecules (543 Da for ATP versus 1,449 Da for vancomycin) or from better capping ability of aptamer gate structure (35 nucleotide for ATP binding aptamer versus 49 nucleotide for *S. aureus* binding aptamers sequence).

The cumulative amount of vancomycin increased up to 5 hours and levelled off afterwards, which corresponded to about  $12.1 \pm 0.2$  pmol of encapsulated vancomycin molecules in one mg of nanoparticles as determined by UV absorbance analysis at the end of 24 hours. This proved that the aptamer nanovalves were generally functional in the sense that the hairpin aptamer blocked the pores prior to addition of cells, whereas the presence of *S. aureus* cells triggered their opening and hence release of vancomycin. The half-life of *S. aureus*-triggered release was estimated to be 45 min. A control experiment with the same nanoparticles, but *S. epidermidis* cells addition was performed for 24 hours. The vancomycin release was lower than release by *S. aureus* at about 15% (Figure 27, blue line).



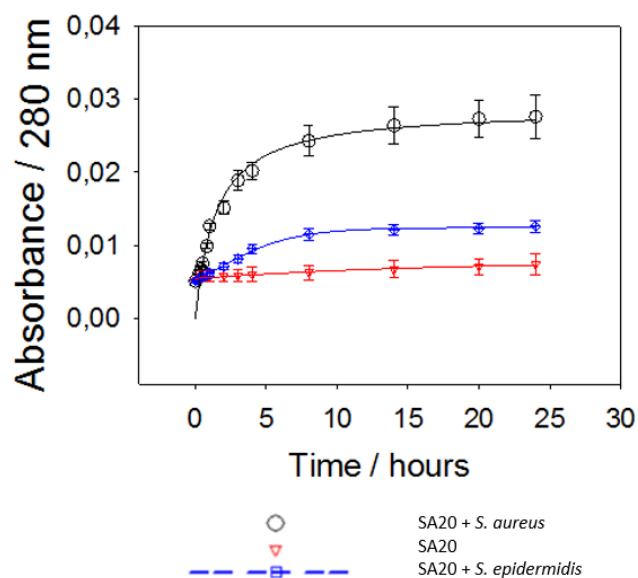


Figure 27 Evaluation of aptamer-capped nanoparticles loading with vancomycin under simulated physiological conditions (10% human serum in 0.01 M PBS at 37 °C). Black line represents the nanoparticles containing SA20 aptamer in serum with  $10^4$  CFU/mL *S. aureus* bacteria. Blue represents the SA20-capped nanoparticles with control microorganism, *S. epidermidis*. Red line represents only vancomycin loaded, SA20-capped nanoparticle. Y-axis represent the absorbance measurement with respect to times of sample taking for measurement depicted in X-axis. Triple measurements were carried out in each sample; the results show average fluorescence intensity and the error bars were standard deviations (n=3 independent experiments,  $p < 0.05$ ).

### 3.3.4 MIC Analysis of Aptamer-Capped Silica Nanoparticles

Minimum inhibitory concentrations (MICs) are defined as the lowest concentration of an antimicrobial agent inhibiting the growth of a microorganism after overnight incubation. The therapeutic efficiency of aptamer-gated vancomycin nanoparticles was subsequently evaluated in two strains of *Staphylococcus* cultures. Mesoporous nanoparticles were loaded with vancomycin (a common antibiotic for treating *S. aureus* infections) and capped with *S. aureus* binding aptamer hairpin. During 24h, the susceptibility of two cultures was monitored, namely that of *S. aureus* which is a

genus of Staphylococcus that has specific affinity to the aptamer sequence of this study and that of *S. epidermidis* which is another strain of Staphylococcus that has not any affinity to the aptamer sequence (Cao et al., 2009).

As can be seen in Figure 28, the MICs of vancomycin-nanoparticles for *S. aureus* and *S. epidermidis* (control) were found to be 0.420 µg/mL and 6.295 µg/mL, respectively. Susceptibility of a) *S. aureus* and b) *S. epidermidis* cultures were challenged against serial two-fold dilutions of vancomycin-nanoparticles (red lines) or vancomycin only as control (black lines). After a 24 h incubation period at 37 °C, the cell viability was determined by measuring optical density (OD) at 600 nm, and the minimum inhibitory concentrations (MICs) were calculated. All the measurements were performed in triplicate; the error bars indicate the standard deviations.

These results mean a 15-fold increased efficiency between *S. aureus* and *S. epidermidis*, thus indicating specific targeting in the case of *S. aureus* and lower toxicity for *S. epidermidis*. The MIC for vancomycin only, used as control in our study, amounted to 1.1-2.4 µg/mL (Figure 28) which is in agreement with previous studies (Rehm & Tice, 2010). Importantly, *S. epidermidis* was only affected by high doses of vancomycin-nanoparticles (6.295 µg/mL). This suggests that at an appropriate dose (e.g. at 1 MIC = 0.420 µg/mL), aptamer-gated vancomycin nanoparticles approach could be safe for non-targeted bacteria or cells while efficiently killing the targeted bacteria *S. aureus*. We verified this hypothesis by comparing kill curves and growth curves of *S. aureus* and *S. epidermidis* in presence and absence, respectively, of vancomycin-loaded aptamer-gated nanoparticles. Time-kill curves have been previously used *in vitro* to provide more detailed information about the time course of the antimicrobial effects (Dilworth et al., 2014). Statistical background these findings was given in Appendix D.

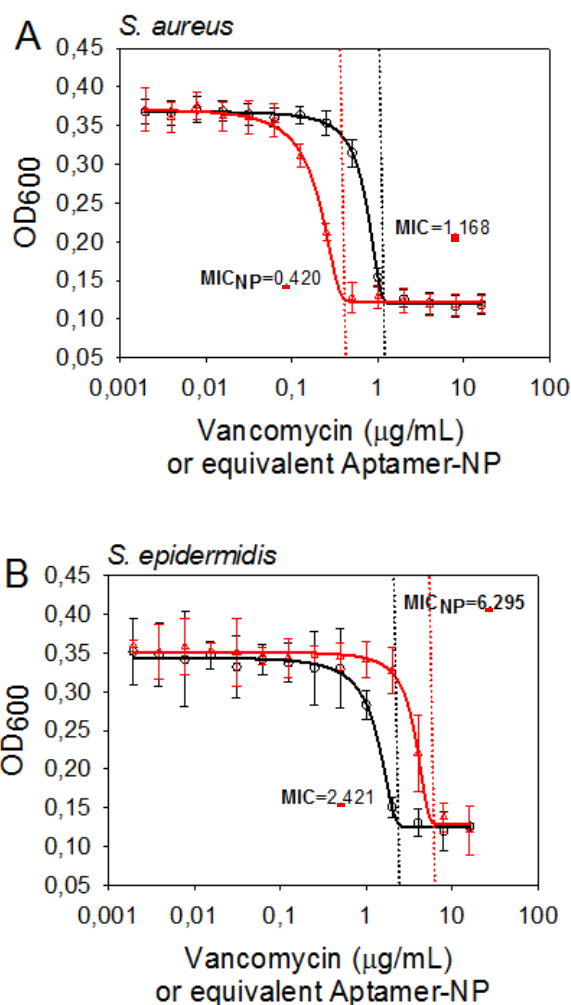


Figure 28 Bactericidal efficiency of aptamer-gated vancomycin loaded mesoporous silica particles. Susceptibility of a) *S. aureus* and b) *S. epidermidis* cultures were challenged against serial two-fold dilutions of vancomycin-NanoKeepers (red lines) or vancomycin only as control (black lines). After a 24 h incubation period at 37 °C, the cell viability was measured by optical density (OD) detection at 600 nm, and the minimum inhibitory concentrations (MICs) were determined. All the measurements were performed in triplicate; the error bars indicate the standard deviations. Statistical background was given in Appendix D.

Figure 28 depicts the effect of 1 MIC concentration of vancomycin-loaded nanoparticles and the change in density of viable bacteria as a function of time. Vancomycin-loaded nanoparticles with aptamer caps can be considered an effective

therapeutic strategy against *S. aureus*, by inhibiting bacterial growth after 2 h; followed by a strong and prolonged bactericidal activity from 2 to 24 h (blue dashed line), and as compared to the *S. aureus* growth curve (black line). In contrast, the viability of *S. epidermidis* was only slightly affected by vancomycin-nanoparticles (green line), being similar to the control *S. epidermidis* growth curve (red line). The growth curve of *S. epidermidis* in presence of NP was inhibited about 12 % compared to control growth curve. After each time indicated in the Figure 29, the log of CFU/mL was determined by culturing method.

MIC results clearly demonstrate the bactericidal efficiency of aptamer-gated nanoparticles for *S. aureus* and the limited effects on the viability of non-targeted bacteria, in this case *S. epidermidis*. For verification purposes, time-kill plots of different bacteria/nanoparticle combinations. This verification was carried out by comparing kill curves and growth curves of *S. aureus* and *S. epidermidis* in presence and absence, respectively, of vancomycin-loaded aptamer oligonucleotide-capped nanoparticles. The aim was also to confirm the safety and efficiency of aptamer-gated nanoparticles as a potential therapeutic approach. Since aptamers are well-established technology to obtain high affinity oligonucleotides, it is relatively more available for any kind of pathogenic microorganism or other human conditions. Thus, time-kill performance of aptamer-capped mesoporous silica nanoparticles enlightened new approaches with different aptamers against different targets faster than searching for nuclease specific oligo sequences.

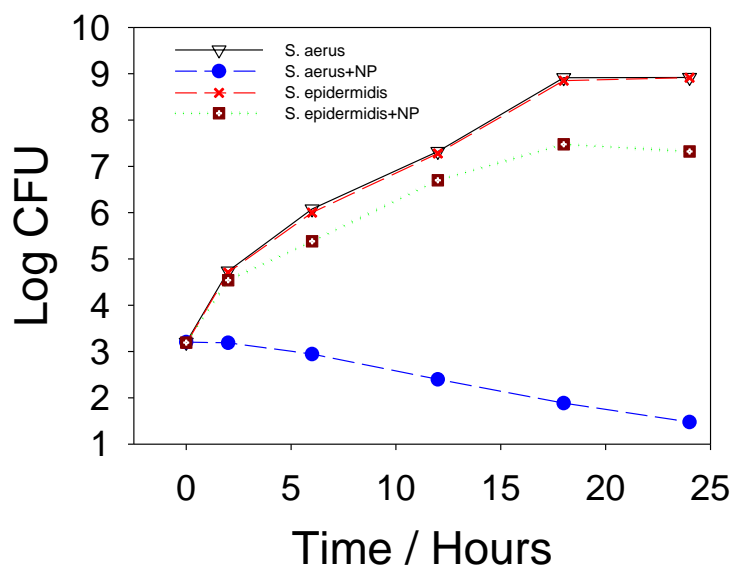


Figure 29 Time-kill curves for *S. aureus* and *S. epidermidis* cultures after treating with aptamer-nanoparticles with a concentration of 1 MIC calculated. Time-kill curves for *S. aureus* and *S. epidermidis* cultures.  $10^3$  CFU/mL initial concentrations of *S. aureus* and *S. epidermidis* cultures were used for normal growth in TSB medium at 37 °C (black and blue lines). Same bacteria concentration was challenged against 1 MIC of (0.420  $\mu\text{g/mL}$ ) vancomycin encapsulated by aptamer-capped mesoporous silica nanoparticles (green and red lines). After a 24 h incubation period at 37 °C and sampling at different time intervals, the cell viability was measured by optical density (OD) detection at 600 nm, with further TSB agar plate colony counting. Y-axis represents the log scale of bacteria counting while X-axis represents time for expressing sampling intervals. All the measurements were performed in triplicate; the error bars indicate the standard deviations.

Aptamers for antibiotic delivery were demonstrated in a limited number of reports. A nanocarrier for antibiotic neomycin was developed by using aptamers for on-demand delivery, (Sundaram, Wower, & Byrne, 2012) in which neomycin aptamers immobilize the antibiotic molecules through affinity binding and released with temperature increase *in vitro*. Thus, aptamers were used for affinity-immobilizing antibiotic molecules rather than targeting them. The aptamer utilization as a functional gate system was unique in its research area. The results also confirm the safety and efficiency of aptamer-capped mesoporous silica nanoparticles as a potential

therapeutic approach. In addition, a decrease in MIC values is one of the promising results of this study since, resistance level of pathogenic bacteria is considered and classified according to the MIC values. As long as the MIC values decrease, the risk of side effects and unwanted new antimicrobial resistances and number of new resistance cases will also decrease which can be regarded as an ultimate application potential of the systems proposed and experimented in this study.

## CHAPTER 4

### CONCLUSION

In this study, a targeted drug delivery mechanism was proposed, constructed and experimented based on two different targeting approaches. The usage of mesoporous silica nanoparticles is not new and there are various studies in the literature, some of which was summarized in this study, utilizing mesoporous silica particles. However the capping and targeting strategies used, constructed the innovative part of the study. Both the micrococcal serum nuclease resistant modified oligonucleotide and *S. aureus* aptamer are results of recent studies, and the incorporation of their so called “interaction” against the bacteria with the drug loading / carrying capability of the mesoporous silica nanoparticles marked the strategy of the study.

In this study, targeted delivery and release of antibiotics has been investigated for proof-of-concept via two different gating mechanisms; affinity-oriented aptamers and cleavage-oriented specific oligo sequence. *Staphylococcus aureus* and *Staphylococcus epidermidis* were used as model and control organisms respectively, vancomycin was used as model antibiotic for experimenting this concept. The minimum inhibitory concentration (MIC) and time-kill curve studies showed compatible results with the hypothesized performance and two different mechanisms gave us comparable inhibitory efficiency between each other. Nanoparticles with cleavage-oriented oligo sealing mechanism decreased the MIC of vancomycin against *S. aureus* strain from 1.168 µg/mL to 0.332 µg/mL, while increased the MIC of vancomycin to a non-targeted *S. epidermidis* from 2.101 µg/mL to 10.483 µg/mL. Similar results obtained with affinity-oriented aptamer sealing mechanism with a decreased MIC for *S. aureus*

strain from 1.168  $\mu\text{g/mL}$  to 0.420  $\mu\text{g/mL}$  and an increased MIC for *S. epidermidis* from 2.421  $\mu\text{g/mL}$  to 6.295  $\mu\text{g/mL}$ . Time-kill curve of both gating mechanisms showed promising results with a leakage-related less growth of *S. epidermidis* was observed in aptamer-gated nanoparticles. The inhibitory performance of proposed targeted drug delivery mechanism proved its potential for further applications and developments.

At the basis of this research, oligo and aptamer sequences were adapted from previous studies and modified according to the need of constructed drug delivery system. Then release kinetics of the system with Rhodamine B, followed by MIC and time-kill analysis of vancomycin with proposed drug delivery system against *S. aureus* for target and *S. epidermidis* for control. While oligo capping was opened with cleavage-oriented approach; micrococcal nuclease activity specifically cleaves the oligo cap allowing the leakage of the drug outside, the aptamer capping was opened with affinity-oriented approach; specific binding of aptamer (selected by cell-SELEX) to *S. aureus* cell, thus change its conformation allowing the drug to release.

While both of the capping mechanisms achieved to lower the MIC of vancomycin administration about 0.7  $\mu\text{g/mL}$ , each gating mechanism has its own advantages and disadvantages. Modified oligo gating had a better sealing than aptamer gating, which can be seen in release kinetics, MIC analysis and time-kill graphs of two gating mechanisms comparatively. This is most probably because the oligo caps are smaller in size and not particularly engineered for binding targets as in the case of aptamer. On the other hand, aptamer sequences are larger in size and complex 3D structure makes it less rigid on sealing the caps. In addition, aptamer has a tendency to bind a cell surface, which makes it attractive to other molecules or surfaces in serum, following an opening of the seal effect of which depends on the strength of its binding to any unwanted target. From these perspectives modified oligo capping seems to be advantageous.



However, aptamer-based capping has its own advantages. First of all, it is easier to find an aptamer from literature or new researches than finding a nuclease specific to the target to be issued. With cell-SELEX, no need for discovering whether there is an enzyme to be utilized, just synthetically choosing the right sequence will give the result at least in theory. Another advantage of aptamer is in fact a disadvantageous of nuclease specific oligo capping mechanism. The aim of the targeted drug delivery is literally “target” the disease itself than administrating the drug for therapy. Unlike aptamer-gating, oligo-gating mechanism “target” not the disease itself but an indication of its presence; micrococcal nuclease. And since micrococcal nuclease is an enzyme assumed to be found in the bloodstream in case of a disease, the “targeting” of such a mechanism will direct the release of the drug theoretically anywhere in the bloodstream, certainly with higher accuracy toward the location of disease, where is also the source of micrococcal nuclease. On the other hand aptamer-gating mechanism allow the drug to release only in case of the presence of the “target” itself. In addition, if the oligo-capping is cleaved once, the sealing mechanism will be lost completely. In the case of aptamer-gating, opening of aptamer has a potential to seal back, which may have further application potential in different strategies.

Both of the capping mechanisms achieved to lower the MIC of vancomycin administration about 0.7  $\mu\text{g}/\text{mL}$  and such a decrease in MIC can be regarded as a “game changer” from the resistance classification of pathogenic microorganisms to clinical treatment strategy of drugs. However, any advantageous or disadvantageous proposed here are remained to be weak and unstable assumptions as long as experimented *in vivo*. This study is only a proof-of-concept for observing the potential of such a drug delivery system combining both the capping and targeting of drug in a simplified system. It can be anticipated that the concept of gated antibiotic nanoparticles is not limited to bacterial infections, but that it bears the potential to be transformed into therapeutic alternatives for other infectious diseases (e.g. virus and

fungi) or cancer treatment. The result of this study may be expanded with *in vivo* experiments, including using completely modified aptamers for resistance. As long as antibiotics are used, new resistance challenges and new theranostic approaches encompassing both diagnostic and therapeutic actions will emerge. This study has been an attempt to pave a way on behalf of innovative approaches.

#### **4.1 Future Studies**

New studies and research topics can be derived based on the different perspective of from this study. For future studies to be determined, sectional approach is assumed: future studies for nanoparticle construct, drug to be delivered, diseases to be challenged, supportive and *in vivo* studies.

New research projects can be performed is to try out the mesoporous silica particles with different pore sizes and pore morphologies other than used in this study and to determine the limits of utilization of a system fitted on this platform. In addition, modification of the nanoparticles can be diversified (for example amine modification of the surface and glutaraldehyde coupling of oligonucleotides (Bayramoglu, Ozalp, Dincbal, & Arica, 2018)) in order to determine more effective binding method with respect to change in the construct or target to be issued. Since the nanoparticles by themselves (even loaded with antibiotics) did not effect of the bacterial growth in a negative manner (observed from the MIC analysis and time-kill curves of control organism *S. epidermidis*) possible unloaded nanoparticles were not in the focus of the research. However, with a possibility of clinical usage, parameters like unloaded particles, loading efficiency and leakage in long term (as a shelf-life) should be thoroughly experimented and a following research project may be initiated focusing on these challenges.

For antibiotic administration only one molecule; vancomycin has been used in this study, but clinical applications can be subject to a new challenge with usage of more than one drug. There are two strategies for this purpose; combinations of two or more antibiotics and antibiotic/adjuvant combinations. In the first one, different antibiotics are utilized for; targeting of different pathways, targeting different stages of same target (for example cell wall synthesis) and, targeting same step in different ways. In the second strategy, adjuvant molecules (such as  $\beta$ -lactamase inhibitor; clavulanic acid) aiming the resistance mechanism can be coupled with the antibiotic in order to overcome antibiotic resistance and increase the efficiency of antibiotic (Worthington & Melander, 2013). The pathway of the pathogenic bacterium is particularly successful. The potential of the system for clinical situations can be tested *in vitro* with both drug-drug combinations and drug-adjuvant combinations.

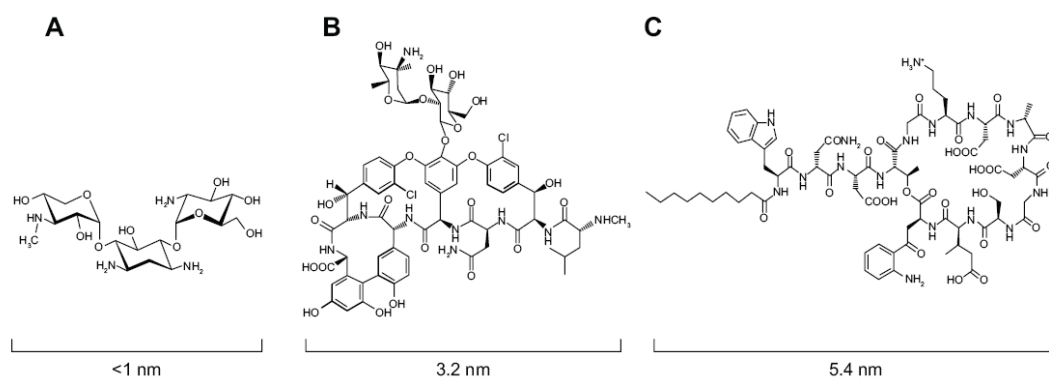


Figure 30 Chemical structures of different antibiotics for experimenting mesoporous particle release kinetics. A) gentamicin as an example for small antibiotic, B) vancomycin as an example of medium-sized antibiotic, C) daptomycin as an example of large antibiotic molecule (Atefyekta et al., 2016).

Vancomycin has been used as a large molecule in this work to force the system. However, when other antibiotic molecules are considered, it can be termed a medium-sized molecule. For example, gentamicin has a size of 1 nanometer, while daptomycin has a size of 5.4 nanometers (Figure 30). This study may also be repeated with these

antibiotics as a derivative and to demonstrate the effectiveness of mesoporous silica particle-based drug delivery system. Experiments with larger molecules may gain importance when it is thought that some of the new generation antibiotics developed against antibiotic resistance are various modifications of the current antibiotics and thus are increasing in size. Gentamicin, being a small molecule, can be used as a model for unwanted leakage challenge until the drug reaches its target, may exemplify the struggle against a small scale molecules, another challenge for the system of this study. These molecules have been tried in another study for the release performance of mesoporous titania particles for modelling molecules with different hydrophobicity and size (Atefyekta et al., 2016) and clinical potential of mesoporous particles can be examined with the system developed in this study.

Within the scope of the study, target and control organisms were provided from ATCC strains for proof-of-concept. This study can be repeated with moderate or high grade resistance clinical strains to examine the performance of the system because the resistance gained by the bacteria usually includes mutations that greatly increase the minimum inhibitory concentrations of the antibiotics. It has been shown in this study that the developed system is released at a high concentration near the pathogenic bacterial site but the drug concentration from the covers to be opened besides the bacteria with resistance at a certain scale can be examined by conventional methods against the bacteria which can not break the resistance. In the event of such a positive outcome, there is the possibility that many antibiotics that we think have lost function in our arsenal may be used again clinically. Thus, such a research project is worth initiating.

This developed system can be also be tested against other bacteria as well as against the pathogenic microorganisms like fungi or viruses for both diagnosis and treatment purposes. With respect to the effective environment of the target issued, different mediums apart form the human serum should be studied in order to prove the

robustness of the system. For example, microflora and environmental conditions of human mouth is unlike any other environment. A research project with respect to such conditions may flourish new scientific and technological findings.

Both this study and other researches found in the literature utilizing mesoporous silica particles has been based on the inhibition or killing of bacterial or cancer cells. Future studies may be diversified against cardiovascular diseases such as plaque formation or autoimmune diseases such as rheumatoid arthritis. Such studies will demonstrate the robustness and clinical applicability of the system. Alternative uses, such as the repair of damaged tissues or the prevention of apoptosis mechanisms leading to cell death in organ transplants, are also potential areas of use that need to be investigated by scientific and technological studies.

It is possible to use this system in combination with different systems for the sake of future studies. For example, boron-containing chemicals can be used in the applications to be used as a radioactive therapy of cancer cells in the treatment of tumor cells called Boron-Neutron Capture Therapy (BNCT). BNCT is radiation therapy with less side effect, having clinical usage and equipment currently in hospitals (Mitsumoto et al., 2018). When Boron-10, a stable isotope, is irradiated with low-energy thermal neutrons to yield  $\alpha$  particles (Helium-4) and recoiling lithium-7 nuclei, the gamma rays can destruct with high energy and low effective area. Thus, targeting any boron containing agent near enough and concentrated enough, treatment can be achieved (Nedunchezian, Aswath, Thirupathy, & Thirugnanamurthy, 2016). For the sake of using the proposed system in this study (either with enzymatic or affinity-oriented capping/targeting approach) sodium borocaptate ( $\text{Na}_2\text{B}_{12}\text{H}_{11}\text{SH}$ ) can be used as delivered drug which is one of the two boron delivery agents used by clinical practice.

It has been found that the cost of the system can be analyzed in two different ways. Considering the usage of modified nucleotides the aptamer gating mechanisms seems

to be cheaper. However, most probably *in vivo* trials, aptamer sequence will also be modified and the cost of the aptamer has a potential to outrun the serum nuclease resistant modified oligonucleotide sequence due to difference in lengths. In such a scenario, the cost of the system changes dramatically whether a modification will be performed before or after the synthesis of the sequence. Another consideration of the cost comparison can be made specific to the application. Vancomycin, which is used in particular for the study, is higher in cost than the proposed system. Thus, when it is considered specifically for vancomycin, since effective vancomycin concentration is nearly 1/3 of the conventional usage, incorporation of such system to clinical trials may have a potential to decrease the cost of the treatment. In addition, such system may apply to many drugs that are above a certain price like drugs for cancer treatment.

In combination with the biotechnology experiments computer modeling can be performed as the derivation and supporter of this work. In particular, the mechanism and dynamics of nucleic acid valve system before any *in vivo* experiments and clinical trials can be examined by modeling the dynamics of involuntary parameters and the opening of the flap from the opening. The computer modelling is both outside the scope of the study and expertise of the researcher, such modelling studies can provide an advantage for the commercial and technological success of the targeted drug delivery platform being developed. However, in the final step of all studies, this system should be experimented *in vivo* conditions in order to understand the real application potential for clinical uses. Decreasing the MIC of drug was an achievement but without real-life applications, all such studies will remain to be a “step” rather than “achievement” toward combating antimicrobial resistance mechanisms.

In conclusion, a convention-alternative therapeutic strategy for *S. aureus* with high efficiency, specificity and active drug delivery capabilities were proposed and tested. In principle, the described aptamer-gated or serum nuclease resistant-gated silica nanoparticles allow administering of antibiotics at a lower dosage. The same delivery

method can be further expanded to the use of stronger therapeutic compounds or combination of drugs (polytherapy) in a safer manner. In this way, the approach proposed may contribute to diminishing bacterial resistance development against our last standing antibacterial arsenal.





## REFERENCES

- Abbaspour, A., Norouz-Sarvestani, F., Noori, A., & Soltani, N. (2015). Aptamer-conjugated silver nanoparticles for electrochemical dual-aptamer-based sandwich detection of staphylococcus aureus. *Biosensors and Bioelectronics*, *68*, 149–155. <https://doi.org/10.1016/j.bios.2014.12.040>
- Adam Raw. (n.d.). Mesoporous Materials: Properties and Applications. Retrieved September 4, 2017, from <http://www.sigmaaldrich.com/technical-documents/articles/materials-science/mesoporous-materials.html>
- Ajnai, G., Chiu, A., Kan, T., Cheng, C.-C., Tsai, T.-H., & Chang, J. (2014). Trends of Gold Nanoparticle-based Drug Delivery System in Cancer Therapy. *Journal of Experimental & Clinical Medicine*, *6*(6), 172–178. <https://doi.org/10.1016/j.jecm.2014.10.015>
- Allothman, Z. (2012). *A Review: Fundamental Aspects of Silicate Mesoporous Materials*. *Materials* (Vol. 5). <https://doi.org/10.3390/ma5122874>
- Atefyekta, S., Ercan, B., Karlsson, J., Taylor, E., Chung, S., Webster, T. J., & Andersson, M. (2016). Antimicrobial performance of mesoporous titania thin films: role of pore size, hydrophobicity, and antibiotic release. *International Journal of Nanomedicine*, *11*, 977–990. <https://doi.org/10.2147/IJN.S95375>
- Ball, L.-J., Goult, C. M., Donarski, J. A., Micklefield, J., & Ramesh, V. (2004). NMR structure determination and calcium binding effects of lipopeptide antibiotic daptomycin. *Organic & Biomolecular Chemistry*, *2*(13), 1872–1878. <https://doi.org/10.1039/B402722A>
- Baltz, R. H. (2009). Daptomycin: mechanisms of action and resistance, and biosynthetic engineering. *Current Opinion in Chemical Biology*, *13*(2), 144–151. <https://doi.org/http://dx.doi.org/10.1016/j.cbpa.2009.02.031>

- Barna, J. C., & Williams, D. H. (1984). The structure and mode of action of glycopeptide antibiotics of the vancomycin group. *Annual Review of Microbiology*, 38, 339–357. <https://doi.org/10.1146/annurev.mi.38.100184.002011>
- Bayramoglu, G., Ozalp, V. C., Dincbal, U., & Arica, M. Y. (2018). Fast and Sensitive Detection of Salmonella in Milk Samples Using Aptamer-Functionalized Magnetic Silica Solid Phase and MCM-41-Aptamer Gate System. *ACS Biomaterials Science & Engineering*, 4(4), 1437–1444. <https://doi.org/10.1021/acsbiomaterials.8b00018>
- Berends, E. T. M., Horswill, A. R., Haste, N. M., Monestier, M., Nizet, V., & von Kückritz-Blickwede, M. (2010). Nuclease Expression by *Staphylococcus aureus* Facilitates Escape from Neutrophil Extracellular Traps. *Journal of Innate Immunity*, 2(6), 576–586. <https://doi.org/10.1159/000319909>
- Boisgard, R., Kuhnast, B., Vonhoff, S., Younes, C., Hinnen, F., Verbavatz, J. M., ... Tavitian, B. (2005). In vivo biodistribution and pharmacokinetics of F-18-labelled Spiegelmers: a new class of oligonucleotidic radiopharmaceuticals. *European Journal of Nuclear Medicine and Molecular Imaging*, 32(4), 470–477. <https://doi.org/10.1007/s00259-004-1669-8>
- Boychev, H., & Parsons, V. (2016). British study’s claim 10 million people a year could die because of antibiotic resistance dismissed as “unreliable.” Retrieved December 11, 2017, from <http://www.independent.co.uk/news/science/antimicrobial-resistance-superbugs-death-toll-new-study-flawed-assumptions-british-amr-review-david-a7481396.html>
- BRENDA. (2017). Information on EC 3.1.31.1 - micrococcal nuclease. Retrieved September 4, 2017, from <http://www.brenda-enzymes.org/enzyme.php?ecno=3.1.31.1>
- Brigham, R. B., & Pittenger, R. C. (1956). *Streptomyces orientalis*, n. sp., the source of vancomycin. *Antibiotics & Chemotherapy (Northfield, Ill.)*, 6(11), 642–647.
- Brunauer, S., Emmett, P. H., & Teller, E. (1938). Adsorption of Gases in Multimolecular Layers. *Journal of the American Chemical Society*, 60(2), 309–319. <https://doi.org/10.1021/ja01269a023>

- Bruno, J. G., & Carrillo, M. P. (2012). Development of Aptamer Beacons for Rapid Presumptive Detection of Bacillus Spores. *Journal of Fluorescence*, 22(3), 915–924. <https://doi.org/10.1007/s10895-011-1030-0>
- Bruno, J. G., Carrillo, M. P., & Phillips, T. (2008). In Vitro antibacterial effects of antilipopolsaccharide DNA aptamer-C1qrs complexes. *Folia Microbiologica*, 53(4), 295–302. <https://doi.org/10.1007/s12223-008-0046-6>
- Cao, X., Li, S., Chen, L., Ding, H., Xu, H., Huang, Y., ... Shao, N. (2009). Combining use of a panel of ssDNA aptamers in the detection of Staphylococcus aureus. *Nucleic Acids Research*, 37(14), 4621–4628. <https://doi.org/10.1093/nar/gkp489>
- Cauda, V., Onida, B., Platschek, B., Muhlstein, L., & Bein, T. (2008). Large antibiotic molecule diffusion in confined mesoporous silica with controlled morphology. *Journal of Materials Chemistry*, 18(48), 5888–5899. <https://doi.org/10.1039/B805395B>
- Chang, C.-C., Wei, S.-C., Wu, T.-H., Lee, C.-H., & Lin, C.-W. (2013). Aptamer-based colorimetric detection of platelet-derived growth factor using unmodified gold nanoparticles. *Biosensors & Bioelectronics*, 42, 119–123. <https://doi.org/10.1016/j.bios.2012.10.072>
- Chen, B., Dai, W., He, B., Zhang, H., Wang, X., Wang, Y., & Zhang, Q. (2017). Current Multistage Drug Delivery Systems Based on the Tumor Microenvironment. *Theranostics*, 7(3), 538–558. <https://doi.org/10.7150/thno.16684>
- Cho, E. C., Glaus, C., Chen, J., Welch, M. J., & Xia, Y. (2010). Inorganic nanoparticle-based contrast agents for molecular imaging. *Trends in Molecular Medicine*, 16(12), 561–573. <https://doi.org/10.1016/j.molmed.2010.09.004>
- Choi, S. K., Lee, C., Lee, K. S., Choe, S.-Y., Mo, I. P., Seong, R. H., ... Jeon, S. H. (2011). DNA aptamers against the receptor binding region of hemagglutinin prevent avian influenza viral infection. *Molecules and Cells*, 32(6), 527–533. <https://doi.org/10.1007/s10059-011-0156-x>

Clarivate Analytics. (2018). Web of Science. Retrieved February 16, 2018, from [http://0-apps.webofknowledge.com.library.metu.edu.tr/WOS\\_AdvancedSearch\\_input.do?product=WOS&SID=D1EINOVfUs1qNKrt1bu&search\\_mode=AdvancedSearch](http://0-apps.webofknowledge.com.library.metu.edu.tr/WOS_AdvancedSearch_input.do?product=WOS&SID=D1EINOVfUs1qNKrt1bu&search_mode=AdvancedSearch)

Clinical and Laboratory Standards Institute. (2006). *Methods for Dilution Antimicrobial Susceptibility Tests for Bacteria That Grow Aerobically; Approved Standard—Ninth Edition. Clinical and Laboratory Standards Institute* (Vol. 32).

Coates, A. R. M., Halls, G., & Hu, Y. (2011). Novel classes of antibiotics or more of the same? *British Journal of Pharmacology*, *163*(1), 184–194. <https://doi.org/10.1111/j.1476-5381.2011.01250.x>

Collins, A. M. (2012). Chapter 3 - Common Analytical Techniques for Nanoscale Materials BT - Nanotechnology Cookbook (pp. 17–33). Oxford: Elsevier. <https://doi.org/https://doi.org/10.1016/B978-0-08-097172-8.00003-5>

Conly, J. M., & Johnston, B. L. (2005). Where are all the new antibiotics? The new antibiotic paradox. *The Canadian Journal of Infectious Diseases & Medical Microbiology*, *16*(3), 159–160. Retrieved from <http://www.ncbi.nlm.nih.gov/pmc/articles/PMC2095020/>

Cruz-Toledo, J., McKeague, M., Zhang, X., Giamberardino, A., McConnell, E., Francis, T., ... Dumontier, M. (2012). Aptamer base: a collaborative knowledge base to describe aptamers and SELEX experiments. *Database: The Journal of Biological Databases and Curation*, *2012*, bas006. <https://doi.org/10.1093/database/bas006>

Davies, J., & Davies, D. (2010). Origins and Evolution of Antibiotic Resistance. *Microbiology and Molecular Biology Reviews: MMBR*, *74*(3), 417–433. <https://doi.org/10.1128/MMBR.00016-10>

De Jong, W. H., & Borm, P. J. A. (2008). Drug delivery and nanoparticles:

Applications and hazards. *International Journal of Nanomedicine*, 3(2), 133–149. Retrieved from <http://www.ncbi.nlm.nih.gov/pmc/articles/PMC2527668/>

- Deng, Q., Watson, C. J., & Kennedy, R. T. (2003). Aptamer affinity chromatography for rapid assay of adenosine in microdialysis samples collected in vivo. *Journal of Chromatography A*, 1005(1–2), 123–130. [https://doi.org/10.1016/s0021-9673\(03\)00812-4](https://doi.org/10.1016/s0021-9673(03)00812-4)
- Dilworth, T. J., Sliwinski, J., Ryan, K., Dodd, M., & Mercier, R.-C. (2014). Evaluation of vancomycin in combination with piperacillin-tazobactam or oxacillin against clinical methicillin-resistant *Staphylococcus aureus* Isolates and vancomycin-intermediate *S. aureus* isolates in vitro. *Antimicrobial Agents and Chemotherapy*, 58(2), 1028–1033. <https://doi.org/10.1128/AAC.01888-13>
- Dingwall, C., Lomonosoff, G. P., & Laskey, R. A. (1981). High sequence specificity of micrococcal nuclease. *Nucleic Acids Research*, 9(12), 2659–2673.
- Doessing, H., Hansen, L. H., Veedu, R. N., Wengel, J., & Vester, B. (2012). Amplification and Re-Generation of LNA-Modified Libraries. *Molecules*, 17(11), 13087–13097. <https://doi.org/10.3390/molecules171113087>
- Dortet, L., Anguel, N., Fortineau, N., Richard, C., & Nordmann, P. (2013). In vivo acquired daptomycin resistance during treatment of methicillin-resistant *Staphylococcus aureus* endocarditis. *International Journal of Infectious Diseases*, 17(11), e1076–e1077. <https://doi.org/http://dx.doi.org/10.1016/j.ijid.2013.02.019>
- Drolet, D. W., Moon-McDermott, L., & Romig, T. S. (1996). An enzyme-linked oligonucleotide assay. *Nature Biotechnology*, 14, 1021. Retrieved from <http://dx.doi.org/10.1038/nbt0896-1021>
- Duan, N., Wu, S., Chen, X., Huang, Y., & Wang, Z. (2012). Selection and identification of a DNA aptamer targeted to *Vibrio parahemolyticus*. *Journal of Agricultural and Food Chemistry*, 60(16), 4034–4038. <https://doi.org/10.1021/jf300395z>
- Dubois, C., Campbell, M. A., Edwards, S. L., Wengel, J., & Veedu, R. N. (2012). Stepping towards highly flexible aptamers: enzymatic recognition studies of

unlocked nucleic acid nucleotides. *Chemical Communications*, 48(44), 5503–5505. <https://doi.org/10.1039/c2cc31316b>

Dwivedi, H. P., Smiley, R. D., & Jaykus, L.-A. (2010). Selection and characterization of DNA aptamers with binding selectivity to *Campylobacter jejuni* using whole-cell SELEX. *Applied Microbiology and Biotechnology*, 87(6), 2323–2334. <https://doi.org/10.1007/s00253-010-2728-7>

Eisenstein, B. I., Oleson Frederick B., J., & Baltz, R. H. (2010). Daptomycin: From the Mountain to the Clinic, with Essential Help from Francis Tally, MD. *Clinical Infectious Diseases*, 50(Supplement\_1), S10–S15. Retrieved from <http://dx.doi.org/10.1086/647938>

Ellington, A. D., & Szostak, J. W. (1990). In vitro selection of RNA molecules that bind specific ligands. *Nature*, 346(6287), 818–822. Retrieved from <http://dx.doi.org/10.1038/346818a0>

Escudero-Abarca, B. I., Suh, S. H., Moore, M. D., Dwivedi, H. P., & Jaykus, L.-A. (2014). Selection, Characterization and Application of Nucleic Acid Aptamers for the Capture and Detection of Human Norovirus Strains. *PLoS ONE*, 9(9), e106805. <https://doi.org/10.1371/journal.pone.0106805>

Flenker, K. S., Burghardt, E. L., Dutta, N., Burns, W. J., Grover, J. M., Kenkel, E. J., ... McNamara, J. O. (2017). Rapid Detection of Urinary Tract Infections via Bacterial Nuclease Activity. *Molecular Therapy*, 25(6), 1353–1362. <https://doi.org/https://doi.org/10.1016/j.ymthe.2017.03.015>

Gardete, S., & Tomasz, A. (2014). Mechanisms of vancomycin resistance in *Staphylococcus aureus*. *The Journal of Clinical Investigation*, 124(7), 2836–2840. <https://doi.org/10.1172/JCI68834>

Golezani, A. S., Fateh, A. S., & Mehrabi, H. A. (2016). Synthesis and characterization of silica mesoporous material produced by hydrothermal continues pH adjusting path way. *Progress in Natural Science: Materials International*, 26(4), 411–414. <https://doi.org/http://dx.doi.org/10.1016/j.pnsc.2016.07.003>

- Gopinath, S. C. B., Hayashi, K., & Kumar, P. K. R. (2012). Aptamer that binds to the gD protein of herpes simplex virus 1 and efficiently inhibits viral entry. *Journal of Virology*, 86(12), 6732–6744. <https://doi.org/10.1128/JVI.00377-12>
- Gupta, N., Limbago, B. M., Patel, J. B., & Kallen, A. J. (2011). Carbapenem-Resistant Enterobacteriaceae: Epidemiology and Prevention. *Clinical Infectious Diseases*, 53(1), 60–67. Retrieved from <http://dx.doi.org/10.1093/cid/cir202>
- Hamula, C. L., Le, X. C., & Li, X. F. (2011). DNA aptamers binding to multiple prevalent M-types of *Streptococcus pyogenes*. *Anal Chem*, 83(10), 3640–3647. <https://doi.org/10.1021/ac200575e>
- Hanrahan, J. P., O'Mahony, T. F., Tobin, J. M., & Hogan, J. J. (n.d.). Mesoporous Silica and their Applications. Retrieved September 4, 2017, from <http://www.sigmaaldrich.com/technical-documents/articles/materials-science/renewable-alternative-energy/mesoporous-silica.html>
- Hernandez, F. J., Hernandez, L. I., Pinto, A., Schäfer, T., & Özalp, V. C. (2013). Targeting cancer cells with controlled release nanocapsules based on a single aptamer. *Chemical Communications*, 49(13), 1285. <https://doi.org/10.1039/c2cc37370j>
- Hernandez, F. J., Huang, L., Olson, M. E., Powers, K. M., Hernandez, L. I., Meyerholz, D. K., ... McNamara, J. O. (2014). Noninvasive imaging of *Staphylococcus aureus* infections with a nuclease-activated probe. *Nat Med*, 20(3), 301–306. <https://doi.org/10.1038/nm.3460><http://www.nature.com/nm/journal/v20/n3/abs/nm.3460.html#supplementary-information>
- Hernandez, F. J., Huang, L., Olson, M. E., Powers, K. M., Hernandez, L. I., Meyerholz, D. K., ... McNamara, J. O. (2014). Non-invasive Imaging of *Staphylococcus aureus* Infections with a Nuclease-Activated Probe. *Nature Medicine*, 20(3), 301–306. <https://doi.org/10.1038/nm.3460>
- Hernandez, F. J., Kalra, N., Wengel, J., & Vester, B. (2009). Aptamers as a model for functional evaluation of LNA and 2'-amino LNA. *Bioorganic & Medicinal Chemistry Letters*, 19(23), 6585–6587.

<https://doi.org/10.1016/j.bmcl.2009.10.039>

Hunter, A. C., Elsom, J., Wibroe, P. P., & Moghimi, S. M. (2012). Polymeric particulate technologies for oral drug delivery and targeting: A pathophysiological perspective. *Maturitas*.  
<https://doi.org/10.1016/j.maturitas.2012.05.014>

Hur, J., Jawale, C., & Lee, J. H. (2012). Antimicrobial resistance of Salmonella isolated from food animals: A review. *Food Research International*, 45(2), 819–830. <https://doi.org/10.1016/j.foodres.2011.05.014>

Hwang, J., Son, J., Seo, Y., Jo, Y., Lee, K., Lee, D., ... Choi, J. (2018). Functional silica nanoparticles conjugated with beta-glucan to deliver anti-tuberculosis drug molecules. *Journal of Industrial and Engineering Chemistry*, 58, 376–385. <https://doi.org/https://doi.org/10.1016/j.jiec.2017.09.051>

Hyeon, J.-Y., Chon, J.-W., Choi, I.-S., Park, C., Kim, D.-E., & Seo, K.-H. (2012). Development of RNA aptamers for detection of *Salmonella Enteritidis*. *Journal of Microbiological Methods* (Vol. 89).  
<https://doi.org/10.1016/j.mimet.2012.01.014>

Igarashi, M., Sawa, R., Kinoshita, N., Hashizume, H., Nakagawa, N., Homma, Y., ... Akamatsu, Y. (2008). Pargamicin A, a novel cyclic peptide antibiotic from *Amycolatopsis* sp. *The Journal of Antibiotics*, 61(6), 387–393. <https://doi.org/10.1038/ja.2008.54>

Jayasena, S. D. (1999). Aptamers: An Emerging Class of Molecules That Rival Antibodies in Diagnostics. *Clinical Chemistry*, 45(9), 1628–1650. Retrieved from <http://www.clinchem.org/content/45/9/1628.abstract>

Joshi, R., Janagama, H., Dwivedi, H. P., Kumar, T., Jaykus, L. A., Scheffers, J., & Sreevatsan, S. (2009). Selection, characterization, and application of DNA aptamers for the capture and detection of *Salmonella enterica* serovars. *Molecular and Cellular Probes*, 23(1), 20–28. <https://doi.org/10.1016/j.mcp.2008.10.006>



- Kalhapure, R. S., Jadhav, M., Rambharose, S., Mocktar, C., Singh, S., Renukuntla, J., & Govender, T. (2017). pH-responsive chitosan nanoparticles from a novel twin-chain anionic amphiphile for controlled and targeted delivery of vancomycin. *Colloids and Surfaces. B, Biointerfaces*, 158, 650–657. <https://doi.org/10.1016/j.colsurfb.2017.07.049>
- Khan, N. T. (2017). *Nanoparticles Mediated Drug Delivery*. *Journal of Pharmacogenomics & Pharmacoproteomics* (Vol. 08). <https://doi.org/10.4172/2153-0645.1000172>
- Khati, M., Schuman, M., Ibrahim, J., Sattentau, Q., Gordon, S., & James, W. (2003). Neutralization of infectivity of diverse R5 clinical isolates of human immunodeficiency virus type 1 by gp120-binding 2'F-RNA aptamers. *Journal of Virology*, 77(23), 12692–12698.
- Kompella, U. B., Amrite, A. C., Ravi, R. P., & Durazo, S. A. (2013). Nanomedicines for Back of the Eye Drug Delivery, Gene Delivery, and Imaging. *Progress in Retinal and Eye Research*, 36, 172–198. <https://doi.org/10.1016/j.preteyeres.2013.04.001>
- Kraemer, S., Vaught, J. D., Bock, C., Gold, L., Katilius, E., Keeney, T. R., ... Sanders, G. M. (2011). From SOMAmer-Based Biomarker Discovery to Diagnostic and Clinical Applications: A SOMAmer-Based, Streamlined Multiplex Proteomic Assay. *PLoS ONE*, 6(10), e26332. <https://doi.org/10.1371/journal.pone.0026332>
- Kresge, C. T., Leonowicz, M. E., Roth, W. J., Vartuli, J. C., & Beck, J. S. (1992). Ordered mesoporous molecular sieves synthesized by a liquid-crystal template mechanism. *Nature*, 359(6397), 710–712. Retrieved from <http://dx.doi.org/10.1038/359710a0>
- Kruk, M., Jaroniec, M., & Sayari, A. (1997). Application of Large Pore MCM-41 Molecular Sieves To Improve Pore Size Analysis Using Nitrogen Adsorption Measurements. *Langmuir*, 13(23), 6267–6273. <https://doi.org/10.1021/la970776m>
- Kruspe, S., Dickey, D. D., Urak, K. T., Blanco, G. N., Miller, M. J., Clark, K. C., ... Giangrande, P. H. (2017). Rapid and Sensitive Detection of Breast Cancer Cells in Patient Blood with Nuclease-Activated Probe Technology. *Molecular Therapy - Nucleic Acids*, 8, 542–557.

<https://doi.org/https://doi.org/10.1016/j.omtn.2017.08.004>

- Kubik, M. F., Bell, C., Fitzwater, T., Watson, S. R., & Tasset, D. M. (1997). Isolation and characterization of 2'-fluoro-, 2'-amino-, and 2'-fluoro-/amino-modified RNA ligands to human IFN-gamma that inhibit receptor binding. *Journal of Immunology (Baltimore, Md. : 1950)*, *159*(1), 259–267.
- Kujau, M. J., & Wöfl, S. (1998). Intramolecular derivatization of 2'-amino-pyrimidine modified RNA with functional groups that is compatible with re-amplification. *Nucleic Acids Research*, *26*(7), 1851–1853. Retrieved from <http://www.ncbi.nlm.nih.gov/pmc/articles/PMC147467/>
- Kulkarni, V., Kulkarni, D., Nilekar, S., & More, S. (2017). Methicillin, Vancomycin and Multidrug-Resistance Among Staphylococcus Aureus. *National Journal of Integrated Research in Medicine*, *8*(3), 68–74. Retrieved from <http://www.nicpdjournals.com/?mno=271323>
- Kumar, B., Jalodia, K., Kumar, P., & Gautam, H. K. (2017). Recent advances in nanoparticle-mediated drug delivery. *Journal of Drug Delivery Science and Technology*, *41*, 260–268. <https://doi.org/https://doi.org/10.1016/j.jddst.2017.07.019>
- Kumar, S., Malik, M. M., & Purohit, R. (2017). Synthesis Methods of Mesoporous Silica Materials. *Materials Today: Proceedings*, *4*(2, Part A), 350–357. <https://doi.org/https://doi.org/10.1016/j.matpr.2017.01.032>
- Labib, M., Zama, A. S., Muharemagic, D., Chechik, A. V., Bell, J. C., & Berezovski, M. V. (2012). Aptamer-Based Viability Impedimetric Sensor for Viruses. *Analytical Chemistry*, *84*(4), 1813–1816. <https://doi.org/10.1021/ac203412m>
- Lee, Y. J., Han, S. R., Maeng, J.-S., Cho, Y.-J., & Lee, S.-W. (2012). In vitro selection of Escherichia coli O157:H7-specific RNA aptamer. *Biochemical and Biophysical Research Communications*, *417*(1), 414–420. <https://doi.org/10.1016/j.bbrc.2011.11.130>
- Li, H., Ding, X., Peng, Z., Deng, L., Wang, D., Chen, H., & He, Q. (2011). Aptamer

selection for the detection of Escherichia coli K88. *Canadian Journal of Microbiology*, 57(6), 453–459. <https://doi.org/10.1139/w11-030>

Li, Z., Barnes, J. C., Bosoy, A., Stoddart, J. F., & Zink, J. I. (2012). Mesoporous silica nanoparticles in biomedical applications. *Chemical Society Reviews*, 41(7), 2590–2605. <https://doi.org/10.1039/C1CS15246G>

Liss, M., Petersen, B., Wolf, H., & Prohaska, E. (2002). An aptamer-based quartz crystal protein biosensor. *Analytical Chemistry*, 74(17), 4488–4495. <https://doi.org/10.1021/ac011294p>

Liu, G., Yu, X., Xue, F., Chen, W., Ye, Y., Yang, X., ... Zong, K. (2012). Screening and preliminary application of a DNA aptamer for rapid detection of Salmonella O8. *Microchimica Acta*, 178(1), 237–244. <https://doi.org/10.1007/s00604-012-0825-2>

Liu, X., & Yuan, Q. (2018). Fluorescence Sandwich Assays for Nucleic Acid Detection BT - Biosensors Based on Sandwich Assays. In F. Xia, X. Zhang, X. Lou, & Q. Yuan (Eds.) (pp. 107–125). Singapore: Springer Singapore. [https://doi.org/10.1007/978-981-10-7835-4\\_7](https://doi.org/10.1007/978-981-10-7835-4_7)

Loomba, P. S., Taneja, J., & Mishra, B. (2010). Methicillin and Vancomycin Resistant *S. aureus* in Hospitalized Patients. *Journal of Global Infectious Diseases*, 2(3), 275–283. <https://doi.org/10.4103/0974-777X.68535>

Lübbecke, M., Walter, J.-G., Stahl, F., & Scheper, T. (2012). Aptamers as detection molecules on reverse phase protein microarrays for the analysis of cell lysates. *Engineering in Life Sciences*, 12(2), 144–151. <https://doi.org/10.1002/elsc.201100100>

Ma, X., Jiang, Y., Jia, F., Yu, Y., Chen, J., & Wang, Z. (2014). An aptamer-based electrochemical biosensor for the detection of Salmonella. *Journal of Microbiological Methods*, 98, 94–98. <https://doi.org/10.1016/j.mimet.2014.01.003>

Mai, W. X., & Meng, H. (2013). Mesoporous silica nanoparticles: A multifunctional

- nano therapeutic system. *Integrative Biology: Quantitative Biosciences from Nano to Macro*, 5(1), 19–28. <https://doi.org/10.1039/c2ib20137b>
- Mairal, T., Ozalp, V. C., Lozano Sanchez, P., Mir, M., Katakis, I., & O’Sullivan, C. K. (2008). Aptamers: molecular tools for analytical applications. *Anal Bioanal Chem*, 390(4), 989–1007. <https://doi.org/10.1007/s00216-007-1346-4>
- Marimuthu, C., Tang, T.-H., Tominaga, J., Tan, S.-C., & Gopinath, S. C. B. (2012). Single-stranded DNA (ssDNA) production in DNA aptamer generation. *The Analyst*, 137(6), 1307–1315. <https://doi.org/10.1039/c2an15905h>
- Marty, F. M., Yeh, W. W., Wennersten, C. B., Venkataraman, L., Albano, E., Alyea, E. P., ... Pillai, S. K. (2006). Emergence of a Clinical Daptomycin-Resistant *Staphylococcus aureus* Isolate during Treatment of Methicillin-Resistant *Staphylococcus aureus* Bacteremia and Osteomyelitis. *Journal of Clinical Microbiology*, 44(2), 595–597. <https://doi.org/10.1128/JCM.44.2.595-597.2006>
- Mayer, G., Ahmed, M.-S. L., Dolf, A., Endl, E., Knolle, P. A., & Famulok, M. (2010). Fluorescence-activated cell sorting for aptamer SELEX with cell mixtures. *Nat. Protocols*, 5(12), 1993–2004. Retrieved from <http://dx.doi.org/10.1038/nprot.2010.163>
- McKenna, M. (2013, July). Antibiotic resistance: the last resort. *Nature*. England. <https://doi.org/10.1038/499394a>
- McKenzie, C. (2011). Antibiotic dosing in critical illness. *Journal of Antimicrobial Chemotherapy*, 66(suppl\_2), ii25-ii31. Retrieved from <http://dx.doi.org/10.1093/jac/dkq516>
- Meletis, G. (2016). Carbapenem resistance: overview of the problem and future perspectives. *Therapeutic Advances in Infectious Disease*, 3(1), 15–21. <https://doi.org/10.1177/2049936115621709>
- Mitsumoto, T., Fujita, K., Ogasawara, T., Tsutsui, H., Yajima, S., Heavy Industries, S., ... Tanaka, H. (2018). *BNCT SYSTEM USING 30 MEV H -CYCLOTRON*.
- Moore, M. D., Bunka, D. H. J., Forzan, M., Spear, P. G., Stockley, P. G., McGowan,

- I., & James, W. (2011). Generation of neutralizing aptamers against herpes simplex virus type 2: potential components of multivalent microbicides. *The Journal of General Virology*, 92(Pt 7), 1493–1499. <https://doi.org/10.1099/vir.0.030601-0>
- Murphy, C. J., Gole, A. M., Stone, J. W., Sisco, P. N., Alkilany, A. M., Goldsmith, E. C., & Baxter, S. C. (2008). Gold Nanoparticles in Biology: Beyond Toxicity to Cellular Imaging. *Accounts of Chemical Research*, 41(12), 1721–1730. <https://doi.org/10.1021/ar800035u>
- NCBI. (2018a). Rhodamine B. Retrieved May 12, 2018, from [https://pubchem.ncbi.nlm.nih.gov/compound/rhodamine\\_b#section=Top](https://pubchem.ncbi.nlm.nih.gov/compound/rhodamine_b#section=Top)
- NCBI. (2018b). Vancomycin. Retrieved May 12, 2018, from <https://pubchem.ncbi.nlm.nih.gov/compound/14969>
- Nedunchezian, K., Aswath, N., Thiruppathy, M., & Thirugnanamurthy, S. (2016). Boron Neutron Capture Therapy - A Literature Review. *Journal of Clinical and Diagnostic Research : JCDR*, 10(12), ZE01-ZE04. <https://doi.org/10.7860/JCDR/2016/19890.9024>
- Nieto, M., & Perkins, H. R. (1971). Physicochemical properties of vancomycin and iodovancomycin and their complexes with diacetyl-l-lysyl-d-alanyl-d-alanine. *Biochemical Journal*, 123(5), 773-.
- Ohk, S. H., Koo, O. K., Sen, T., Yamamoto, C. M., & Bhunia, A. K. (2010). Antibody-aptamer functionalized fibre-optic biosensor for specific detection of *Listeria monocytogenes* from food. *Journal of Applied Microbiology*, 109(3), 808–817. <https://doi.org/10.1111/j.1365-2672.2010.04709.x>
- Özalp, V. C., Nielsen, L. J., & Olsen, L. F. (2010). An Aptamer-Based Nanobiosensor for Real-Time Measurements of ATP Dynamics. *ChemBioChem*, 11(18), 2538–2541. <https://doi.org/10.1002/cbic.201000500>
- Ozalp, V. C., Pedersen, T. R., Nielsen, L. J., & Olsen, L. F. (2010). Time-resolved measurements of intracellular ATP in the yeast *Saccharomyces cerevisiae* using a new type of nanobiosensor. *J Biol Chem*, 285(48), 37579–37588. <https://doi.org/10.1074/jbc.M110.155119>

- Ozalp, V. C., & Schafer, T. (2011). Aptamer-based switchable nanovalves for stimuli-responsive drug delivery. *Chemistry*, *17*(36), 9893–9896. <https://doi.org/10.1002/chem.201101403>
- Özalp, V. C., & Schäfer, T. (2011). Aptamer-Based Switchable Nanovalves for Stimuli-Responsive Drug Delivery. *Chemistry - A European Journal*, *17*(36), 9893–9896. <https://doi.org/10.1002/chem.201101403>
- Padilla, R., & Sousa, R. (1999). Efficient synthesis of nucleic acids heavily modified with non-canonical ribose 2'-groups using a mutant T7 RNA polymerase (RNAP). *Nucleic Acids Research*, *27*(6), 1561–1563. Retrieved from <http://www.ncbi.nlm.nih.gov/pmc/articles/PMC148355/>
- Pan, Q., Zhang, X.-L., Wu, H.-Y., He, P.-W., Wang, F., Zhang, M.-S., ... Wu, J. (2005). Aptamers that preferentially bind type IVB pili and inhibit human monocytic-cell invasion by *Salmonella enterica* serovar typhi. *Antimicrobial Agents and Chemotherapy*, *49*(10), 4052–4060. <https://doi.org/10.1128/AAC.49.10.4052-4060.2005>
- Papayannopoulos, V. (2017). Neutrophil extracellular traps in immunity and disease. *Nature Reviews Immunology*, *18*, 134. Retrieved from <http://dx.doi.org/10.1038/nri.2017.105>
- Park, K. (2014). The Controlled Drug Delivery Systems: Past Forward and Future Back. *Journal of Controlled Release : Official Journal of the Controlled Release Society*, *190*, 3–8. <https://doi.org/10.1016/j.jconrel.2014.03.054>
- Park, S. Y., Kim, S., Yoon, H., Kim, K.-B., Kalme, S. S., Oh, S., ... Kim, D.-E. (2011). Selection of an antiviral RNA aptamer against hemagglutinin of the subtype H5 avian influenza virus. *Nucleic Acid Therapeutics*, *21*(6), 395–402. <https://doi.org/10.1089/nat.2011.0321>
- Pogliano, J., Pogliano, N., & Silverman, J. A. (2012). Daptomycin-Mediated Reorganization of Membrane Architecture Causes Mislocalization of Essential Cell Division Proteins. *Journal of Bacteriology*, *194*(17), 4494–4504. <https://doi.org/10.1128/JB.00011-12>

- Prosperi, M., Veras, N., Azarian, T., Rathore, M., Nolan, D., Rand, K., ... Salemi, M. (2013). Molecular epidemiology of community-associated methicillin-resistant *Staphylococcus aureus* in the genomic era: a cross-sectional study. *Scientific Reports*, 3, 1902. <https://doi.org/10.1038/srep01902>
- Rehm, S. J., & Tice, A. (2010). *Staphylococcus aureus*: Methicillin-Susceptible *S. aureus* to Methicillin-Resistant *S. aureus* and Vancomycin-Resistant *S. aureus*. *Clinical Infectious Diseases*, 51(Supplement\_2), S176–S182. Retrieved from <http://dx.doi.org/10.1086/653518>
- Reynolds, P. E. (1989). Structure, biochemistry and mechanism of action of glycopeptide antibiotics. *European Journal of Clinical Microbiology & Infectious Diseases : Official Publication of the European Society of Clinical Microbiology*, 8(11), 943–950.
- Rouquerol, J., Avnir, D., Fairbridge, C. W., Everett, D. H., Haynes, J. M., Pernicone, N., ... Unger, K. K. (1994). Recommendations for the characterization of porous solids (Technical Report). *Pure and Applied Chemistry*. <https://doi.org/10.1351/pac199466081739>
- Schäfer, M., Schneider, T. R., & Sheldrick, G. M. (2017). Crystal structure of vancomycin. *Structure*, 4(12), 1509–1515. [https://doi.org/10.1016/S0969-2126\(96\)00156-6](https://doi.org/10.1016/S0969-2126(96)00156-6)
- Sée, V., Free, P., Cesbron, Y., Nativo, P., Shaheen, U., Rigden, D. J., ... Lévy, R. (2009). Cathepsin L Digestion of Nanobioconjugates upon Endocytosis. *ACS Nano*, 3(9), 2461–2468. <https://doi.org/10.1021/nn9006994>
- Seper, A., Fengler, V. H. I., Roier, S., Wolinski, H., Kohlwein, S. D., Bishop, A. L., ... Schild, S. (2011). Extracellular nucleases and extracellular DNA play important roles in *Vibrio cholerae* biofilm formation. *Molecular Microbiology*, 82(4), 1015–1037. <https://doi.org/10.1111/j.1365-2958.2011.07867.x>
- Shi, B., Shin, Y. K., Hassanali, A. A., & Singer, S. J. (2015). DNA Binding to the Silica Surface. *The Journal of Physical Chemistry B*, 119(34), 11030–11040. <https://doi.org/10.1021/acs.jpcc.5b01983>

- Shi, H., He, X., Cui, W., Wang, K., Deng, K., Li, D., & Xu, F. (2014). Locked nucleic acid/DNA chimeric aptamer probe for tumor diagnosis with improved serum stability and extended imaging window in vivo. *Analytica Chimica Acta*, *812*, 138–144. <https://doi.org/10.1016/j.aca.2013.12.023>
- Shwetha, N., Selvakumar, L. S., & Thakur, M. S. (2013). Aptamer–nanoparticle-based chemiluminescence for p53 protein. *Analytical Biochemistry*, *441*(1), 73–79. <https://doi.org/http://dx.doi.org/10.1016/j.ab.2013.06.006>
- Sigma-Aldrich. (2017a). Nuclease micrococcal from *Staphylococcus aureus*. Retrieved September 4, 2017, from <http://www.sigmaaldrich.com/catalog/product/sigma/n3755?lang=en&region=NL#>
- Sigma-Aldrich. (2017b). Silica, mesostructured MCM-41 type (hexagonal). Retrieved June 6, 2017, from <http://www.sigmaaldrich.com/catalog/product/aldrich/643645?lang=en&region=TR>
- Silver, L. L. (2011). Challenges of antibacterial discovery. *Clinical Microbiology Reviews*, *24*(1), 71–109. <https://doi.org/10.1128/CMR.00030-10>
- Silverman, J. A., Perlmutter, N. G., & Shapiro, H. M. (2003). Correlation of daptomycin bactericidal activity and membrane depolarization in *Staphylococcus aureus*. *Antimicrobial Agents and Chemotherapy*, *47*(8), 2538–2544.
- Spellberg, B., Powers, J. H., Brass, E. P., Miller, L. G., & Edwards, J. E. J. (2004). Trends in antimicrobial drug development: implications for the future. *Clinical Infectious Diseases : An Official Publication of the Infectious Diseases Society of America*, *38*(9), 1279–1286. <https://doi.org/10.1086/420937>
- Stjern, L., Voittoinen, S., Weldemichel, R., Thuresson, S., Agnes, M., Benkovics, G., ... Valetti, S. (2017). Cyclodextrin-mesoporous silica particle composites for controlled antibiotic release. A proof of concept toward colon targeting. *International Journal of Pharmaceutics*, *531*(2), 595–605. <https://doi.org/https://doi.org/10.1016/j.ijpharm.2017.05.062>



- Sundaram, P., Wower, J., & Byrne, M. E. (2012). A nanoscale drug delivery carrier using nucleic acid aptamers for extended release of therapeutic. *Nanomedicine: Nanotechnology, Biology and Medicine*, 8(7), 1143–1151. <https://doi.org/http://dx.doi.org/10.1016/j.nano.2012.01.010>
- Swenson, J. M., Anderson, K. F., Lonsway, D. R., Thompson, A., McAllister, S. K., Limbago, B. M., ... Patel, J. B. (2009). Accuracy of Commercial and Reference Susceptibility Testing Methods for Detecting Vancomycin-Intermediate Staphylococcus aureus. *Journal of Clinical Microbiology*, 47(7), 2013–2017. <https://doi.org/10.1128/JCM.00221-09>
- Tang, F., Li, L., & Chen, D. (2012). Mesoporous Silica Nanoparticles: Synthesis, Biocompatibility and Drug Delivery. *Advanced Materials*, 24(12), 1504–1534. <https://doi.org/10.1002/adma.201104763>
- Tang, J., Hu, J., Kang, L., Deng, Z., Wu, J., & Pan, J. (2015). The use of vancomycin in the treatment of adult patients with methicillin-resistant Staphylococcus aureus (MRSA) infection: a survey in a tertiary hospital in China. *International Journal of Clinical and Experimental Medicine*, 8(10), 19436–19441. Retrieved from <http://www.ncbi.nlm.nih.gov/pmc/articles/PMC4694488/>
- Thati, V., Shivannavar, C. T., & Gaddad, S. M. (2011). Vancomycin resistance among methicillin resistant Staphylococcus aureus isolates from intensive care units of tertiary care hospitals in Hyderabad. *The Indian Journal of Medical Research*, 134(5), 704–708. <https://doi.org/10.4103/0971-5916.91001>
- Theuretzbacher, U. (2012). Accelerating resistance, inadequate antibacterial drug pipelines and international responses. *International Journal of Antimicrobial Agents*, 39(4), 295–299. <https://doi.org/10.1016/j.ijantimicag.2011.12.006>
- Thommes, M., Kaneko, K., V. Neimark, A., Olivier, J., Rodriguez-Reinoso, F., Rouquerol, J., & Sing, K. (2015). *Physisorption of gases, with special reference to the evaluation of surface area and pore size distribution (IUPAC Technical Report)*. *Pure and Applied Chemistry* (Vol. 87). <https://doi.org/10.1515/pac-2014-1117>

- Tjørve, K. M. C., & Tjørve, E. (2017). The use of Gompertz models in growth analyses, and new Gompertz-model approach: An addition to the Unified-Richards family. *PLOS ONE*, *12*(6), e0178691. Retrieved from <https://doi.org/10.1371/journal.pone.0178691>
- Tuerk, C., & Gold, L. (1990). Systematic Evolution of Ligands by Exponential Enrichment - RNA Ligands to Bacteriophage-T4 DNA-Polymerase. *Science*, *249*(4968), 505–510. <https://doi.org/10.1126/science.2200121>
- Uchil, R. R., Kohli, G. S., Katekhaye, V. M., & Swami, O. C. (2014). Strategies to Combat Antimicrobial Resistance. *Journal of Clinical and Diagnostic Research*: *JCDR*, *8*(7), ME01-ME04. <https://doi.org/10.7860/JCDR/2014/8925.4529>
- Upadhyay, R. K. (2014). Drug Delivery Systems, CNS Protection, and the Blood Brain Barrier. *BioMed Research International*, *2014*, 869269. <https://doi.org/10.1155/2014/869269>
- Veedu, R. N., & Wengel, J. (2009). Locked nucleic acid nucleoside triphosphates and polymerases: on the way towards evolution of LNA aptamers. *Molecular BioSystems*, *5*(8), 787–792. <https://doi.org/10.1039/b905513b>
- von Köckritz-Blickwede, M., & Nizet, V. (2009). Innate immunity turned inside-out: antimicrobial defense by phagocyte extracellular traps. *Journal of Molecular Medicine (Berlin, Germany)*, *87*(8), 775–783. <https://doi.org/10.1007/s00109-009-0481-0>
- Wang, Y., Ding, X., Chen, Y., Guo, M., Zhang, Y., Guo, X., & Gu, H. (2016). Antibiotic-loaded, silver core-embedded mesoporous silica nanovehicles as a synergistic antibacterial agent for the treatment of drug-resistant infections. *Biomaterials*, *101*, 207–216. <https://doi.org/https://doi.org/10.1016/j.biomaterials.2016.06.004>
- West, L., Isotta-Day, H., Ba-Break, M., & Morgan, R. (2016). Factors in use of family planning services by Syrian women in a refugee camp in Jordan. *Journal of Family Planning and Reproductive Health Care*. Retrieved from

<http://jfprhc.bmj.com/content/early/2016/03/08/jfprhc-2014-101026.abstract>

- Wilczewska, A. Z., Niemirowicz, K., Markiewicz, K. H., & Car, H. (2012). Nanoparticles as drug delivery systems. *Pharmacological Reports*, *64*(5), 1020–1037. [https://doi.org/https://doi.org/10.1016/S1734-1140\(12\)70901-5](https://doi.org/https://doi.org/10.1016/S1734-1140(12)70901-5)
- Wink, J. M., Kroppenstedt, R. M., Ganguli, B. N., Nadkarni, S. R., Schumann, P., Seibert, G., & Stackebrandt, E. (2003). Three new antibiotic producing species of the genus *Amycolatopsis*, *Amycolatopsis balhimycina* sp. nov., *A. tolypomycina* sp. nov., *A. vancoresmycina* sp. nov., and description of *Amycolatopsis keratiniphila* subsp. *keratiniphila* subsp. nov. and *A. keratiniph.* *Systematic and Applied Microbiology*, *26*(1), 38–46. <http://doi.org/10.1078/072320203322337290>
- World Health Organization. (2011). *The 10 leading causes of death by broad income group, 2008*. Retrieved from [http://www.who.int/mediacentre/factsheets/fs310\\_2008.pdf](http://www.who.int/mediacentre/factsheets/fs310_2008.pdf)
- Worthington, R. J., & Melander, C. (2013). Combination approaches to combat multidrug-resistant bacteria. *Trends in Biotechnology*, *31*(3), 177–184. <https://doi.org/10.1016/j.tibtech.2012.12.006>
- Xiong, M.-H., Bao, Y., Yang, X.-Z., Zhu, Y.-H., & Wang, J. (2014). Delivery of antibiotics with polymeric particles. *Advanced Drug Delivery Reviews*, *78*(0), 63–76. <https://doi.org/http://dx.doi.org/10.1016/j.addr.2014.02.002>
- Yeh, F.-Y., Liu, T.-Y., Tseng, I. H., Yang, C.-W., Lu, L.-C., & Lin, C.-S. (2014). Gold nanoparticles conjugates-amplified aptamer immunosensing screen-printed carbon electrode strips for thrombin detection. *Biosensors and Bioelectronics*, *61*(0), 336–343. <https://doi.org/http://dx.doi.org/10.1016/j.bios.2014.05.007>
- Zhou, J., & Rossi, J. J. (2011). Cell-specific aptamer-mediated targeted drug delivery. *Oligonucleotides*, *21*(1), 1–10. <https://doi.org/10.1089/oli.2010.0264>
- Zhou, W., Ding, J., & Liu, J. (2017). Theranostic DNazymes. *Theranostics*, *7*(4), 1010–1025. <https://doi.org/10.7150/thno.17736>
- Zhou, X., Weng, W., Chen, B., Feng, W., Wang, W., Nie, W., ... He, C. (2018).

Mesoporous silica nanoparticles/gelatin porous composite scaffolds with localized and sustained release of vancomycin for treatment of infected bone defects. *Journal of Materials Chemistry B*, 6(5), 740–752. <https://doi.org/10.1039/C7TB01246B>

Zwanikken, J. W., Guo, P., Mirkin, C. A., & Olvera de la Cruz, M. (2011). Local Ionic Environment around Polyvalent Nucleic Acid-Functionalized Nanoparticles. *The Journal of Physical Chemistry C*, 115(33), 16368–16373. <https://doi.org/10.1021/jp205583j>

## APPENDIX A

### PERMISSIONS FOR PUBLICATIONS

Issue 40, 2015

From the journal: **Chemical Communications**


### Antibiotic loaded nanocapsules functionalized with aptamer gates for targeted destruction of pathogens

M. Kavruk,<sup>ab</sup> O. Celikbıcak,<sup>c</sup> V. C. Ozello,<sup>ad</sup> B. A. Borsa,<sup>e</sup> F. J. Hernandez,<sup>g</sup> G. Bayramoglu,<sup>h</sup> B. Sali,<sup>c</sup> and M. Y. Arca<sup>f</sup>

Author affiliations

**Abstract**

In this study, we designed aptamer-gated nanocapsules for the specific targeting of cargo to bacteria with controlled release of antibiotics based on aptamer-receptor interactions. Aptamer-gates caused a specific decrease in minimum inhibitory concentration (MIC) values of vancomycin for *Staphylococcus aureus* when mesoporous silica nanoparticles (MSNs) were used for bacteria-targeted delivery.



Antibiotic (Vancomycin)  
Capsule  
Aptamer  
MSNs

Targeted Antibiotic Delivery  
For Specific Bacteria

Bacteria (*Staphylococcus aureus*)

About Cited by Related

#### Antibiotic loaded nanocapsules functionalized with aptamer gates for targeted destruction of pathogens

M. Kavruk, O. Celikbıcak, V. C. Ozalp, B. A. Borsa, F. J. Hernandez, G. Bayramoglu, B. Sali and M. Y. Arca, *Chem. Commun.*, 2015, 51, 8492  
DOI: 10.1039/C5CC01869B

If you are not the author of this article and you wish to reproduce material from it in a third party non-RSC publication you must formally request permission using RightsLink. Go to our [instructions for using RightsLink page](#) for details.

Authors contributing to RSC publications (journal articles, books or book chapters) do not need to formally request permission to reproduce material contained in this article provided that the correct acknowledgement is given with the reproduced material.

Reproduced material should be attributed as follows:

- For reproduction of material from NJC:  
Reproduced from Ref. XX with permission from the Centre National de la Recherche Scientifique (CNRS) and The Royal Society of Chemistry.
- For reproduction of material from PCCP:  
Reproduced from Ref. XX with permission from the PCCP Owner Societies.
- For reproduction of material from PPS:  
Reproduced from Ref. XX with permission from the European Society for Photobiology, the European Photochemistry Association, and The Royal Society of Chemistry.
- For reproduction of material from all other RSC journals and books:  
Reproduced from Ref. XX with permission from The Royal Society of Chemistry.

If the material has been adapted instead of reproduced from the original RSC publication "Reproduced from" can be substituted with "Adapted from".

In all cases the Ref. XX is the XXth reference in the list of references.

If you are the author of this article you do not need to formally request permission to reproduce figures, diagrams etc. contained in this article in third party publications or in a thesis or dissertation provided that the correct acknowledgement is given with the reproduced material.

Figure 31 Permission for publication “Antibiotic loaded nanocapsules functionalized with aptamer Gates for targeted destruction of pathogens” as a research paper.

Publishing Journals Books Databases  Advanced ROYAL SOCIETY OF CHEMISTRY

Log in / register

Issue 67, 2014 Previous Article | Next Article

From the journal: **Chemical Communications**

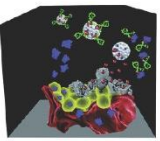
## NanoKeepers: stimuli responsive nanocapsules for programmed specific targeting and drug delivery

Frank J. Hernandez,<sup>a,b</sup> Luiza L. Hernandez,<sup>b</sup> Alurat Kavruk,<sup>c</sup> Yakup M. Arica,<sup>d</sup> Gulay Bayramoglu,<sup>e</sup> Saris A. Borsa,<sup>e</sup> Huseyin A. Ozkaya,<sup>f</sup> Thomas Schaefer<sup>g</sup> and Veli C. Ozalp<sup>g\*</sup>

Author affiliations

**Abstract**

Bacterial resistance is a high priority clinical issue worldwide. Thus, an effective system that rapidly provides specific treatment for bacterial infections using controlled dose release remains an unmet clinical need. Herein, we report on the NanoKeepers approach for the specific targeting of *S. aureus* with controlled release of antibiotics based on nuclease activity.



**About** | **Cited by** | **Related**

**NanoKeepers: stimuli responsive nanocapsules for programmed specific targeting and drug delivery**

F. J. Hernandez, L. L. Hernandez, M. Kavruk, Y. M. Arica, G. Bayramoglu, B. A. Borsa, H. A. Ozkaya, T. Schaefer and V. C. Ozalp, *Chem. Commun.*, 2014, **50**, 9489  
DOI: 10.1039/C4CC04248D

If you are not the author of this article and you wish to reproduce material from it in a third party non-RSC publication you must: [formally request permission](#) using RightsLink. Go to our [instructions for using RightsLink](#) page for details.

Authors contributing to RSC publications (journal articles, books or book chapters) do not need to formally request permission to reproduce material contained in this article provided that the correct acknowledgement is given with the reproduced material.

Reproduced material should be attributed as follows:

- For reproduction of material from NJC:  
Reproduced from Ref. XX with permission from the Centre National de la Recherche Scientifique (CNRS) and The Royal Society of Chemistry.
- For reproduction of material from PCCP:  
Reproduced from Ref. XX with permission from the PCCP Owner Societies.
- For reproduction of material from PPS:  
Reproduced from Ref. XX with permission from the European Society for Photobiology, the European Photochemistry Association, and The Royal Society of Chemistry.
- For reproduction of material from all other RSC journals and books:  
Reproduced from Ref. XX with permission from The Royal Society of Chemistry.

If the material has been adapted instead of reproduced from the original RSC publication "Reproduced from" can be substituted with "Adapted from".

In all cases the Ref. XX is the XXth reference in the list of references.

If you are the author of this article you do not need to formally request permission to reproduce figures, diagrams etc. contained in this article in third party publications or in a thesis or dissertation provided that the correct acknowledgement is given with the reproduced material.

Figure 32 Permission for publication “NanoKeepers: stimuli responsive nanocapsules for programmed specific targeting and drug delivery” as a research paper.

## BENTHAM SCIENCE PUBLISHERS LICENSE TERMS AND CONDITIONS

May 05, 2017

This Agreement between Murat Kavruk ("You") and Bentham Science Publishers ("Bentham Science Publishers") consists of your license details and the terms and conditions provided by Bentham Science Publishers and Copyright Clearance Center.

License Number	4102441097641
License date	May 05, 2017
Licensed Content Publisher	Bentham Science Publishers
Licensed Content Publication	Current Topics in Medicinal Chemistry
Licensed Content Title	Aptamers: Molecular Tools for Medical Diagnosis
Licensed Content Author	Veli Cengiz Ozalp, Murat Kavruk, Ozlem Dilek et al
Licensed Content Date	June 2017
I would like to...	Thesis/Dissertation
Requestor type	Author of requested content
Format	Print, Electronic
Portion	chapter/article
Rights for	Main product
Duration of use	Life of current edition
Creation of copies for the disabled	no
With minor editing privileges	no
In the following language(s)	Original language of publication
With incidental promotional use	no
The lifetime unit quantity of new product	0 to 499
The requesting person/organization is:	Murat Kavruk / Middle East Technical University
Title of your thesis / dissertation	NUCLEIC ACID GATED NANOPORE DELIVERY OF ANTIBIOTICS

Figure 33 Permission for publication "Aptamers: Molecular Tools for Medical Diagnosis" as a book chapter.



Confirmation Number: 11642549  
Order Date: 05/05/2017

Customer Information

Customer: Murat Kavruk  
Account Number: 3001148012  
Organization: Murat Kavruk  
Email: murat.kavruk@outlook.com  
Phone: +90 (531)2929008  
Payment Method: Invoice

This is not an invoice

Order Details

Future microbiology

Billing Status:  
N/A

Order detail ID: 70414029  
ISSN: 1746-0913  
Publication Type: Journal  
Volume:  
Issue:  
Start page:  
Publisher: FUTURE MEDICINE LTD

Permission Status: **Granted**  
Permission type: Republish or display content  
Type of use: Thesis/Dissertation  
Order License Id: 4102461272254

Requestor type	Author of requested content
Format	Print, Electronic
Portion	chapter/article
Title or numeric reference of the portion(s)	Figure 1, paragraphs from Page 1125, 1226, 1129, 1131, 1132
Title of the article or chapter the portion is from	Antimicrobial aptamers for detection and inhibition of microbial pathogen growth
Editor of portion(s)	N/A
Author of portion(s)	N/A
Volume of serial or monograph	8
Issue, if republishing an article from a serial	3
Page range of portion	
Publication date of portion	Mar 1, 2013
Rights for	Main product
Duration of use	Life of current edition
Creation of copies for the disabled	no
With minor editing privileges	no
For distribution to	Worldwide
In the following language(s)	Original language of publication
With incidental promotional use	yes

Figure 34 Permission for publication “Antimicrobial aptamers for detection and inhibition of microbial pathogen growth” as a review paper.



## APPENDIX B

### SHAPE CHARACTERISTICS OF GOMBERTZ MODEL

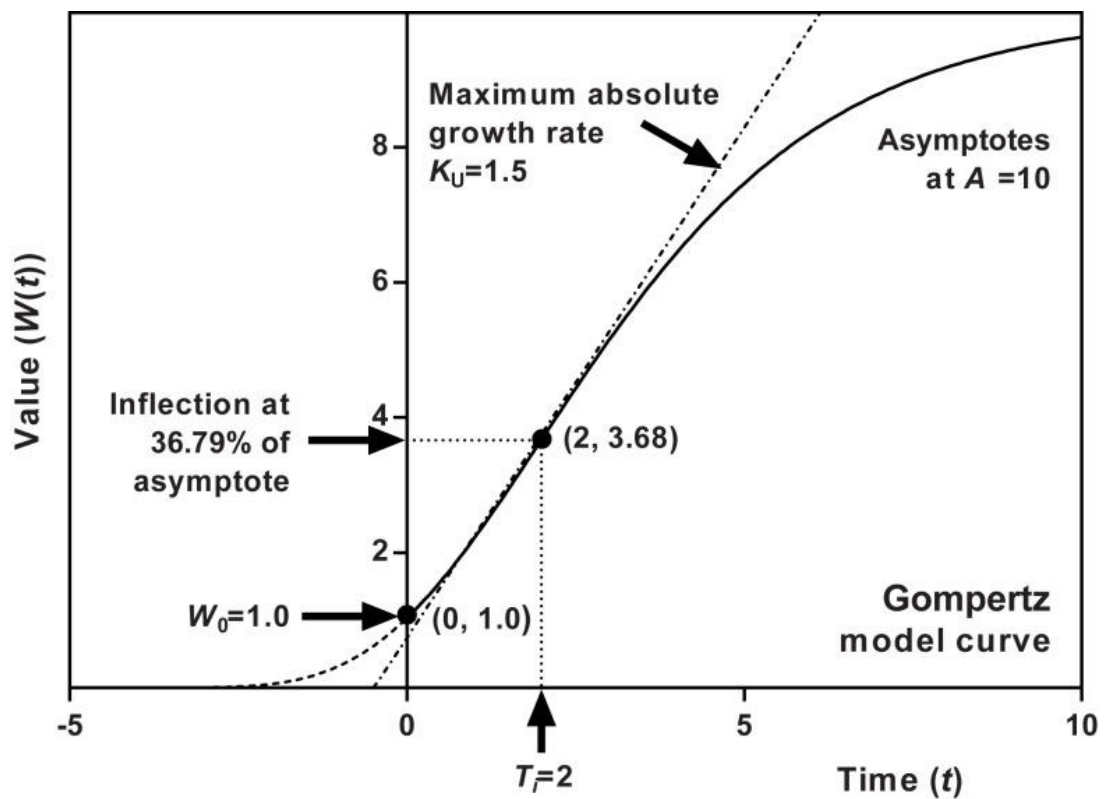


Figure 35 Shape characteristics of the Gompertz model. “The inflection value is fixed at 36.79% of the upper asymptote. Here the upper asymptote ( $A$ ) is set at 10.0, maximum absolute growth rate ( $K_U$ ) to 1.5, time at inflection ( $T_i$ ) to 2.0, and the starting point ( $W_0$ ) to 1.0. With a set asymptote and growth rate, time of inflection follows from a given starting point or vice versa. Maximum growth rate is represented by the tangent at inflection (dashed line).” (Tjørve & Tjørve, 2017).



## APPENDIX C

### BET ANALYSIS METHOD AND SUPPORTIVE GRAPHICS

Gas adsorption is the gold-standard tool for the characterization of the porous solids and fine powders for the determination of the surface area and pore size distribution on the surface. Nitrogen (at 77 K) is the recommended adsorptive gas for determining the surface area and mesopore size distribution, but it is necessary to employ a range of probe molecules to obtain a reliable assessment of the micropore size distribution (Thommes et al., 2015). Various procedures have been devised for determining the amount of gas adsorbed. Related with these methods, different computational procedures have been offered to measure the mesopore size distribution from nitrogen adsorption data. These procedures are based on the emptying of the mesopores by the step-wise reduction ( $p / p^0$ ), leading to the thinning of the multilayer in the pores already emptied of condensate gas. The meniscus curvature at the interface is controlled by the pore size and shape, assuming that the pores are rigid and confined to the mesopore range and that there are no pore blocking effects. Furthermore, the derived pore size distribution is dependent on whether the adsorption or desorption branch of the hysteresis loop is used for the computation. Moreover, if these two fluids are a pure liquid, of molar volume  $V_m$ , and its vapour, then under conditions of equilibrium the vapor pressure ( $p$ ) at the temperature ( $T$ ) will differ from the normal saturation vapor pressure ( $p^0$ ) according to Kelvin equation (IUPAC, 1994).

$$(RT / V_m^l) \ln (p / p^0) = \sigma C \text{ (Kelvin equation)}$$

where  $R$  is the universal gas constant. Measurements of either  $(p / p^0)$  or of  $\Delta P$  can be used to determine  $C$  and, then, the pore radius  $r$ .

The Brunauer–Emmett–Teller (BET) method has been the most widely used procedure for evaluating the surface area of porous and finely-divided materials (Brunauer, Emmett, & Teller, 1938). According to the BET theory, the parameter  $C$  is exponentially related to the energy of monolayer adsorption. It is now generally agreed that the value of  $C$  rather gives a useful indication of the shape of the isotherm in the BET range. It was this characteristic point which was first identified by Brunauer and Emmett as the stage of monolayer completion and the beginning of multilayer adsorption. Under certain predetermined conditions, the BET-area of a nonporous, macroporous or a mesoporous solid (i.e., giving a well-defined Type II or a Type IV(a) isotherm) can be regarded as the area available for the adsorption of the specified adsorptive gas (i.e. nitrogen). In the application of BET method, it is first necessary to transform a physisorption isotherm into the BET plot and a value of the BET monolayer capacity ( $n_m$ , the specific monolayer capacity) is derived. Then, the BET-area is calculated from  $n_m$  by assuming an appropriate value of the molecular cross-sectional area,  $\sigma$ . The linear BET equation is given below where  $n$  is the specific amount adsorbed at the relative pressure  $p/p^0$  and  $n_m$  is the specific monolayer capacity.

$$[(p / p^0) / n (1 - (p / p^0))] = (1 / n_m C) + (C-1) / [ (n_m C) (p / p^0) ]$$

Generally, the methods for mesopore size analysis, based on the modified Kelvin equation, including Barrett, Joyner and Halenda (BJH) method have been used. For many years mesopore size analysis was mostly based on the application of the Kelvin equation. Thus, the shift of the gas-liquid phase transition of a confined fluid from bulk coexistence, is expressed in terms of the Physisorption of gases, with special reference to the evaluation of the surface tension  $\gamma$  of the bulk fluid and the molar

liquid volume  $V_m$ . For cylindrical pores the modified Kelvin equation is formulized as follows:

$$\ln (p / p^0) = 2 \gamma V_m / RT (r_p - t_c)$$

where  $r_p$  is the pore radius and  $t_c$  the thickness of the adsorbed multilayer film, which is formed prior to pore condensation.

The Kelvin equation is evaluated along with a standard isotherm, t-curve, for nonporous solids to account for the preadsorbed multilayer films. However, for the size analysis of narrow mesopores, the standard t-curve is not entirely satisfactory, because the curvature and enhanced surface forces are not exactly considered. Similarly, the validity of the Kelvin equation is questionable as the mesopore width is reduced because macroscopic concepts can no longer be safely applied. It was demonstrated that the Kelvin equation based procedures, such as the BJH method, significantly underestimate the pore size for narrow mesopores (for pore diameter less than 10 nm size will be underestimated by 20-30%). Thus, the limitations of the Kelvin equation can be avoided by applying microscopic methods based on molecular simulation or DFT to obtain yield the thermodynamics and density profiles of confined fluids and a description of the adsorbed phase on a molecular level. This method combine the essential features of both micropore and mesopore filling and hysteresis. Hence, a more reliable assessment of the pore size distribution over the complete range would be obtained. Furthermore, useful information from both the adsorption and desorption branches of the hysteresis loop can be extracted. With certain ordered mesoporous materials, these methods are capable of quantitatively predicting the pore condensation and hysteresis type behavior by taking into account the underlying adsorption-desorption mechanisms including the delay in condensation due to metastability of the pore fluid. These advantages are crucial in the pore size

analysis of materials which give rise to H2, H3, H4 and H5 hysteresis loops (Thommes et al., 2015).

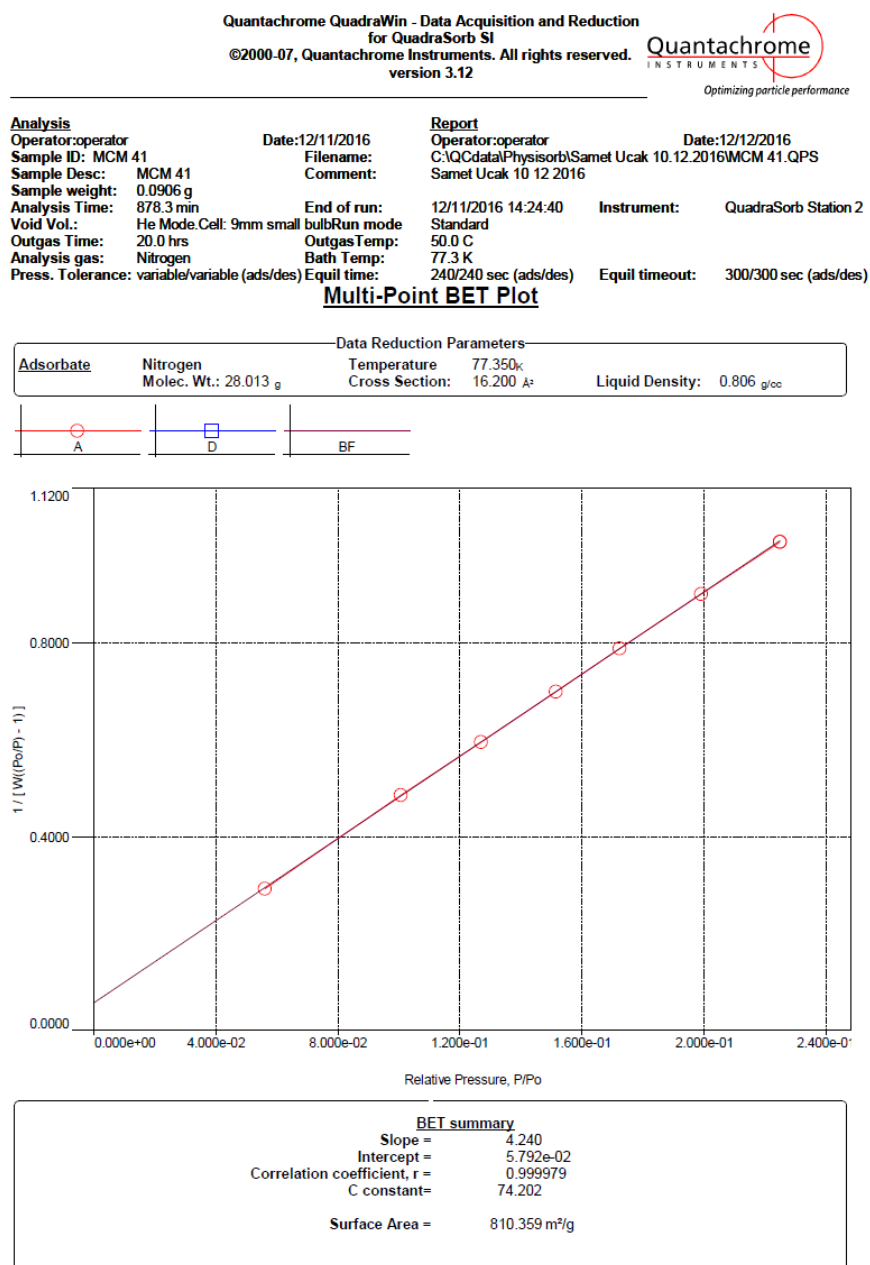
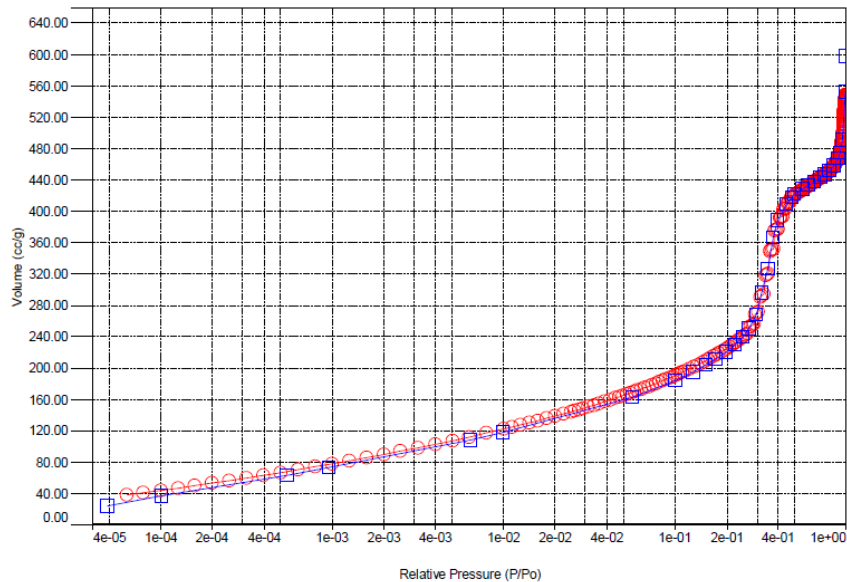
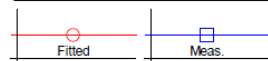


Figure 36 Multi-point BET plot of BET analysis

<b>Analysis</b>		<b>Report</b>	
Operator:operator	Date:12/11/2016	Operator:operator	Date:12/12/2016
Sample ID: MCM 41	Filename:	C:\QCdata\Physisorb\Samet Ucak 10.12.2016\MCM 41.QPS	
Sample Desc: MCM 41	Comment:	Samet Ucak 10.12.2016	
Sample weight: 0.0906 g			
Analysis Time: 878.3 min	End of run:	12/11/2016 14:24:40	Instrument: QuadraSorb Station 2
Void Vol.: He Mode.Cell: 9mm small bulb	Run mode:	Standard	
Outgas Time: 20.0 hrs	Outgas Temp:	50.0 C	
Analysis gas: Nitrogen	Bath Temp:	77.3 K	
Press. Tolerance: variable/variable (ads/des)	Equil time:	240/240 sec (ads/des)	Equil timeout: 300/300 sec (ads/des)

**DFT \* Fitting Comparison**

Data Reduction Parameters			
<b>DFT method</b>	Calc. Model: N2 at 77 K on silica (cylindr. pore, NLDFT adsorption branch model) Rel. press. range: 0.0000 - 1.00		
<b>Adsorbate</b>	Moving pt. avg: off		
	Temperature	77.350 K	
	Molec. Wt.: 28.013 g	Cross Section: 16.200 Å²	Liquid Density: 0.806 g/cc



DFT method summary	
Pore volume =	0.816 cc/g
Lower confidence limit =	2.122 nm
Fitting error =	0.686 %
Pore width (Mode) =	4.093 nm
Moving point average :	off

Figure 37 DFT Fitting Comparison of BET analysis





## APPENDIX D

### ANOVA CALCULATIONS OF MIC ANALYSIS

**Data Source: Data 2 in mic**

**Equation: Sigmoidal; Gompertz, 4 Parameter**

$f=y_0+a*\exp(-\exp(-(x-x_0)/b))$

R	Rsqr	Adj Rsqr	Standard Error of Estimate
0,9975	0,9950	0,9935	0,0111

	Coefficient	Std. Error	t	P
a	0,2805	0,0090	31,0885	<0,0001
b	-0,0565	0,0204	-2,7729	0,0197
x0	0,2722	0,0099	27,3808	<0,0001
y0	0,1242	0,0045	27,3642	<0,0001

**Analysis of Variance:**

Analysis of Variance:

	DF	SS	MS
Regression	4	1,2776	0,3194
Residual	10	0,0012	0,0001
Total	14	1,2789	0,0913

Corrected for the mean of the observations:

	DF	SS	MS	F	P
Regression	3	0,2440	0,0813	658,4852	<0,0001
Residual	10	0,0012	0,0001		
Total	13	0,2453	0,0189		

**Statistical Tests:**

**Normality Test (Shapiro-Wilk)** Passed (P = 0,5572)

W Statistic= 0,9498      Significance Level = <0,0001

**Constant Variance Test** Passed (P = 0,0719)

Figure 38 ANOVA statistics for MIC calculations of modified oligonucleotide-capped nanoparticles against *S. aureus*

**Data Source:** Data 3 in mic  
**Equation:** Sigmoidal; Gompertz, 4 Parameter  
 $f=y_0+a*\exp(-\exp(-(x-x_0)/b))$

<b>R</b>	<b>Rsqr</b>	<b>Adj Rsqr</b>	<b>Standard Error of Estimate</b>
0,9839	0,9680	0,9584	0,0125

	<b>Coefficient</b>	<b>Std. Error</b>	<b>t</b>	<b>P</b>
a	0,2071	0,0182	11,4019	<0,0001
b	-2,5202	0,8076	-3,1207	0,0109
x0	7,6260	0,4959	15,3775	<0,0001
y0	0,2028	0,0125	16,2354	<0,0001

**Analysis of Variance:**

Analysis of Variance:

	<b>DF</b>	<b>SS</b>	<b>MS</b>
Regression	4	1,9921	0,4980
Residual	10	0,0016	0,0002
Total	14	1,9936	0,1424

Corrected for the mean of the observations:

	<b>DF</b>	<b>SS</b>	<b>MS</b>	<b>F</b>	<b>P</b>
Regression	3	0,0472	0,0157	100,8473	<0,0001
Residual	10	0,0016	0,0002		
Total	13	0,0488	0,0038		

**Statistical Tests:**

**Normality Test (Shapiro-Wilk)** Passed (P = 0,3856)

W Statistic= 0,9374      Significance Level = <0,0001

**Constant Variance Test** Passed (P = 0,0026)

Figure 39 ANOVA statistics for MIC calculations of modified oligonucleotide-capped nanoparticles against *S. epidermis*

Data Source: Data 2 in mic

Equation: Sigmoidal; Gompertz, 4 Parameter

$f=y_0+a*\exp(-\exp(-(x-x_0)/b))$

R	Rsqr	Adj Rsqr	Standard Error of Estimate
0,9973	0,9946	0,9930	0,0109

	Coefficient	Std. Error	t	P
a	0,2932	0,0127	23,1319	<0,0001
b	-0,2759	0,0412	-6,6994	<0,0001
x0	0,7816	0,0363	21,5388	<0,0001
y0	0,1290	0,0054	23,7366	<0,0001

**Analysis of Variance:**

Analysis of Variance:

	DF	SS	MS
Regression	4	1,4869	0,3717
Residual	10	0,0012	0,0001
Total	14	1,4881	0,1063

Corrected for the mean of the observations:

	DF	SS	MS	F	P
Regression	3	0,2185	0,0728	615,9905	<0,0001
Residual	10	0,0012	0,0001		
Total	13	0,2197	0,0169		

**Statistical Tests:**

Normality Test (Shapiro-Wilk) Passed (P = 0,3591)

W Statistic= 0,9351 Significance Level = <0,0001

Constant Variance Test Passed (P = 0,0211)

Figure 40 ANOVA statistics for MIC calculations of aptamer-capped nanoparticles against *S. aureus*

Data Source: Data 3 in Figure3-5

Equation: Sigmoidal; Logistic, 4 Parameter

$f = \text{if}(x < 0; \text{if}(b < 0; y_0; y_0 + a); \text{if}(b > 0; y_0 + a / (1 + \text{abs}(x/x_0)^b); y_0 + a * \text{abs}(x/x_0)^{(\text{abs}(b))} / (1 + (\text{abs}(x/x_0)^{(\text{abs}(b))})))$

R	Rsqr	Adj Rsqr	Standard Error of Estimate
0,9979	0,9959	0,9946	0,0006

	Coefficient	Std. Error	t	P
a	0,0243	0,0011	22,1175	<0,0001
b	-1,1879	0,1077	-11,0296	<0,0001
x0	140,2080	11,6421	12,0431	<0,0001
y0	0,0046	0,0005	8,8984	<0,0001

Analysis of Variance:

Analysis of Variance:

	DF	SS	MS
Regression	4	0,0042	0,0011
Residual	10	4,0493E-006	4,0493E-007
Total	14	0,0042	0,0003

Corrected for the mean of the observations:

	DF	SS	MS	F	P
Regression	3	0,0010	0,0003	805,8906	<0,0001
Residual	10	4,0493E-006	4,0493E-007		
Total	13	0,0010	7,5618E-005		

Statistical Tests:

Normality Test (Shapiro-Wilk) Passed (P = 0,1033)

W Statistic= 0,8974 Significance Level = <0,0001

Constant Variance Test Passed (P = 0,0211)

Figure 41 ANOVA statistics for MIC calculations of aptamer-capped nanoparticles against *S. epidermis*

## CURRICULUM VITAE

### PERSONAL INFORMATION

Surname, Name: Kavruk, Murat  
Nationality: Türkiye  
Date and Place of Birth: 15/05/1984 - Kocaeli  
Marital Status: Married  
Phone: 533 – 422 60 13  
E-mail: murat.kavruk@outlook.com

### EDUCATION

Degree	Institution	Year of Graduation
MS	METU Biotechnology	2010
BS	METU Biology	2007
High School	Gazi Anatolian H.S., Ankara	2002

### WORK EXPERIENCE

Year	Place	Enrollment
2013-Present	Turkish Standards Institution	TSE Specialist
2007-2013	NANObiz Ltd	R&D Specialist

### FOREIGN LANGUAGES

Advanced English

### PUBLICATIONS

- Hernandez, F. J., M. Kavruk, L. I. Hernandez, V. C. Ozalp (2015), “8. Nanocapsules in Biomedicine: Promises and Challenges”. Advanced Theranostic Materials, Wiley, July 2015.
- M. Kavruk, O. Celikbicak, V. C. Ozalp, B. A. Borsa, F. J. Hernandez, G. Bayramoglu. Salih and M. Y. Arica (2015). “Antibiotic loaded nanocapsules

functionalized with aptamer gates for targeted destruction of pathogens." *Chem Commun (Camb)* 51(40): 8492-8495.

- Hernandez, F. J., L. I. Hernandez, M. Kavruk, Y. M. Arica, G. Bayramoglu, B. A. Borsa, H. A. Oktem, T. Schafer and V. C. Ozalp (2014). "NanoKeepers: stimuli responsive nanocapsules for programmed specific targeting and drug delivery." *Chem Commun (Camb)* 50(67): 9489-9492.
- Ozalp, V. C., G. Bayramoglu, M. Kavruk, B. B. Keskin, H. A. Oktem and M. Y. Arica (2014). "Pathogen detection by core-shell type aptamer-magnetic preconcentration coupled to real-time PCR." *Analytical Biochemistry* 447(0): 119-125.
- Ozalp, V. C., U. S. Zeydanlı, A. Lunding, M. Kavruk, M. T. Oz, F. Eyidogan, L. F. Olsen and H. A. Oktem (2013). "Nanoparticle embedded enzymes for improved lateral flow sensors." *Analyst* 138(15): 4255-4259.
- Kavruk, M., V. C. Ozalp and H. A. Oktem (2013). "Portable Bioactive Paper-Based Sensor for Quantification of Pesticides." *Journal of Analytical Methods in Chemistry* 2013: 8.
- Ozalp, V. C., K. Bilecen, M. Kavruk and H. Avni Öktem (2013). "Antimicrobial aptamers for detection and inhibition of microbial pathogen growth." *Future Microbiology* 8(3): 387-401.
- Cansız, S., C. Özen, C. Bayraç, A. T. Bayraç, F. Gül, M. Kavruk, R. Yılmaz, F. Eyidogan and H. Öktem (2012). "A sandwich-type DNA array platform for detection of GM targets in multiplex assay." *European Food Research and Technology* 235(3): 429-437.

## **HOBBIES**

Jogging, cycling, reading, documentaries